UNDERSTANDING THE ROLE OF DIBENZOFURAN 4,4A DIOXYGENASE REVEALS A SILENT PATHWAY FOR BIPHENYL DEGRADATION IN *SPHINGOMONAS WITTICHII* RW1 AND HELPS IN ENGINEERING DIOXIN DEGRADING STRAINS

By

RAYAN MAZIN FAISAL

A dissertation submitted to the

School of Graduate Studies

Rutgers, The State University of New Jersey

In partial fulfillment of the requirements

For the degree of

Doctor of Philosophy

Graduate Program in Microbial biology

Written under the direction of

Gerben Zylstra

And approved by

_____

_____

_____

_____

New Brunswick, New Jersey

October, 2019

ABSTRACT OF THE DISSERTATION

Understanding the Role of Dibenzofuran 4,4a Dioxygenase Reveals a Silent Pathway for Biphenyl Degradation in *Sphingomonas wittichii* RW1 and Helps in Engineering Dioxin Degrading Strains

by RAYAN MAZIN FAISAL

Dissertation Director:

Dr. Gerben Zylstra

Sphingomonas wittichii RW1 is one of three strains known to degrade dibenzo-*p*-dioxin (DXN) and dibenzofuran (DBF). Due to the toxic, carcinogenic, and endocrine disruption characteristics of these compounds molecular and biochemical studies of the enzymes involved in the DXN and DBF degradative pathways has been of great interest. Dibenzofuran 4,4a-dioxygenase (DBFDO) is the first enzyme involved in the DXN and DBF degradation pathways. This enzyme is a heterodimer of two polypeptides DxnA1 (45KDa) and DxnA2 (23KDa) which functions to add two atoms of molecular oxygen at two adjacent carbon atoms where one of the carbons is a bridge atom between the two benzene rings. This enzyme is thus often called an angular dioxygenase. Based on studies with the purified enzyme DBFDO is known to be capable of hydroxylating other aromatic compounds, however, the exact product made and the location where the dioxygenation occurs on these aromatics are unknown. For that purpose, we cloned the four genes necessary for DBFDO into *E. coli* in the pET30a expression vector. This

included the genes for the two oxygenase subunits *dxnA1* and *dxnA2*, the reductase *redA2*, and the ferredoxin *fdx3*. Results based on the HPLC, GC-MS, and NMR analysis showed that *E. coli* BL21 strains harboring this clone when induced had the ability to perform three types of oxygenations: angular dioxygenation towards DBF, DXN, 2-hydroxyDBF, xanthene, and xanthone; *cis*-dihydroxylation towards biphenyl, phenanthrene, anthracene, and xanthone; and monooxygenation to the benzylic methylenic group in fluorene as well as monooxygenation and dioxygenation to the sulfur heteroatom in dibenzothiophene. On the other hand, no oxygenation was seen for diphenylmethane, diphenyl ether, carbazole, chrysene, naphthalene, pyrene, anthrone, salicylate, and toluene.

Our next goal was to engineer a DXN and DBF degrading strain which was achieved through cloning the *S. wittichii* RW1 *dxnA1-dxnA2-redA2-fdx3* genes into the biphenyl degrading organism *S. yanoikuyae* B1 in place of the *bphA1f-bphA2f* genes thus placing the RW1 oxygenase under control of the B1 biphenyl pathway promoter. This allowed us to examine if the enzymatic activity of DBFDO towards biphenyl is sufficient to allow growth on biphenyl as the sole carbon source. More importantly, the engineered *S. yanoikuyae* B1 (B1DR, DR for dioxygenase replacement) will now have the ability to perform angular dioxygenation towards DXN and DBF which will allow us to identify if *S. yanoikuyae* B1 contains genes that metabolize these aromatics. Our results showed that B1DR had the ability to grow on biphenyl and DXN but not DBF indicating the presence of downstream DXN degrading enzymes in this organism and showing that the enzymes do not function on DBF. Gene knockout and gene insertion experiments showed that the biphenyl extradiol dioxygenase, BphC, and the HOPDA hydrolase, BphD, from *S.*

yanoikuyae B1 are the enzymes that showed activity on DXN metabolites, as deleting *bphC* abolished the ability of B1DR to metabolize DXN but not biphenyl. However, deletion of *bphD* abolished growth of B1DR on both DXN and biphenyl. On the other hand complementing B1DRΔbphC with the specific DXN extradiol dioxygenase, SWIT3046, from RW1 retained growth on DXN, while complementing B1DRΔbphD with RW1 hydrolase, *dxnB*, retained growth on both DXN and biphenyl to similar growth rates as of B1DR. These results show that *bphC* and *bphD* from *S. yanoikuyae* B1 carry similar activity to specific DXN metabolizing genes from *S. wittichii* RW1 and shows that more than one extradiol dioxygenase is involved in biphenyl degradation in *S. yanoikuyae* B1 but only BphC functions on DXN metabolites. This work also shows that *S. yanoikuyae* B1 uses a single hydrolase, BphD, for biphenyl degradation which also has activity towards DXN. DBF was metabolized by B1DR only after inserting both an extradiol dioxygenase (*dbfB* or SWIT3046) and a hydrolase (*dxnB*) from *S. wittichii* RW1, indicating the lack of DBF degrading genes in *S. yanoikuyae* B1.

Even though *S. wittichii* RW1 is unable to use biphenyl as a sole carbon source, the present work showed that it contains an angular dioxygenase that can attack biphenyl at a lateral position producing *cis*-2,3-dihydro-2,3-dihydroxybiphenyl. Also, a previous study showed that its 2,2',3-trihydroxybiphenyl dioxygenase involved in the DBF pathway, *dbfB*, showed activity towards 2,3-dihydroxybiphenyl. Finally, its hydrolase, *dxnB*, is able to hydrolyze HOPDA generated from biphenyl degradation. All these facts collectively led us to hypothesize that the only missing gene for *S. witichii* RW1 to grow on biphenyl would be the *cis*-dihydrodiol dehydrogenase. To prove our hypothesis, the gene for *cis*-dihydrodiol dehydrogenase, *bphB*, from the biphenyl degrader *Sphingobium*

yanaikuyae B1 was placed downstream of the *fdx3* gene under the control of the constitutive promoter of the *dxn* locus in *S. wittichii* RW1. Interestingly, this engineered strain grew on biphenyl revealing a hidden pathway for biphenyl degradation in RW1. Using a series of knockout mutant strains we showed the involvement of two different ring-cleavage dioxygenases and two different hydrolases in the biphenyl degradation pathway. This work demonstrates that the enzymes in the upper pathway for DBF and DXN degradation have a wide substrate range with activity towards other aromatic hydrocarbons.

DEDICATION

This work is dedicated to the brave Iraqi soilders who liberated my city Mosul from the control of ISIS and to the soules of all innocent civilians who had lost their lives during this period.

To all my instructors who I have learned from at the University of Mosul and here at Rutgers University, you have all contributed to what I achieve today.

ACKNOWLEDGMENT

It has been a great honor for me to work under the guidance and support of Dr. Gerben Zylstra, without whom, this thesis would not have been finished. Dr. Zylstra is one of the pioneers in the field of "genetics of biodegradation" and by following his advice I was able to achieve my goals. He introduced me to the field of biodegradation and supported me with all materials and feedback required. He always appreciated new ideas that I brought and gave me the chance to test them in real life. Dr. Zylstra's guidance was not only restricted to research needs but went further for support outside the lab. For that, I owe him much thanks.

I would also like to express appreciation to the members of my qualifying exam and dissertation committee Dr. Gerben Zylstra, Dr. Jerome Kukor, Dr. Donna Fennell, Dr. Donald Kobayashi, and Dr. Tamar Barkay for making the time to serve as committee members for my dissertation. I appreciate their time and respect their ideas and suggestions.

I would like to express my sincere gratitude to Dr. Hung-Kuang Chang for all his valuable suggestions especially when I first started working in the lab. He guided me through most of the procedures I used in lab and showed me how to organize my data. I would also like to thank our visiting professor Dr. Xing Huang and my lab mate, Thamer Mutter, for sharing some of their knockout strains. Thanks to all my lab mates Suha, Aakansha, Ahmed, Igor, and Aveen for providing a great laboratory environment which made the six years pass smoothly. I would also like to thank Dr. Thomas Hartman and his lab members Bin and Joseph for their help in running my GC-MS samples. Thanks to Dr.

Daniel Seidel and his wonderful lab members, Wazo, Zhingbo, and Kaidong for running and analyzing my NMR research.

I am indebted to the higher committee for education development in Iraq for this great opportunity they provided for me to study at Rutgers University. This was one of my biggest dreams that by their support and funding came true. I would also like to thank the Department of Biochemistry and Microbiology for providing me with several fellowships, travel awards, and a teaching assistant position which helped me extend my study and be able to present my work in several conferences and meetings around the United States. All these benefits were kindly arranged by my thesis advisor Dr. Gerben Zylstra to whom I show my respect.

No matter what I say it would not be enough to express my gratitude and appreciation to my wife, Noor, who dedicated her life to support and encourage me throughout these years. Without her I would not had dared to study abroad. All my love to my wonderful kids Naba, Younis, Bilal, and Deema you were my true source of motivation. Sorry, for spending too much time in lab away from you.

Last but not least, I would like to acknowledge my Dad and Mom for their endless support. If I feel that I have succeeded one day in my life, it is definitely due to their prayers.

Table of Contents

List of Tables

List of Illustrations

Chapter 1: Introduction

Chemical and physical properties of polycyclic aromatic hydrocarbons

Polycyclic aromatic hydrocarbons (PAHs) are a class of organic compounds that consist of 2-7 benzene rings. They are found as colorless, white/pale yellow solids that are highly lipophilic and as a result have very low solubility in water. These compounds have high melting and boiling points and low vapor pressure (1, 2). PAHs are classified according to their molecular weight into two categories: low molecular weight compounds, consisting of 2-4 benzene rings, and high molecular weight compounds possessing more than 4 rings (1). As more rings are added to the PAH, their aqueous solubility and vapor pressure decreases while their melting and boiling points increases. PAHs are also distinct by some physical characteristics such as light sensitivity, heat resistance, conductivity, and corrosion resistance. Most PAHs are fluorescent and each PAH has its unique UV spectrum which can be used for their identification (3). Due to the chemical and physical properties of PAHs, they are highly persistent and mobile in the environment allowing them to distribute in the ecosystems. Accordingly, they are considered one of the first environmental pollutants that have been identified for their toxicity and carcinogenicity (4).

Sources of polycyclic aromatic hydrocarbons

The major source for PAHs formation in the environment is the incomplete combustion of organic matter. This can be either from natural sources such as forest fires, volcanoes, high-temperature pyrolysis of organic matter, and direct biosynthesis from microorganisms and plants. PAHs can also be generated from anthropogenic sources such

as domestic burning of wood, coal, and peat in fireplaces; burning of municipal wastes and tobacco; incomplete combustion of fuel emitted from different transportation vehicles (automobiles, ships, trains, and airplanes); industrial wastes from aluminum production, coke production, creosote and wood preservation, asphalt formation, tire and petrochemical industries; and oil spills (2-4). Once PAHs are formed they can be mobilized in the environment depending on different factors. High molecular weight PAHs absorb more efficiently to soil particles hence transfer less distances, while gaseous PAHs travel longer. Organic matter also tends to effect PAHs concentration in soil, as soils enriched with organic matter contain higher concentrations of PAHs than mineral soil (5). Even though PAHs are toxic to many organisms, they are still produced and used commercially for pesticide production, plastic industry, and in the manufacture of dyes. Examples of commercially produced PAHs are pyrene, fluoranthene, phenanthrene, anthracene, fluorene, and naphthalene (4). Due to the presence of PAHs in our ecosystem, studies have estimated that a person intakes around 3 mg of carcinogenic PAHs per day which corresponds to a low risk of cancer. However, intake may increase among workers in aluminum and coke factories or among smokers. In such cases the risk of lung, skin, and bladder cancer has been found to be more prevalent (6, 7).

Health effects of polycyclic aromatic hydrocarbons

Humans and mammals are exposed to mixtures of PAHs through inhalation, ingestion, and skin contact. As a result, it has been difficult to assess the effects of each PAH individually especially in humans (6). However, some PAHs such as benzo[a]pyrene, benzo[a]fluoranthene, chrysene, and indeno [1,2,3-c, d] pyrene have

been experimentally proven to have carcinogenic, mutagenic, and genotoxic effects on animals (8).

For a PAH to show its toxicity it has to be absorbed through body membrane barriers and enter the bloodstream where it can be distributed by the lymph to different locations in the body, mainly the liver and kidneys. Due to the lipophilic nature of PAHs, they tend to accumulate in lipid-rich tissues of the body. PAHs at this step are called procarcinogens because they do not show toxicity until they are metabolized through different enzymatic pathways in the body, most of these enzymatic processes occur in the liver. Metabolism of PAHs occur through three major pathways: the CYP1A1/1B1 and epoxide hydrolase pathway, CYP peroxidase pathway, and aldo-keto reductase pathway. As a result, electrophilic metabolites such as epoxides, radical cations, or reactive and redox-active quinones are produced that can cause direct damage to DNA, protein, or lipid (6, 9).

The relationship between environmental pollution and human health has always generated hot topics for research of biologists. PAHs have taken a large portion from these researches due to their association with several cases of skin, lung, and bladder cancer (8). Smokers and people who work in places where air is polluted with PAHs have been associated with DNA adducts and P53 mutations that led to lung cancer which is probably due to the presence of 100 ng or more of PAHs for each group of tobacco (8, 9). Studies have shown that PAHs can travel through the placenta and reach the fetus causing more severe toxicological effects on the fetus compared to adults (10). These effects are specific to the central nervous system and were found to cause brain tumor, behavior deficits, and disorders in the differentiation of the brain (11).

Dioxins

Polychlorinated dibenzofurans (PCDF), polychlorinated dibenzo-*p*-dioxins (PCDD) and polychlorinated biphenyls (PCBs) are toxic polycyclic aromatic hydrocarbons (PAHs) known as dioxins (12). These compounds are insoluble in water, semi-volatile to nonvolatile, and chemically and metabolically stable. Even though their concentrations in different environmental samples are low, their stability and lipophilicity enables them to accumulate in human and animal lipids to reach up to 9 and 14 pg/g for tetrachloro-dibenzo-*p*-dioxin and heptachloro-dibenzo-*p*-dioxin, respectively (13, 14). Dioxins are released to the environment naturally through forest fires or by human activities through the incineration of municipal and hospital wastes; combustion of wood and diesel vehicles; and as by products from pesticide, herbicide, and paper manufacturing. Chlorinated dioxins can also be formed naturally by the reaction of peroxidases on chlorophenols leading to the formation of some toxic chlorinated dioxins such as 2,3,7,8-tetrachlorodioxin which is the most toxic and persistent form of dioxin with an approximate half-life of 1-10 years in soil and sediments (15). These sources collectively, are responsible for air, water, and soil pollution leading to incorporation of dioxins in the food chain (13, 16). One of the best studies that showed the effect of dioxins on humans was carried out in Italy on a group of people accidentally exposed to 2,3,7,8-TCDD from a plant near Seveso. This study found an increase in cases of hepatobiliary cancer, hematologic neoplasm, multiple myeloma, myeloid leukemia, and soft tissue tumors especially in people who lived in this area for more than 5 years. An increase in diabetes was also observed among women besides chronic circulatory and respiratory disorders. Their results led them to support the evaluation of dioxin as a

carcinogen (17, 18). Once dioxins are introduced into the environment, they can be remediated chemically, physically, or biologically. Due to the high cost of the first two methods, scientists have focused on finding bacteria capable of using these toxic compounds as a sole source for carbon and energy, thereby avoiding their toxic danger (19).

Microorganisms that degrade dibenzo-*p*-dioxin

Since dioxins are generated from forest fires, one would hypothesize that bacteria have been exposed to such compounds for thousands or millions of years and that we would have many bacteria capable of degrading them. Unfortunately, dioxin degradation is only limited to three strains, *Rhodococcus opacus* SAO101 (20), *Pseudomonas veronii* PH03 (21), and *Sphingomonas wittichii* RW1 (22). No further research has been conducted on both *Rhodococcus opacus* SAO101 and *Pseudomonas veronii* PH03 since their isolation in 2001 and 2004, respectively. All knowledge regarding the genetics, physiology, and biochemistry of the dioxin degradation pathway is obtained from work done with *Sphingomonas wittichii* RW1 (23-25).

***Sphingomonas wittichii* RW1**

S. wittichii RW1 was first isolated from a water sample from the River Elbe (Germany) by R. Wittich in 1992 for its ability to completely metabolize DXN and DBF as the sole source of carbon and energy for growth (22). Later, this strain was found to be capable of transforming several chlorinated congeners of DXN and DBF including 2-chlorodibenzo-*p*-dioxin, 2,7-dichlorodibenzo-*p*-dioxin, and 1,2,3,4-tetrachlorodibenzo-*p*-dioxin (26, 27). Cells of *S. wittichii* RW1 are gram negative rods (0.4–0.6 × 0.9–1.5 μm),

non-spore forming, and motile with a single polar or subpolar flagellum. Colonies of this strain are 1 mm in diameter, smooth, and show a faint yellow color after three days of incubation at 30°C on Bacto-heart infusion agar (28). *Sphingomonas* is classified within the α-proteobacteria under the α-4 subclass along with *Rhizomonas*, *Zymomonas*, and *Blastomonas*. Phylogenetic analysis of the 16S rRNA sequence sub-divides *Sphingomonas* into 4 distinct clusters, *S. wittichii* RW1 is placed in the second cluster with the species *S. yanoikuyae*, *S. herbicidovorans*, *S. chlorophenolica*, and *S. xenophaga* (29). Members of this cluster are known for their ability to degrade a wide variety of mono and polycyclic aromatic hydrocarbons (30-33).

Aerobic degradation of dibenzo-*p*-dioxin and dibenzofuran by *S. wittichii* RW1

DXN and DBF have been used as model compounds for the isolation of bacterial degraders and to study pathways of their degradation. Since then, many bacteria capable of metabolizing DBF as a sole carbon source have been isolated including *Sphingomonas* sp. HH69, *Terrabacter* sp. strain YK3, *Pseudomonas* sp. strain CA10, and *Serratia marcescens* (34). Even though these isolates were able to use DBF as a sole carbon source, they were unable to completely metabolize DXN. The isolation of *S. wittichii* RW1 in 1992 revealed for the first time a DBF degrader that can completely metabolize dibenzo-*p*-dioxin and from that time, the actual era for dioxin degradation research began (22). The full genome sequence of *S. wittichii* RW1 shows that it consists of a 5.3 Mbp chromosome in addition to two megaplasmids designated pSWIT01 (310 kb) and pSWIT02 (222 kb), all the genes required for DBF and DXN degradation are thought to be located on pSWIT02, but scattered in different loci (25, 35). The proposed pathway

for DXN and DBF degradation is illustrated in Figure 1 and details regarding the genetics and biochemistry of each enzymatic step are discussed below.

Initial angular dioxygenation

In the first step of the DXN and DBF degradation pathway both compounds are activated by the addition of two atoms of molecular oxygen in the angular position at carbon 4 and 4a to produce an unstable phenolic hemiacetal that spontaneously rearomatizes to the more stable intermediate 2,2',3-trihydroxydiphenylether (2,2',3-THD-ether) and 2,2',3-trihydroxybiphenyl (2,2',3-THB) for DXN and DBF, respectively (22). This step is catalyzed by a three component enzyme system that was purified by Bunz and Cook in 1993 and found to consist of the dibenzofuran 4,4a-dioxygenase (DBFDO), a reductase, and a ferredoxin. Electrons from NADH are carried by the reductase, a monomeric flavoprotein, to the ferredoxin that eventually transports them to DBFDO (36). Two reductases designated RedA1 and RedA2 were isolated from *S. wittichii* RW1 and found to carry electrons from NADH to a ferredoxin and when expressed with DBFDO were capable of producing 2,2',3-THD-ether and 2,2',3-THB from DXN and DBF, respectively (25, 37). The genome sequence of *S. wittichii* RW1 shows that both reductases are not linked with the angular dioxygenase itself, rather *redA2* is located on pSWIT02, 20 kb away from the *dxn* locus and in the opposite orientation, while *redA1* is located on the chromosome (35). The reductase transfers its electrons to the second component of the dioxygenase system, a ferredoxin. Two ferredoxins were identified in *S. wittichii* RW1 and were named Fdx1 (SWIT5088) and Fdx3 (SWIT4893). Both ferredoxins were able to donate electrons to DBFDO. *fdx3* is located on the pSWIT02 megaplasmid in the *dxn* operon along with the genes for the two

subunits of the DBFDO, while *fdx1* is found in a different loci on pSWIT02 (35). Amino acid analysis of the N-terminal end of these ferredoxins showed more similarities to putidaredoxin type ferredoxins. These ferredoxins contain [2Fe-2S] clusters coordinated by four cysteine residues arranged in the pattern Cys-Xaa_5-Cys-Xaa_2-Cys-Xaa_n-Cys and are different from the Rieske type ferredoxins that contain a [2Fe-2S] cluster coordinated by two cysteines and two histidines (38, 39). Due to the unusual electron transport system represented by the flavoprotein reductase (lacks iron-sulfur cofactor) and the putidaredoxin type ferredoxin (not Rieske type), the angular dioxygenase system in *S. wittichii* RW1 is classified as a class-IIA ring-hydroxylating oxygenase according to the Batie et al. classification of oxygenases (36). Electrons from the ferredoxin are transferred to the third component of the system, the oxygenase, a heterotetrameric protein composed of 2α (45Kd) and 2β (23Kd) subunits designated DxnA1 and DxnA2, respectively. Even though the DNA sequence of the N-terminus of the α subunit is distinct from all other known dioxygenases, its overall sequence shows 40% similarities to dioxygenases from class IIB and class III. In addition, consensus sequences for the Rieske-type [2Fe-2S] cluster binding site and the residues Glu200, Asp205, His208, and His213 surrounding the Fe(II) prosthetic group were identified in this subunit with respect to some minor differences surrounding the Fe(II) prosthetic group (25, 36). The locus containing DBFDO was identified by screening a genomic library of *S. wittichii* RW1 with a probe generated by degenerate primers for the N-terminal region of DBFDO and the C-terminal region from the hydrolase. Sequencing of the positive clones showed that DBFDO is linked to two other genes, a HOPDA hydrolase (*dxnB*) and a TonB-dependent transporter (*dxnC*), but not to its electron transport system and that the *meta*

cleavage dioxygenase for the DBF pathway was located on a separate operon upstream of the *dxn* locus and in the opposite orientation (25). Later, the second ferredoxin, Fdx3, involved in DBF oxygenation was found to be the last gene of the *dxn* locus (39). Attempts to express a functional dioxygenase system in *E. coli* have failed when using the genes for the dioxygenase subunits (*dxnA1* and *dxnA2*) alone, which indicate that the class-IIB electron transfer system from *E. coli* is incapable of transferring electrons to this dioxygenase. However, when the electron transfer system from RW1 was expressed with the dioxygenase, DBF and DXN were oxygenated via angular attack to trihydroxybiphenyl and trihydroxydiphenyl ether, respectively (25).

Meta cleavage (extradiol) dioxygenase

In the second step of DBF and DXN degradation pathway, THB and THD-ether formed are *meta* cleaved by DbfB, a *meta* cleavage dioxygenase. Even though it was not possible to identify the structure of the *meta* cleaved product formed from DBF and DXN by NMR or GC-MS, *meta* cleavage was more likely accepted over ortho cleavage due to multiple reasons. First, *S. wittichii* RW1 lacked the ability to utilize or oxidize, 2-(2-hydroxyphenoxy)-muconate, the ortho ring cleavage product from DXN. Second, this pathway was inhibited by the *meta* cleavage inhibitor, 3-chlorocatechol (22). As mentioned above, the gene encoding DbfB is not linked to the initial dioxygenase but rather located 4.5 kb upstream of the *dxn* locus and in the opposite orientation. This gene was isolated from a cosmid library of *S. wittichii* RW1 that had the ability to *meta* cleave the biphenyl intermediate, 2,3-dihydroxybiphenyl (2,3-DHB), to a yellow colored intermediate. Sequence of this fragment showed the presence of a 32 kDa polypeptide that was designated DbfB. Unlike many other *meta* cleavage dioxygenases which have an

oligomeric quaternary structure, DbfB was a monomeric protein that lost most of its activity when purified aerobically (40). There is a conflict about whether DBF and DXN are degraded using the same extradiol dioxygenase based on the kinetics of the DbfB enzyme with different substrates. DbfB had a very low K_m value for 2,3-DHB and 2,2',3-THB compared to the K_m values for catechol, 3-methylcatechol, and 4-methylcatechol (1000-fold lower). However, the activity of this enzyme for 2,2',3-THD-ether was undetectable using standard procedures which made the likelihood of having a second extradiol dioxygenase involved in DXN degradation more acceptable, especially because the genome of *S. wittichii* RW1 possesses 34 different extradiol dioxygenases (24, 40, 41). In order to solve such issues, two separate studies were conducted in *S. wittichii* RW1 based on observing the proteomic changes when growing on DBF and DXN compared to acetate (41, 42). Results of these studies showed the possibility of the involvement of a second extradiol dioxygenase located on the chromosome designated SWIT3046. This enzyme has 31% sequence identity with DbfB and was shown to be more expressed on DXN and chlorinated DXN (2.51X and 3.04X, respectively) than DBF (0.8X) and acetate. In addition, SWIT3046 was the only extradiol dioxygenase out of the 34 others present in *S. wittichii* RW1 that was upregulated on chlorinated and non-chlorinated dioxin. Due to the redundancy of proteins in this bacterium, more research should be conducted to characterize this enzyme and proof its role in DXN and DBF pathway (41).

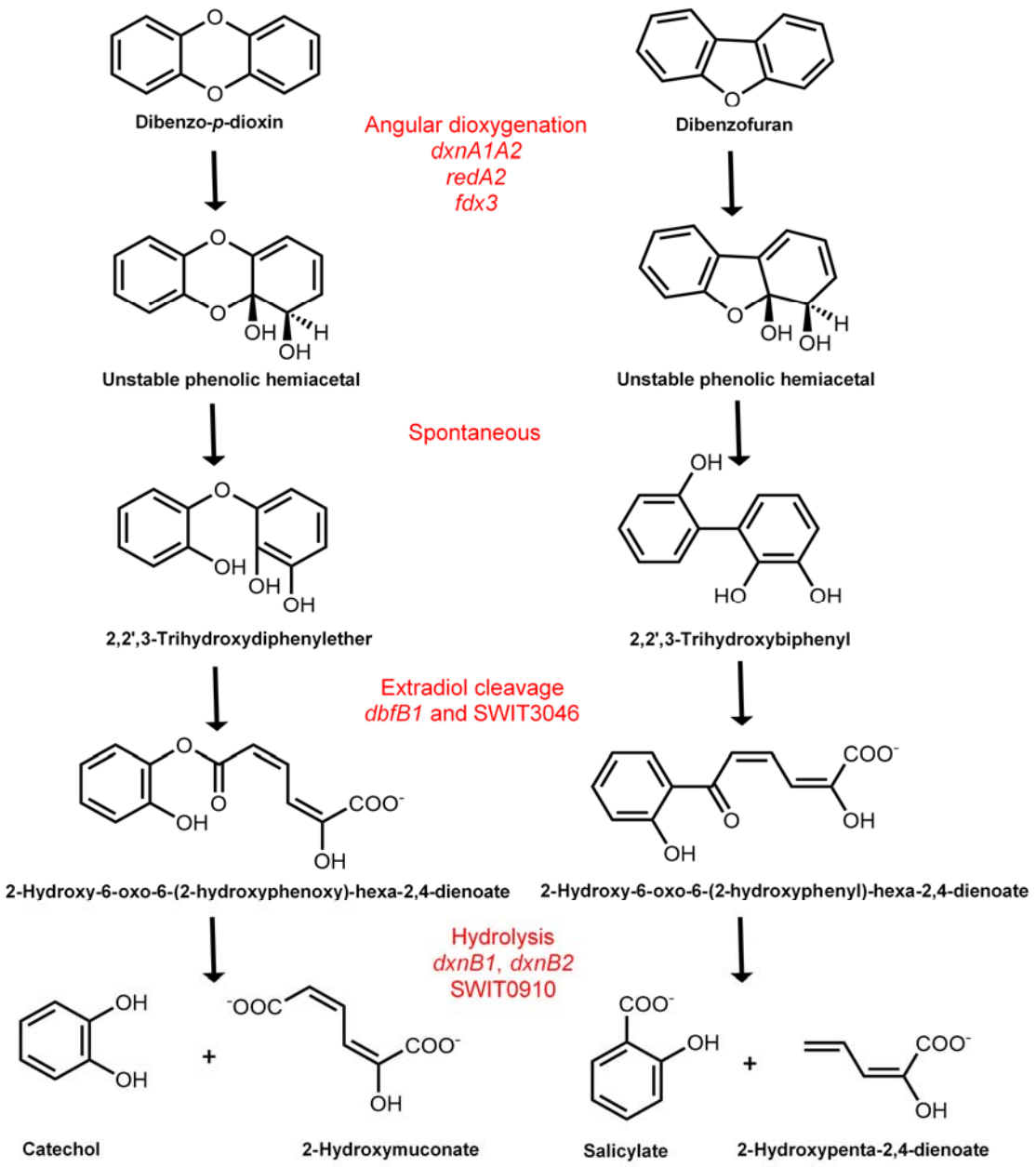

Figure 1. Degradation pathway for dibenzo-*p*-dioxin and dibenzofuran.

Hydrolysis of *meta* cleavage products

The third step of the DBF and DXN degradation pathway involves the hydrolysis of the *meta* cleavage product catalyzed by a hydrolase. Two isofunctional hydrolases designated DxnB1 and DxnB2 were isolated and purified from *S. wittichii* RW1 and were found to be capable of converting 2-hydroxy-6-oxo-6-(2-hydroxyphenyl)hexa-2,4-dienoate (8-OH HOPDA) to salicylate as well as converting the biphenyl intermediate 2-hydroxy-6-oxo-6-phenylhexa-2,4-dienoate (HOPDA) to benzoate. Comparison of N-terminal amino acid sequence showed 50% similarity between both enzymes and according to native and denature gel electrophoresis both proteins were found to be monomeric having a molecular weight of 31 and 29 kDa for DxnB1 and DxnB2, respectively (43). Genes involved in the upper pathway for DBF and DXN degradation are constitutively expressed in *S. wittichii* RW1. This fact was based on the production of salicylate and catechol from acetate growing cells at a level almost similar to those when grown on selected aromatics (22). As seen with the redundancy of extradiol dioxygenases, at least 40 hydrolases were detected in the genome of *S. wittichii* RW1 (41). *dxnB1* is located on the pSWIT02 megaplasmid adjacent to the genes for the DBFDO subunits, *dxnA1* and *dxnA2*, and followed by *dxnC*, a TonB-dependent transporter. The location was determined from sequencing a 5.5 kb *Eco*RI fragment encoding four polypeptides that were all transcribed from one operon. The amino acid sequence of DxnB1 shows similarities with previously characterized 2-hydroxymuconic semialdehyde hydrolases from *Pseudomonas putida* F1 and *Burkholderia sp.* strain LB400 and contained the consensus amino acids Ser_{108}, Asp_{226}, and His_{255} found in the active sites of such enzymes (25).

The second *meta*-cleavage HOPDA hydrolase, DxnB2, was isolated and genetically characterized from *S. wittichii* RW1 using degenerate primers designed based on the N-terminal and C-terminal ends of the purified DxnB. DxnB2 was found to belong to a separate class of MCP hydrolases that was evolutionary divergent from previously characterized BphDs but contained other hydrolases involved in DBF degradation including DxnB from *S. wittichii* RW1 and $CarC_{J3}$ from *Janthinobacterium* sp. strain J3 involved in carbazole and DBF degradation. This hydrolase was capable of transforming 8-OH HOPDA six times faster than HOPDA which makes it more specific for the degradation of DBF. Moreover, DxnB2 was found to be capable of transforming 3-Cl HOPDA and 4-OH HOPDA with a 10-fold higher specificity compared to $BphD_{LB400}$ and $BphD_{P6}$. Another distinguished feature of DxnB2 is its ability to transform multiple chlorinated substitutes of HOPDA such as 8-Cl HOPDA and 9-Cl HOPDA making it a useful candidate for environmental cleanup of PCBs (44). Even though both hydrolases characterized in *S. wittichii* RW1 were not examined for their ability to hydrolyze *meta* cleavage products of DXN, these enzymes are assigned as hydrolases in both the DBF and DXN proposed pathways. Nevertheless, a third HOPDA hydrolase SWIT0910 was detected in *S. wittichii* RW1 by shotgun proteomics that had 29% and 24% sequence identity to DxnB1 and DxnB2, respectively. The highest detection for this hydrolase was on 2-chloro-DXN (1.80X) compared to DBF and acetate (1.11X for both). Similarity in sequence identity between these three hydrolases with differentiation in expression levels to different substrates led researchers to hypothesize that these enzymes have similar substrate ranges but different specificities to different chlorinated aromatics. Such

redundancy in hydrolases might explain why *S. wittichii* RW1 can transform different chlorinated dioxin congeners (41).

Lower pathways for DBF and DXN degradation

For *S. wittichii* RW1 to make living on the skeleton backbone of DBF and DXN, salicylate and catechol are produced, respectively, from the upper pathway of these aromatics as well as the aliphatic tails from HOPDA cleavage. These single ring aromatics are degraded through multiple enzymatic steps in separate pathways to yield TCA cycle intermediates that eventually fuel the TCA cycle to generate carbon and energy to be used for synthesizing building blocks required for life (22, 45).

Catechol is considered a common intermediate from the degradation pathways of several aromatic hydrocarbons including benzoate, phenol, benzene, and salicylate. Degradation of catechol occurs through two pathways: the ortho cleavage pathway catalyzed by catechol 1,2-dioxygenase and the *meta* cleavage pathway catalyzed by catechol 2,3-dioxygenase (46). In *S. wittichii* RW1, catechol degradation is thought to proceed through *meta* cleavage (45) which was inferred from the ability of 2,2',3-trihydroxybiphenyl dioxygenase, DbfB, to *meta* cleave catechol in addition to its own specific substrate (40, 45). However, ortho cleavage activity of catechol 1,2-dioxygenase was also detected from *S. wittichii* RW1 growing cultures on DXN, DBF, and acetate, indicating constitutive expression of this pathway (22). A recent transcriptomic study on *S. wittichii* RW1 showed that the ortho cleavage pathway for catechol was differentially induced when this bacterium was grown on DXN. Data analysis from the same study helped in identifying the responsible genes involved in each step according to their expression levels on DXN. Multiple enzymatic steps convert catechol to succinyl CoA,

an intermediate from the TCA cycle, as shown in Figure 2. Genetic characterization of these genes is required to confirm their role in catechol metabolism (24).

Salicylate is a monocyclic aromatic hydrocarbon generated as an intermediate from the naphthalene and DBF degradation pathways (22, 47). Degradation of salicylate has been well studied in gram negative bacteria and depending on the type of enzymes present, salicylate can be degraded through two distinct routes. The first route is catalyzed by salicylate hydroxylase that converts salicylate to catechol, while the second is catalyzed by salicylate-5-monooxygenase that converts salicylate to gentisate (48). A full pathway for the degradation of 4-hydroxysalicylate has been characterized in *S. wittichii* RW1. This pathway was located downstream of the *dxn* region on pSWIT02 and was found to include a 4-hydroxysalicylate hydroxylase designated *dxnD*. Heterologous expression of this gene in *E. coli* produced a 72 kDa polypeptide that only had activity against 4-hydroxysalicylate and not to phenol, 2-hydroxybiphenyl, 2,2'-dihydroxybiphenyl, 2,3-dihydroxybiphenyl, 4-hydroxybenzoate, and salicylate (45). Even though the exact pathway for salicylate degradation in *S. wittichii* RW1 has not been confirmed so far, multiple genes annotated as salicylate oxygenases were upregulated in *S. wittichii* RW1 when grow on salicylate or DBF (41). These up regulated genes included the multicomponent oxygenase SWIT3056 that is annotated as a salicylate hydroxylase and is responsible for the conversion of salicylate to catechol. A second multicomponent plasmid-located gene designated SWIT5101 and SWIT5102 (gentisate 1,2 dioxygenase) was upregulated on salicylate and DBF as well. However, both of these genes did not respond immediately when exposed to DBF for short exposure periods (30 minutes). On the other hand, the same study detected a different set of putative

dioxygenases that responded to such exposure. One dioxygenase of interest was SWIT3086, a putative gentisate 1,2-dioxygenase, which infers that salicylate might take the gentisate pathway for its degradation. For that reason, whether salicylate degradation in *S. wittichii* RW1 goes through catechol, gentisate, or both is still unknown (23).

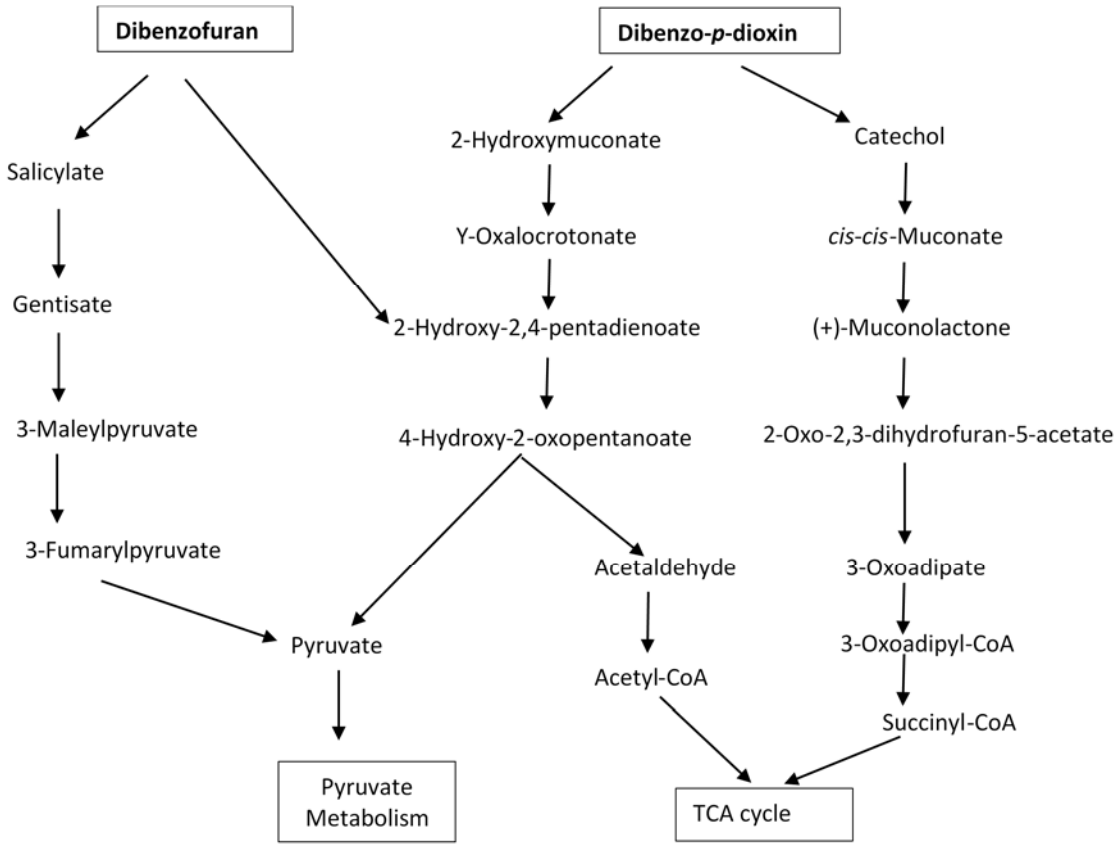

Figure 2. Lower pathway for DBF and DXN degradation in *S. wittichii* RW1.

Aerobic degradation of biphenyl

The biphenyl degradation pathway has been extensively studied in both gram positive and gram negative bacteria as an analog for studying the degradation of polychlorinated biphenyls (PCBs) (49, 50). The upper pathway for biphenyl degradation (Figure 3) consists of four steps which convert biphenyl to benzoate and 2-hydroxypenta 2,4-dienoate (51). The first step of the pathway is catalyzed by biphenyl dioxygenase, a heterohexamer composed of two subunits (BphA1 and BphA2) arranged as $\alpha_3\beta_3$, responsible for activating an oxygen molecule and adding it to the biphenyl structure at carbon 2 and 3 to yield *cis*-2,3-dihydro-2,3-dihydroxybiphenyl. As seen with DBFDO, biphenyl dioxygenase is a three component enzyme system that requires a ferredoxin (BphA3) and a reductase (BphA4) to carry electrons from NADH to reduce the enzyme (52). Substrate specificity is carried out by the BphA1 subunit which contains a Rieske type center [2Fe-2S] involved in electron transport (53). Biphenyl dioxygenases have been shown to have a range in their capabilities in oxygenating different aromatics including DBF and DXN, but no biphenyl degrading organisms were able to use these compounds as the sole source for carbon and energy (54, 55). Unlike how DBFDO catalyzes angular dioxygenation of DBF and DXN, biphenyl dioxygenase performs lateral dioxygenation towards DBF and DXN producing dead end products which prevent biphenyl degraders from fully metabolizing these compounds (56). In addition, biphenyl dioxygenases were found capable of oxygenating different congeners of PCBs at different capabilities depending on amino acid sequence differences between these dioxygenases (57).

The second step in biphenyl degradation pathway is catalyzed by biphenyl *cis*-dihydrodiol dehydrogenase (BphB) that catalyzes the oxidation of *cis*-2,3-dihydro-2,3-dihydroxybiphenyl to 2,3-dihydroxybiphenyl (58). These dehydrogenases were reported to be involved in the oxidation of different *cis*-dihydrodiols other than *cis*-biphenyl dihydrodiol such as dihydrodiols of naphthalene, phenanthrene, DBF, and DXN. Mutants of *bphB* (B8/36) in *Sphingobium yanoikuyae* B1 were extremely important in studying the substrate range of biphenyl dioxygenase in this strain (31).

In the following step, 2,3-dihydroxybiphenyl is subjected to *meta* cleavage by 2,3-dihydroxybiphenyl 1,2-dioxygenase (BphC). This enzyme uses non-heme iron to cleave the aromatic ring adjacent to the hydroxyl substituents to produce HOPDA. Multiple dihydroxybiphenyl 1,2-dioxygenases have been characterized and were found to be capable of cleaving some PCB intermediates at orders of specificities in some cases higher than that for 2,3-dihydroxybiphenyl, while failing to cleave others. For instance, BphC from the PCB degrader *Burkholderia* sp. strain LB400 is inhibited by 2,6-dichloro-2,3-dihydroxybiphenyl as well as by the *meta* cleavage inhibitor 3-chlorocatechol (59).

In the final step of the upper pathway for biphenyl degradation the C-C bond in HOPDA is hydrolyzed via HOPDA hydrolase to benzoate and 2-hydroxypenta-2,4-dienoate. This step is carried out by an α/β-fold serine hydrolase designated BphD and is considered a key determinant in the biphenyl pathway (60). Similarly to extradiol dioxygenases, HOPDA hydrolases possess a range in specificity towards chlorinated substrates showing preference in the order non > *ortho* > *meta* > *para* substituted congeners (61). Hydrolases are more efficient at hydrolyzing HOPDA chlorinated on the phenyl moiety compared to HOPDA chlorinated on the dienoate moiety (62).

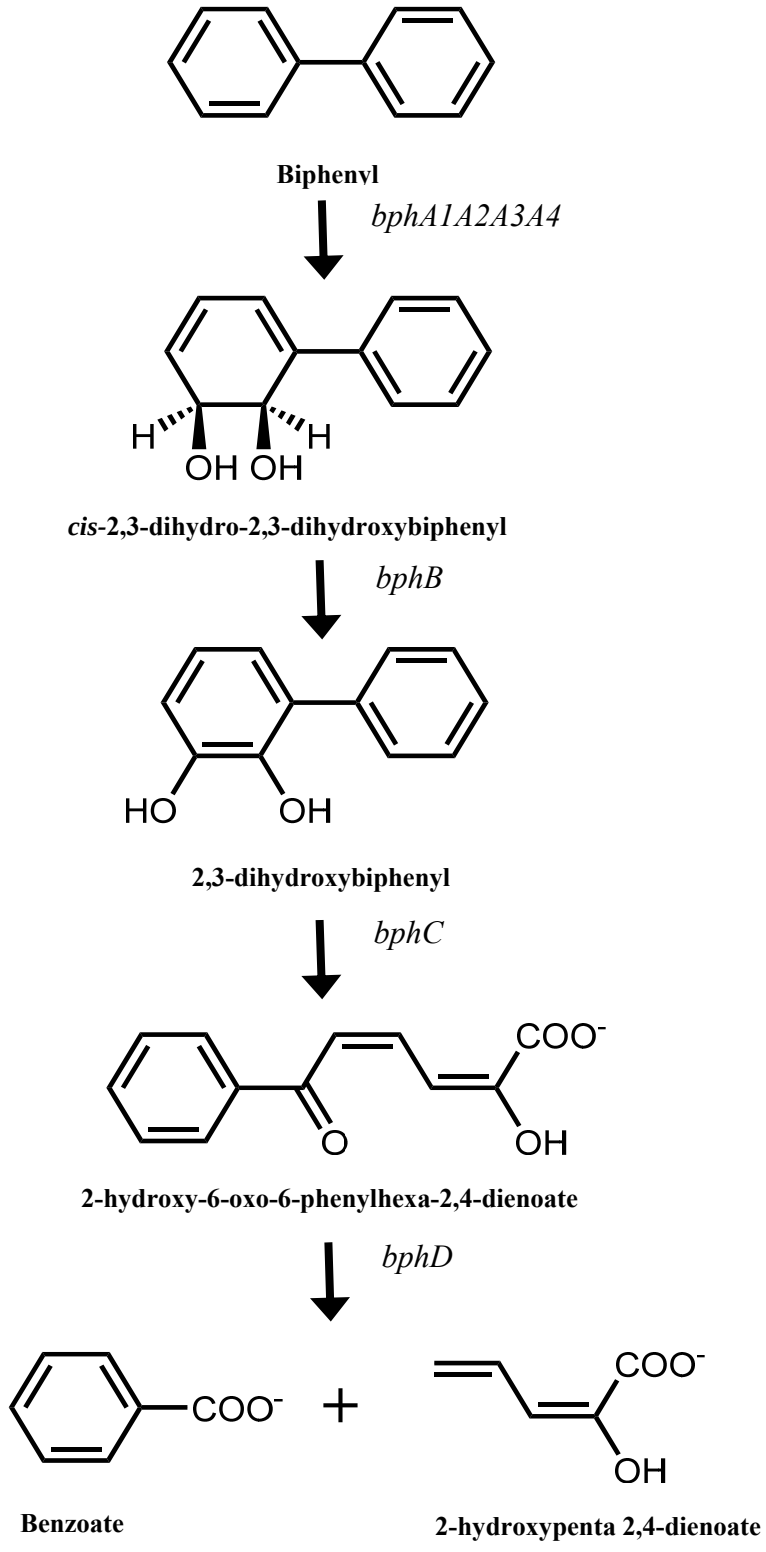

Figure 3. Pathway for biphenyl degradation in bacteria.

Chapter 2: Substrate Specificity of *Sphingomonas wittichii* RW1 Dibenzofuran 4,4a-Dioxygenase

Introduction

Sphingomonas wittichii RW1 was the first strain isolated for its unique ability to use both dibenzo-*p*-dioxin (DXN) and dibenzofuran (DBF) as sole sources of carbon and energy for growth (22). The ability to grow on DBF but not DXN is more widespread and is found in both gram negative and gram positive organisms. Many of these organisms can cometabolize DXN during or after growth on DBF. The genetics underlining the ability of *S. wittichii* RW1 to metabolize both DXN and DBF have been extensively studied including a completed genome sequence (35), cloning of many of the pathway genes (25), and transcriptomic (23, 24) and proteomic studies (41).

The first enzymatic step in DXN and DBF degradation is catalyzed by an angular dioxygenase, dibenzofuran 4,4a-dioxygenase (DBFDO), a three component enzyme system that catalyzes the conversion of DBF and DXN to unstable hemiacetals that rearomatize to 2,2',3-trihydroxybiphenyl and 2,2',3-trihydroxydiphenyl ether, respectively. The three components of DBFDO have been purified and characterized (36) with the discovery that while there is a single common terminal oxygenase component for DXN and DBF oxidation there are two interchangeable reductases (36) and two interchangeable ferredoxins (38, 39) in the electron chain. The genes encoding the terminal oxygenase component, *dxnA1A2*; both of the ferredoxins, *fdx1* and *fdx3*; and one of the reductases, *redA2*, are located in three different places on the large megaplasmid pSWIT02 while the gene encoding the second reductase, *redA1*, is located

on the chromosome. "Scattering" of genes encoding a single catabolic pathway is quite common among the Sphingomonads (25, 63, 64).

Many bacterial multicomponent aromatic dioxygenases have broad substrate ranges and can oxidize many related (and unrelated) hydrocarbons that are not substrates for the cognate metabolic pathway (65). One example among the angular dioxygenases is the carbazole 1,9a dioxygenase of *Pseudomonas* sp. strain CA10 (CARDO) that has angular dioxygenase activity towards carbazole (CAR), DBF, DXN, xanthene and phenoxanthiin and lateral dioxygenase activity towards naphthalene, biphenyl, fluoranthene, anthracene, and phenanthrene. CARDO also catalyzed the monooxygenation of the benzylic methylenic group in fluorene and the sulfur heteroatom in dibenzothiophene (66). The angular dioxygenase from *Sphingomonas* sp. strain LB126 was found to contribute at least twice in the degradation of fluorene, once by the initial monooxygenation of the benzylic methylenic group to form 9-hydroxyfluorene and secondly by the angular attack of 9-fluorenone, the dehydrated product of 9-hydroxyfluorene, to produce 1-hydro-1,1a-dihydroxy-9-fluorenone. This enzyme was also found to perform angular dioxygenation towards DBF and DXN besides *cis* dihydroxylation to other polycyclic aromatic hydrocarbons (67).

Even though *S. wittichii* RW1 has been extensively studied, the ability of its angular dioxygenase to attack different aromatic compounds is still ambiguous. In an earlier study, the ability of purified DBFDO to oxygenate different aromatic compounds was predicted from oxygen consumption followed by HPLC to confirm that a product was made (36). In some cases oxygen consumption by the enzyme did not result in a product and in many cases the identity of the reaction product was not determined (36).

Due to the importance of *S. wittichii* RW1 as a model organism for dioxin degradation and to gain more knowledge about substrate recognition by RW1 DBFDO, we initiated the current work to identify the exact chemical structures of the oxygenated products generated by DBFDO from several polycyclic and heterocyclic aromatic hydrocarbons.

Materials and Methods

Bacterial strains, plasmids, and culture conditions

Escherichia coli DH5α [F^-φ80*lac*ZΔM15 Δ(*lac*ZYA-*arg*F) U169 *rec*A1 *end*A1 *hsd*R17 (r_k^- , m_k^+) *pho*A *sup*E44 thi-1 *gyr*A96 *rel*A1 λ^-] was obtained from Invitrogen (Waltham, Massachusetts) and used as the recipient in transformation experiments. *E. coli* BL21(DE3) was used for gene expression analysis. PCR amplicons were cloned into the pGEM-T easy vector (Promega, Madison, WI) while the pET-30a expression vector (Novagen, Darmstadt, Germany) was used to direct the expression of the dioxygenase system under the control of the strong bacteriophage T7 promoter. Luria-Bertani (LB) broth and agar were used as a complete medium for *E. coli* growth. Kanamycin was added at 50 µg/ml and ampicillin was added at 100 µg/ml when needed. *S. wittichii* RW1 was incubated at 30°C while 37°C was used for *E. coli*.

DNA manipulations and molecular techniques

Genomic DNA was extracted from pure colonies of *S. wittichii* RW1 using the Ultraclean microbial DNA isolation kit and following the recommendations of the manufacturer (MoBio, Carlsbad, CA). Plasmid DNA was purified from *E. coli* cells using Nucleospin plasmid purification kit (Macherey-Nagel, Germany) and following the protocol supplied. Restriction enzyme digestion, ligation, transformation, and gel

electrophoresis were performed using standard methods (68). The Phusion high fidelity PCR kit (New England Biolabs) was used to amplify all DNA fragments used in this study and the Geneclean III kit (MP Biomedicals, Ohio, USA) was used to purify DNA fragments from PCR solutions or agarose gels. All PCR product clones were verified by sequencing (Genewiz, New Jersey, USA).

Construction of the DBFDO expression clone

Genomic DNA from RW1 was used as a template to amplify the *dxnA1A2*, *fdx3*, and *redA2* genes. Since the four genes are not contiguous in the genome, multiple PCR steps were involved to construct the expression clone. The genes (*dxnA1A2*) for the two terminal oxygenase subunits were PCR amplified as a single fragment (1.87 kb) using the primers dxnA1-F (5'-GGGTCTAGAGGATGCAGGAGAGGTTGCATGG-3') and dxnA2-R (5'- CCCGCGGCCGTTACAGGAAGGTTGAGATGCC-3') introducing *Xba*I and *Not*I sites, respectively. The gene for the ferredoxin component (*fdx3*) was PCR amplified (0.35 kb) using the primers fdx3-F (5'-GGGGCGGCCGCCGGATGGGAGATAATAGTGATGC-3') and fdx3-R (5'-CCCGGGCCCTCAATCAAGATTGTTGGACACC-3') introducing *Not*I and *Apa*I sites, respectively. The gene for the reductase component (*redA2*) was PCR amplified (1.28 kb) using the RedA2-F (5'-GGGGGGCCCGAGAAGGAAAGTAGGATGAGATCAGCGG-3') and RedA2-R (5'-CCCAGATCTTAGACCGGGATCAGATCCTTAAGC-3'). In this case the rare start codon, GTG, of *redA2* was replaced with an ATG and restriction sites for *Apa*I and *Bgl*ll were introduced. The three fragments were cloned separately into the pGEM-T Easy vector and sequenced to verify that no changes were introduced by PCR. Each clone was

digested by the restriction enzymes whose cutting sites were included in the PCR primers, the appropriate fragment excised from an agarose gel, and the three fragments were cloned together into the *Xba*I and *BglI*I sites of pET-30A to produce pET_DBFDOS.

Biotransformation of aromatic compounds and HPLC analysis

BL21(DE3) cells harboring pET_DBFDOS growing on LB plates supplemented with 50 µg/ml kanamycin were subcultured into 50 ml LB broth and incubated for 16 hours. This culture was used to inoculate (at 2% by volume) 100 ml of LB broth, which was incubated at 37°C with shaking (180 rpm) until the OD_{600} reached 0.5. At that point, IPTG (isopropyl-β-D-thiogalactopyranoside) was added at a final concentration of 1 mM and the culture was incubated for another 2 hours. Cells were pelleted and washed twice with half the volume of phosphate buffer (50 mM sodium-potassium phosphate buffer, pH 6.8). Cells were resuspended in phosphate buffer plus 20 mM glucose and 3 mM of the aromatic compound tested and incubated at 30°C for 24 hours. BL21(DE3) with the cloning vector pET-30a was processed in a similar fashion as a negative control.

Samples from the supernatant of both BL21(pET_DBFDOS) and BL21(pET-30a) were filtered and analyzed with a Beckman (CA, USA) liquid chromatography system. A reverse phase C_{18} column (4.6mm by 25mm) and a gradient of 0-100% methanol in water under acidic conditions (0.1% acetic acid) and a flow rate of 1 ml/min was used to analyze the oxygenated intermediates. Detection of any peaks was monitored at both 254 nm and 280 nm wavelength.

Analysis by GC-MS

The aqueous phase from samples that showed positive results on the HPLC were extracted by ethyl acetate as described elsewhere (67). One milliliter of each extracted sample was mixed with 50 µl of Sylon BFT reagent (BSTFA+TMCS, 99:1) and incubated for 1 hour at 80°C for derivatization. GC-MS analysis was conducted using a Varian 3400 GC directly interfaced to a Thermo-Finnigan TSQ-7000 triple stage quadrupole mass spectrometer equipped with an Xcalibur data system. The GC capillary column was a 30 meter × 0.32 mm I.D. Guardian-ZB-5MS (Phenomonex) (5% phenyl, poly-dimethylphenylsiloxane) with a 0.25 µm film thickness. Injection volume was 1 µl, while the injection temperature was 300°C (splitless mode with a 100:1 split activated 0.5 min post-injection to serve as a septum purge). The GC column temperature was programmed for 50°C (hold 3 min) to 320°C at a rate of 10°C/min with a 10 min hold at the upper limit. The upper limit was occasionally extended to 340°C for samples containing high boiling migrants. The GC-MS transfer line temperature was 320°C (or 340°C). The TSQ-7000 mass spectrometer was operated in EI mode (70 eV) scanning masses 35-750 m/z once each second. For data management, total ion current (TIC) chromatograms were integrated with the system software and the peak list and area integration values were pasted into spreadsheet-based templates.

Analysis by NMR

Silica gel column chromatography was carried out as follows: The sample was loaded onto a column of silica gel (17 mm [inside diameter] by 20 cm) and eluted with hexanes/EtOAc/HCOOH (69/30/1 or 29/70/1, v/v/v). After analytical TLC, the eluates

containing the products were combined and used for NMR analysis. TLC analysis was performed with hexanes/EtOAc/HCOOH 69:30:1 or 29/70/1, v/v/v.

^{1}H NMR spectra were measured on a Varian VNMRS-400 MHz or a Varian VNMRS-500 MHz instrument at 25°C using residual protonated solvent as internal standard ($CHCl_3$ 7.26 ppm). Resonance assignments were performed using ^{1}H-^{1}H gCOSY and ^{1}H-^{1}H NOESY spectra. NMR spectra were analyzed using Mnova software (Mestrelab Research, S.L., Escondido, CA).

Results

Overview. A functional RW1 DBFDO was produced by the pET-DBFDOS. Three types of oxygenations were detected: angular dioxygenation towards DBF, DXN, 2-hydroxy-DBF, xanthene, and xanthone; *cis*-dihydroxylation towards biphenyl, phenanthrene, anthracene, xanthone; and monooxygenation of the benzylic methylenic group in fluorene as well as monooxygenation and dioxygenation to the sulfur heteroatom in dibenzothiophene. All products were initially detected by the presence of a major HPLC peak(s) from induced cultures of BL21(pET-DBFDOS) and were absent in the BL21(pET-30a) controls. Molecular weights and structures of the intermediates formed were then confirmed by GC-MS (Table 1) and NMR analysis (Table 2). No oxygenated products were detected for carbazole, anthrone, pyrene, chrysene, naphthalene, diphenylmethane, diphenylether, salicylate, and toluene. Structures of the substrates and products are shown in Figure 4. Details for GC-MS and NMR results for each substrate are summarized below and the full data is in the Appendix.

Dibenzofuran: A single peak was seen from the oxygenation of DBF. The TMS derivative for this intermediate had a molecular ion peak at m/z 418 suggesting angular

dioxygenation of DBF. ^{1}H NMR, COSY, and NOESY spectra identified the structure as 2,2',3-trihydroxybiphenyl.

Dibenzo-*p*-dioxin: Based on the GC-MS analysis, DXN was shown to be converted to a single product. The TMS derivative for this product indicated a molecular ion peak at m/z 434 suggesting the presence of three hydroxyl groups due to angular dioxygenation of DXN. ^{1}H NMR, gCOSY, and NOESY analysis identified the intermediate formed from dioxin oxygenation to be 2,2',3-trihydroxydiphenylether.

2-Hydroxydibenzofuran: GC-MS analysis for 2-hydroxy-DBF identified a TMS derivative with a molecular ion peak at m/z 506 suggesting angular dioxygenation for this compound. The structure detected by ^{1}H NMR and gCOSY was 2,2',3,5-tetrahydroxybiphenyl showing the position of the oxygenation to be on the benzene ring that initially contained the hydroxyl group and not the other, unsubstituted, ring.

Xanthene: The GC-MS results from xanthene revealed the presence of a single molecular ion peak at m/z 432. This suggests angular dioxygenation of xanthene on the carbon atoms adjacent to the oxygen and not to the methylenic carbon atom. Our prediction for this angular dioxygenation was proven by ^{1}H NMR and gCOSY identifying the product as 2,2',3-trihydroxybiphenylmethane.

Xanthone: The oxygenation of xanthone yielded two different products that were clearly detected by HPLC. Results from GC-MS identified two different molecular ion peaks, one at m/z 374 that corresponds to a *cis*-hydroxylated product of xanthone, while the second had a molecular ion peak at m/z 446 which suggested an angular attack of xanthone leading to 2,2',3-trihydroxybenzophenone. Both intermediates were identified by ^{1}H NMR, gCOSY, and NOESY analysis which indicates the ability of DBFDO to

perform both angular and lateral dioxygenation towards xanthone producing 2,2',3-triydroxybenzophenone and *cis*-3,4-dihydroxy-3,4-dihydroxanthone, respectively.

Biphenyl: The GC-MS analysis for biphenyl showed a single molecular ion peak at m/z 332. The intermediate that matches this molecular weight could be a *cis*-hydroxylated product of biphenyl. ^{1}H NMR, gCOSY, and NOESY spectra revealed the structure to be *cis*-2,3-dihydro-2,3-dihydroxybiphenyl, indicating the ability of the DBFDO angular dioxygenase to perform lateral oxygenation of biphenyl.

Phenanthrene: A single peak from the oxygenation of phenanthrene was identified from the analysis of the GC-MS results. The TMS derivative for this intermediate had a molecular ion peak at m/z 356 suggesting a lateral dioxygenation of phenanthrene and the formation of a *cis*-dihydrodiol product. Unlike all other known gram negative polycyclic dioxygenases, ^{1}H NMR, gCOSY, and NOESY spectra identified that the angular dioxygenase from RW1 performs lateral dioxygenation of phenanthrene at carbon atom number 9 and 10 and not carbon atoms 3 and 4. The only known dioxygenase that perform this type of dioxygenation is the angular dioxygenase of the gram positive bacteria *Mycobacterium* sp. strain PYR (69).

Anthracene: Dioxygenation of anthracene produced a single product with a TMS derivative at m/z 356. The structure of the oxygenated product was detected by ^{1}H NMR and showed that DBFDO attacked anthracene at carbon atom 1 and 2 producing *cis*-1,2-dihydroxy-1,2-dihydroanthracene.

Dibenzothiophene: Based on our HPLC results, we expected to have two different products from the oxygenation of dibenzothiophene. GC-MS analysis revealed the products to be dibenzothiophene sulfone (m/z 216) and dibenzothiophene sulfoxide

(m/z 200). NMR analysis using ^{1}H NMR and gCOSY, confirmed the structure of both products and identified the ability of DBFDO to perform either two successive monooxygenation attacks or both a monooxygenation and a dioxygenation attack of the sulfur atom in dibenzothiophene.

Fluorene: GC-MS results suggested that DBFDO performs monooxygenation to fluorene as the TMS derivative for the detected intermediate had a molecular ion peak at m/z 254 while no peaks for other oxygenated products were detected. ^{1}H NMR and gCOSY confirmed the final structure for this product to be 9-hydroxyfluorene which indicates that DBFDO performs monooxygenation of the benzylic methylenic group in fluorene.

Discussion

The results obtained from this study definitively identifies that *S. wittichii* RW1 DBFDOS catalyzes the angular dioxygenation of DBF and DXN producing the ring-opened compounds 2,2',3-trihydroxybiphenyl and 2,2',3-trihydroxydiphenylether respectively. This is contrary to certain lateral dioxygenases which attack on the side of the moiety producing *cis*-1,2-dihydroxy-1,2-dihydrodibenzo-*p*-dioxin (56). In the extensive substrate range study presented here many interesting substrate oxidations were observed. In addition to the angular dioxygenation of xanthene, xanthone, and 2-hydroxy-DBF oxidation to a *cis*-dihydrodiol was observed for biphenyl, phenanthrene, anthracene, and xanthone and single oxidations were observed for fluorene and dibenzothiophene. The DBFDOS enzyme was not able to oxidize carbazole, anthrone, pyrene, chrysene, naphthalene, diphenylmethane, diphenylether, salicylate, or toluene This substrate range emphasizes the importance of the compound structure, including the

oxygen atom, in orienting the aromatic compound in the active site of DBFDOS. Different accommodations of the compound in the active site lead to different types of oxygenation as seen with the structurally related compounds DBF, dibenzothiophene, fluorene, and carbazole. No oxidation was seen with carbazole while dibenzothiophene and fluorene were oxidized on the sulfur or methylenic moieties respectively. The importance of the bridging oxygen atom is even more apparent when comparing the ability of the enzyme to oxidize DXN, xanthene, xanthone, and anthrone. DXN has two bridging oxygen atoms between the two aromatic rings while xanthene replaces one of these oxygens with a carbon atom. Both substrates are efficiently oxidized in an angular fashion. Xanthone substitutes a ketone for the bridging carbon atom in xanthone and now two oxidation products are observed: one at the angular position and one at the lateral position. Finally, anthrone, which differs from xanthone by not having any bridging oxygen atoms, is not oxidized at all.

The angular dioxygenase activity of DBFDOS resembles the activity of the angular dioxygenase of the fluorene degrading *Sphingomonas* sp. strain LB126 except for its activity towards fluorene, naphthalene, and carbazole. On the other hand, DBFDOS shows similar angular attacks for DBF, DXN, and xanthene to the carbazole degrading angular dioxygenase CARDO from *Pseudomonas* sp. strain CA10 except for carbazole angular dioxygenation (66). Xanthone was attacked by RW1 DBFDOS at both the angular and lateral positions while xanthone is known to be a growth substrate for *Arthrobacter* sp. strain GFB100 through lateral oxidation (70).

In addition to angular dioxygenation, DBFDO performed *cis* dihydroxylation to biphenyl, anthracene, xanthone, and phenanthrene while it failed to oxidize naphthalene,

diphenylmethane, diphenylether, chrysene, and pyrene. It is interesting to note that the *Pseudomonas* sp. strain CA10 and *Sphingomonas* sp. strain LB126 angular dioxygenases can perform lateral attacks on both biphenyl and naphthalene while RW1 DBFDO oxidized biphenyl but not naphthalene. These results suggest that the RW1 DBFDO active site is different from the two other angular dioxygenases. Phenanthrene was oxidized by DBFDO to produce the unusual product 9,10-dihydroxy-9,10-dihydrophenanthrene and not 3,4-dihydroxy-3,4-dihydrophenanthrene. This unusual type of oxygenation was reported previously in three gram positive strains, *Streptomyces flavovirens*, *Mycobacetrium* sp. strain PYR-1, and *Nocardia otitidiscaviarum* strain TSH1 (69, 71, 72).

Bunz and Cook (36) purified RW1 DBFDOS and examined its substrate range by measuring rates by oxygen consumption and then used simple HPLC to detect if a product were made. Their data matches ours for the substrates DXN, DBF, xanthene, dibenzothiophene, biphenyl, carbazole, anthrone, and naphthalene. Our results differ in that Bunz and Cook did not detect a product from xanthone or fluorene while we did (but they did detect DBFDOS oxygen uptke with these substrates). Interestingly, Bunz and Cook measured significant enzyme activity as measured by oxygen consumption against anthrone but neither we nor they observed a product of the reaction. Uncoupling of oxygen consumption from substrate oxidation is a well-known phenomenon in aromatic oxygenases and illustrates the importance of observing an enzymatic product in addition to measuring dioxygenase enzyme activity.

The ability of DBFDO to oxygenate different substrates that RW1 itself cannot grow on and its ability to perform multiple types of oxygenations, identifies the broad

substrate range of this enzyme and raises a question regarding the ability of its ring cleavage dioxygenases and hydrolases to perform similar reactions to multiple aromatics besides DBF and DXN metabolites. Our results also suggest that the aromatics tested interact with the active site of DBFDOS having the heteroatom facing the active site, no oxygenation occurred at the opposite position. In addition, the presence of oxygen as a heteroatom led to angular dioxygenation and when substituted with sulfur or a benzylic methylenic group led to monooxygenation, but when nitrogen was present all types of oxygenations was abolished.

Table 1. Physical properties of intermediates formed by DBFDO.

No products were detected from the substrates carbazole, anthrone, pyrene, chrysene, naphthalene, diphenylmethane, diphenylether, salicylate, and toluene.

Substrate	R_f on TLC	GC-MS Retention Time (min)	MS Principle ions and relative abundance (% base peak)	Predicted structure
Dibenzo-*p*-dioxin	0.27	20.5	434(100), 331(80), 73(28), 419(13)	2,2',3-trihydroxydiphenyl ether
Dibenzofuran	0.21	19.5	315(100), 418(93), 73(26), 412(10)	2,2',3-trihydroxybiphenyl
2-Hydroxy-dibenzofuran	0.10	21.3	506(100), 403(18), 491(10), 147(4)	2,2',3,5-tetrahydroxybiphenyl
Xanthene	0.24	21.4	432(100), 329(36), 423(27), 179(8)	2,2',3-trihydroxy-diphenylmethane
Xanthone	0.16	21.7	193(100), 73(14), 446(8), 239(7), 151(5)	2,2',3-trihydroxybenzophenone
	0.26	22.2	374(100), 269(63), 345(31), 257(22)	*cis*-3,4-dihydroxy-3,4-dihydroxanthone
Dibenzothiophene	0.12	20.6	216(100), 187(43), 168(32), 139(32), 160(24),	dibenzothiophene sulfone
	0.30	20.7	184(100), 171(73), 200(55), 139(46), 152(13)	dibenzothiophene sulfoxide
Fluorene	0.43	17.3	165(100), 254(79), 239(17), 119(4)	9-hydroxyfluorene
Phenanthrene	0.12	19.7	147(100), 251(93), 165(47), 266(44), 356(42)	*cis*-9,10-dihydroxy-9,10-dihydrophenathrene

Anthracene	0.49	21.1	191(100), 253(94), 356(34), 266(25), 147(26)	*cis*-1,2-dihydroxy-1,2-dihydroanthracene
Biphenyl	0.48	17.5	332(100), 243(13), 211(11), 147(7)	*cis*-2,3-dihydroxy-2,3-dihydrobiphenyl

Table 2. NMR analysis of intermediates formed by DBFDO.

Determined at 500 MHz ^{1}H Larmor frequency in $CDCl_3$ at 25°C. Chemical shift multiplicities are abbreviated as: s, singlet; d. doublet; t, triplet; m, multiplet; dd, doublet of doublets; td, triplet of doublets; ddd, doublet of doublet of doublets.

Substrate	^{1}H Chemical Shifts (δ)	Identification
Dibenzo-*p*-dioxin	7.06 (H-6', dd, *J* = 8.1, 1.6 Hz, 1H), 7.05–7.03 (H-5', m, 1H), 6.88 (H-3', dd, *J* = 7.6, 1.0 Hz, 1H), 6.84 (H-4', ddd, *J* = 9.8, 6.8, 3.8 Hz, 1H), 6.77–6.72 (H-4,6, m, 2H), 6.48–6.42 (H-5, m, 1H), 5.60 (OH, s, 3H).	2,2',3-trihydroxydiphenyl ether
Dibenzofuran	7.33 (H-6', dd, *J* = 7.5, 1.7 Hz, 1H), 7.33–7.30 (H-4', m, 1H), 7.07 (H-5', td, *J* = 7.5, 1.1 Hz, 1H), 7.02 (H-3', dd, *J* = 8.5, 1.1 Hz, 1H), 6.98 (H-4, dd, *J* = 8.0, 2.3 Hz, 1H), 6.97–6.93 (H-5, m, 1H), 6.85 (H-6, dd, *J* = 7.1, 2.3 Hz, 1H). 5.82 (OH, s, 3H).	2,2',3-trihydroxybiphenyl
2-Hydroxy-dibenzofuran	7.34–7.30 (H-4', m, 1H), 7.31 (H-6', d, *J* = 6.9 Hz, 1H), 7.09–7.05 (H-5', m, 1H), 7.01–6.99 (H-3', m, 1H), 6.54 (H-6, d, *J* = 2.9 Hz, 1H), 6.32 (H-4, d, *J* = 2.9 Hz, 1H), 5.73 (OH, s, 1H), 5.61 (OH, s, 1H), 5.46 (OH, s, 1H), 4.47 (OH, s, 1H).	2,2',3,5-tetrahydroxybiphenyl
Xanthene	7.28 (H-6', d, *J* = 7.6 Hz, 1H), 7.11 (H-4', t, *J* = 7.6 Hz, 1H), 6.91 (H-5', t, *J* = 7.4 Hz, 1H), 6.82 (H-5, dd, *J* = 6.5, 3.2 Hz, 1H), 6.80 (H-3', d, *J* = 7.5 Hz, 1H), 6.75 (H-6, d, *J* = 6.2 Hz, 1H), 6.74 (H-4, d, *J* = 3.2 Hz, 1H), 3.92 (CH_2, s, 2H), 1.58 (OH, s, 3H).	2,2',3-trihydroxy-diphenylmethane

Xanthone	8.21 (H-6', d, *J* = 8.0 Hz, 1H), 7.69 (H-4', t, *J* = 7.8 Hz, 1H), 7.46 (H-3', d, *J* = 8.4 Hz, 1H), 7.43 (H-5', t, *J* = 7.6 Hz, 1H), 6.61 (H-5, dd, *J* = 10.0, 3.5 Hz, 1H), 6.39 (H-6, d, *J* = 10.0 Hz, 1H), 5.19 (OH, d, *J* = 6.0 Hz, 1H), 4.57 (OH, s, 1H), 4.55–4.50 (H-4, m, 1H), 3.19 (OH, s, 1H).	2,2',3-trihydroxybenzophenone
	7.90 (H-8, d, *J* = 7.9 Hz, 1H), 7.59 (H-6, t, *J* = 7.0 Hz, 1H), 7.13 (H-7, t, *J* = 7.5 Hz, 1H), 7.09 (H-5, d, *J* = 8.5 Hz, 1H), 6.00 (H-1, d, *J* = 6.1 Hz, 1H), 5.96 (H-2, ddd, *J* = 9.3, 6.2, 2.9 Hz, 1H), 5.67 (H-3, d, *J* = 9.6 Hz, 1H), 5.14 (H-4, d, *J* = 2.3 Hz, 1H), 3.86 (OH, s, 1H), 3.62 (OH, s, 1H).	*cis*-3,4-dihydroxy-3,4-dihydroxanthone
Dibenzothiophene	8.00 (H-1,8, d, *J* = 7.7 Hz, 2H), 7.82 (H-4,5, d, *J* = 7.7 Hz, 2H), 7.61 (H-3,6, td, *J* = 7.6, 0.9 Hz, 2H), 7.51 (H-2,7, td, *J* = 7.6, 0.9 Hz, 2H).	dibenzothiopene sulfone
	7.84 (H-1,8, d, *J* = 7.6 Hz, 2H), 7.81 (H-4,5, d, *J* = 7.8 Hz, 2H), 7.65 (H-3,6, td, *J* = 7.6, 1.2 Hz, 2H), 7.54 (H-2,7, td, *J* = 7.6, 1.0 Hz, 2H).	dibenzothiopene sulfoxide
Fluorene	7.66 (H-4,5, d, *J* = 7.7 Hz, 2H), 7.65 (H-1,8, d, *J* = 7.4 Hz, 2H), 7.39 (H-2,7, t, *J* = 7.4 Hz, 2H), 7.33 (H-3,6, t, *J* = 7.7 Hz, 2H), 5.60 (H-9, d, *J* = 9.7 Hz, 1H), 1.81 (OH, d, *J* = 10.3 Hz, 1H).	9-hydroxyfluorene
Phenanthrene	7.79 (H-4,5, d, *J* = 7.7 Hz, 2H), 7.61 (H-1,8, d, *J* = 7.3 Hz, 2H), 7.43 (H-2,7, t, *J* = 7.3 Hz, 2H), 7.37 (H-3,6, t, *J* = 7.3 Hz, 2H), 4.83 (H-9,10, d, *J* = 7.6 Hz, 2H), 2.19 (OH, s, 2H).	*cis*-9,10-dihydroxy-9,10-dihydrophenanthrene

Anthracene	7.95 (H-10, s, 1H), 7.83–7.70 (H-6,7, m, 2H), 7.53 H-9, (s, 1H), 7.47–7.38 (H-5,8, m, 2H), 6.69 (H-4, d, *J* = 9.7 Hz, 1H), 6.11 (H-3, dd, *J* = 9.6, 4.4 Hz, 1H), 4.83 (H-1, dd, *J* = 8.3, 4.7 Hz, 1H), 4.42 (H-2, dt, *J* = 8.5, 4.4 Hz, 1H), 2.42 (OH, d, *J* = 8.8 Hz, 1H), 1.90 (OH, d, *J* = 8.9 Hz, 1H).	*cis*-1,2-dihydroxy-1,2-dihydroanthracene
Biphenyl	7.55 (H-2',7', d, *J* = 8.0 Hz, 2H), 7.37 (H-3',6', t, *J* = 7.7 Hz, 2H), 7.29 (H-5', t, *J* = 7.3 Hz, 1H), 6.36 (H-6, d, *J* = 5.6 Hz, 1H), 6.14–6.06 (H-5, m, 1H), 5.89 (H-4, d, *J* = 9.6 Hz, 1H), 4.61 (H-3, s, 1H), 4.50 (H-2, s, 1H), 2.62 (OH, s, 1H), 1.92 (OH, s, 1H).	*cis*-2,3-dihydro-2,3-dihydroxybiphenyl

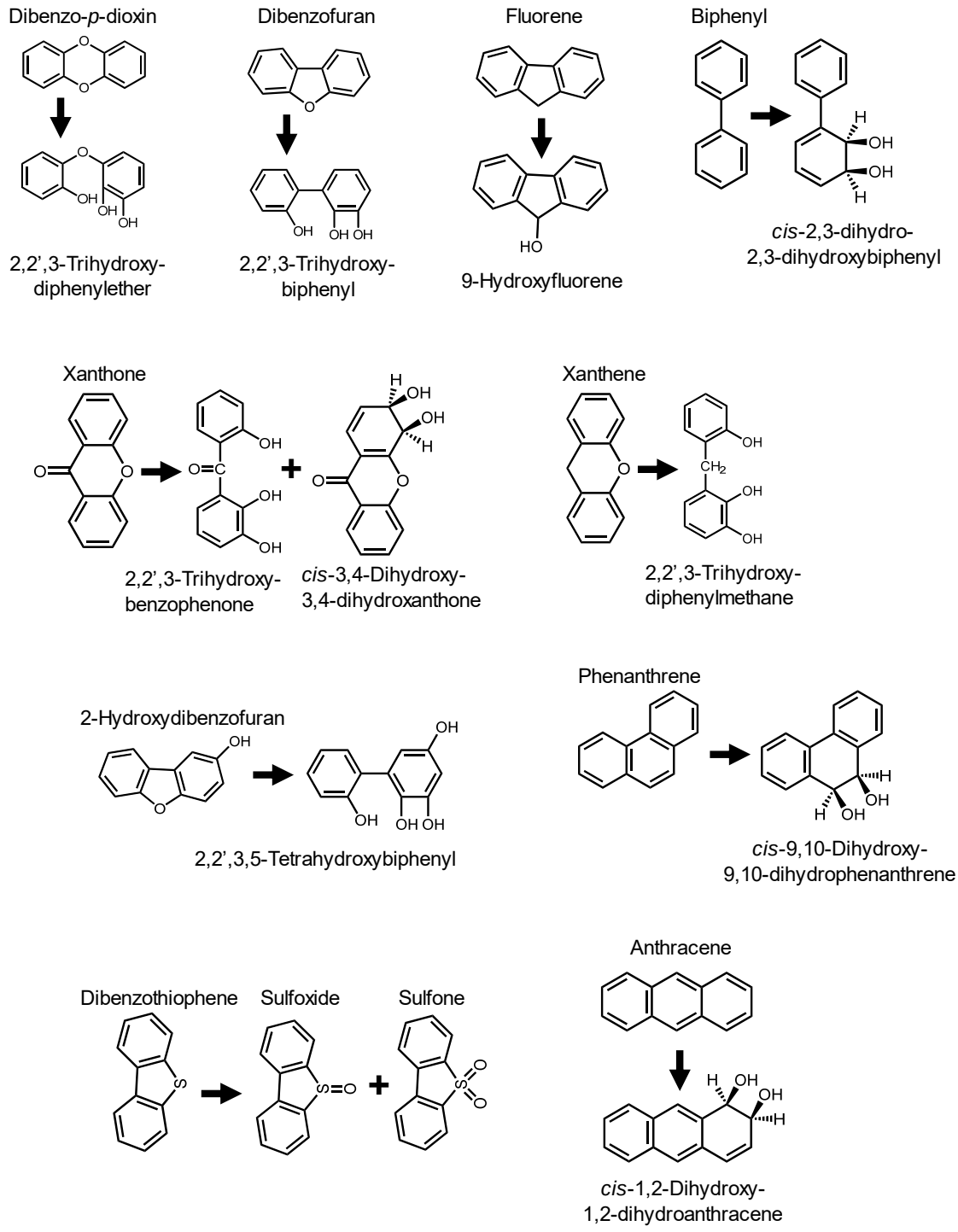

Figure 4. Biotransformations carried out by *S. wittichii* RW1 DBF/DXN dioxygenase.

Chapter 3: Characterization of a silent pathway for biphenyl degradation in *Sphingomonas wittichii* RW1

Introduction

Dioxin and dioxin like compounds are persistent organic pollutants that are known for their ability to bioaccumulate in fat tissue and lead to serious health affects including disruption of hormone function, neurological and behavioral effects, skin lesion, and in some cases cancer (73). Our environment has been a depository site for such persistent pollutants where they have entered either by natural sources such as forest fires or by anthropogenic sources such as oil spills, incomplete combustion of fossil fuels, and many other industrial activities (74). Fortunately, many microorganisms have been isolated for their ability to degrade such pollutants and therefore assist in reducing the toxic effects of these pollutants as well as replenish the carbon cycle (75). However, accumulation of such persistent pollutants in nature is due to multiple reasons such as the insufficient natural metabolic activity of microorganisms, the lack of a fully evolved pathway, or slow degradation rates (76, 77). Recently, recombinant DNA technology has been applied to facilitate the evolution of incomplete pathways and to improve the degradation pathways for other xenobiotic compounds (78, 79).

Extensive genetic and biochemical studies have been conducted on *Sphingomonas wittichii* RW1 due to its unique ability to mineralize dibenzo-*p*-dioxin (DXN) and dibenzofuran (DBF) (23-25). The DXN/DBF catabolic pathway initiates through an angular dioxygenase and subsequent enzymatic steps are highly reminiscent of the biphenyl pathway. Interestingly, despite this catabolic pathway similarity, RW1 is unable to use biphenyl as a sole carbon source. A recent study by us showed that the DBF/DXN

angular dioxygenase can attack biphenyl at the lateral position producing *cis*-2,3-dihydroxy-2,3-dihydrobiphenyl (Chapter 1 of this thesis). Kinetic studies on DbfB, a 2,2',3-trihydroxybiphenyl dioxygenase from *S. wittichii* RW1, showed that this enzyme has similar ring cleavage activity towards both 2,3-dihydroxybiphenyl (a biphenyl pathway intermediate) and 2,2',3-trihydroxybiphenyl (a DBF pathway intermediate) (40). Two hydrolases, DxnB1 and DxnB2, have been purified from RW1 (43, 44, 80) for the hydrolysis of 2-hydroxy-6-oxo-6-(2-hydroxyphenyl)-hexa-2,4-dienoate (8-OH-HOPDA). Both of these purified hydrolases are able to convert 8-OH-HOPDA to salicylate (DBF pathway) and 2-hydroxy-6-oxo-6-phenylhexa-2,4-dienoic acid (HOPDA) to benzoate (biphenyl pathway). Once salicylate or benzoate is formed they can be metabolized by RW1 to TCA cycle metabolites that provide carbon and energy for growth (22, 24). The initial angular dioxygenase, ring cleavage enzyme, and hydrolase are all expressed constitutively by RW1 (22). Interestingly, mutants of *S. wittichii* RW1 capable of growing on biphenyl were isolated at a rate of 10^{-9} after 4 weeks of incubation on biphenyl containing medium (22). While the rate of growth of these RW1 mutants on biphenyl was not reported this fact combined with the information on the other initial enzymes in the pathway suggests that while RW1 does not normally grow on biphenyl it does have the capability to grow on biphenyl.

All these facts collectively led us to hypothesize that biphenyl could potentially be metabolized through the DXN/DBF catabolic pathway. The only missing enzyme that would prevent *S. wittichii* RW1 from growing on biphenyl is the biphenyl *cis*-dihydrodiol dehydrogenase. Engineering a *S. wittichii* RW1 for the capability to degrade biphenyl will not only help in studying the evolution of biodegradation pathways but will also

create a strain carrying PCB degradation capabilities in addition to the DXN/DBF degradation capability.

Materials and Methods

Bacterial strains, plasmids, and growth conditions

S. wittichii RW1 is the wild type strain capable of growth on DXN and DBF but not biphenyl (22). *Sphingobium yanoikuyae* B1 is the wild type strain capable of growing on biphenyl but not DXN and DBF and was the source for the *bphB* gene encoding biphenyl *cis*-dihydrodiol dehydrogenase (81). *Escherichia coli* DH5α [F^-φ80*lac*ZΔM15 Δ(*lac*ZYA-*arg*F) U169 *rec*A1 *end*A1 *hsd*R17 (r_k^- , m_k^+) *pho*A *sup*E44 thi-1 *gyr*A96 *rel*A1 λ^-] was obtained from Invitrogen (Waltham, Massachusetts) and used as a recipient in transformation experiments. *S. wittichii* RW1 ring cleavage mutant strains (RW1ΔdbfB1, RW1ΔSWIT3046, and RW1ΔdbfBΔSWIT3046) and hydrolase mutant strains (RW1ΔdxnB1, RW1ΔdxnB2, RW1Δ0910, RW1ΔdxnB1ΔdxnB2, RW1ΔdxnB1ΔSWIT0910, and RW1ΔdxnB2ΔSWIT0910) were kindly donated by Mutter and Zylstra (82). PCR amplicons were cloned into the pGEM-T easy vector (Promega, Madison, WI) via TA cloning and their sequences verified prior to further use. The low copy number vector pRK415 (83) was used to introduce *bphB* into the different knockout strains of *S. wittichii* RW1 and was also used to insert *bphB* into the genome of *S. wittichii* RW1 by recombination (64, 84). *E. coli* HB101 carrying the helper plasmid pRK2013 (85) was used as a helper strain in all triparental mating experiments to mobilize pRK415 constructs into *S. wittichii* RW1. Mineral salts basal (MSB) medium (86) was used as minimal media to test growth of wild type and engineered strains on

aromatic compounds. DXN, DBF, and biphenyl were added as crystals to the plate lid to test growth on solid media. For growth in liquid medium DXN, DBF, and biphenyl were dissolved in acetone, added to an empty sterile 250 mL Erlenmeyer flask, the acetone allowed to evaporate for 4 hours at room temperature, 50 mL of sterile MSB broth was added, and the flask sonicated for 10 minutes in a Branson 1800 water bath sonicator. The amount of each aromatic compound added was calculated to be 3 mM after the addition of the MSB broth. Growth curves were constructed by subculturing into the appropriate test media at an initial OD of 0.05 as measured at 600 nm. Because crystals of the substrate were present in the medium, all optical density readings were taken after first allowing the crystals to settle in an extracted sample of the culture. All growth curves were performed in triplicate flasks. MSB plates containing tetracycline (15 µg/ml) and supplemented with 20 mM phenylalanine were used to select for *S. wittichii* RW1 transconjugants. Luria-Bertani (LB) broth and agar were used as a complete medium for *E. coli* growth. Ampicillin (100 µg/ml), kanamycin (50 µg/ml), gentamycin (10 µg/ml), and tetracycline (15 µg/mL) were added when needed. *S. yanoikuyae* B1 and *S. wittichii* RW1 were incubated at 30°C while all *E. coli* strains were incubated at 37°C.

Molecular techniques

Genomic DNA was extracted from pure colonies of *S. wittichii* RW1 and *S. yanoikuyae* B1 using the Ultraclean microbial DNA isolation kit and following the recommendations of the manufacturer (MoBio, Carlsbad, CA). Plasmid DNA was isolated from *E. coli* DH5α cells harboring constructs using the Nucleospin plasmid purification kit (Macherey-Nagel, Germany) and following the protocol supplied. Restriction enzyme digestion, ligation, transformation and gel electrophoresis were

performed using standard methods (68). The Phusion high fidelity PCR kit (New England Biolabs) was used to amplify all DNA fragments used in this study and the Geneclean III kit (MP Biomedicals, Ohio, USA) was used to purify DNA fragments from PCR solutions or agarose gels. Sequencing was done through the Genewiz sequencing company (South Plainfield, New Jersey, USA). Sequence analysis was aided by the DNAStar Lasergene package (DNASTAR, Madison, WI).

Introducing *bphB* to the genome of *S. wittichii* RW1

The *bphB* gene encoding the *cis*-biphenyl dihydrodiol dehydrogenase was isolated from genomic DNA of *S. yanoikuyae* B1 using the primers *bphB*-F: GGCTGCAGggcttgaagaggagagtggc and *bphB*-R: GGGAGCTCtcaggcgtcggggcgcttgc and cloned into the *Pst*I and *Sac*I sites of pRK415. The resulting construct, designated pRK_bphB, was delivered to the *S. wittichii* RW1 wild type and mutant strains via triparental mating as described elsewhere (64).

In order to construct a stable engineered RW1 strain containing *bphB* the gene was inserted downstream of *fdx3* under the control of the constitutive promotor of the *dxn* locus (this operon encodes for the angular dioxygenase large and small subunits, one of the hydrolases, and one of the ferredoxins). For genome insertion a plasmid containing *bphB* flanked by upstream and downstream sequences of *fdx3* was constructed. A 1.2 kb region containing *fdx3* and its upstream sequence was amplified from the genomic DNA of *S. wittichii* RW1 using the primers *Upfdx3*-F: GGTCTAGAcgatgtcagcactggtttca and *Upfdx*3-R: GGCTCGAGtcaatcaagattgttggaca that introduced *Xba*I and *Xho*I sites, respectively. Genomic DNA from *S. yanoikuyae* B1 was used as a template to amplify the *bphB* gene using the primers *bphB*-F2: GGCTCGAGggcttgaagaggagagtggc and

bphB-R2: GGGGTACCtcaggcgtcggggcgcttgc which introduced *XhoI* and *Kpn*I sites, respectively. A 1.2kb region downstream of *fdx3* was amplified from genomic DNA of *S. wittichii* RW1 using the primers *Dnfdx3*-F: GGGGTACCacttaacgatcctccaaagt and *Dnfdx3*-R: GGGAGCTCcctcgactgcggtgttgtaa, introducing *Kpn*I and *Sac*I restriction sites, respectively. All three PCR generated fragments were initially cloned into the pGEM-T easy vector and their sequences confirmed. The pGEM-T vectors containing the three fragments above were digested with the appropriate restriction enzymes and the desired fragments were gel purified and cloned into the *XbaI* and *Sac*I sites of pRK415 resulting in the plasmid pRK_UpBphBDn. An ampicillin resistance cassette was PCR amplified from pGEM-T Easy with the primers GGGGTACCggtctgacagttaccaatgc and CCGGTACCcacaccgcatcaggtggcac, digested with *Kpn*I, and introduced into the *Kpn*I site of pRK_UpBphBDn to form pRK_bphBins. Orientation (same direction as the knockout gene) of the ampicillin cassette was confirmed via PCR as well as digestion with appropriate restriction enzymes. The final construct, pRK_bphBins, was delivered to *S. wittichii* RW1 via triparental mating and an insertional mutant carrying the double crossover recombination that is resistant to ampicillin and sensitive to tetracycline was isolated as described previously (64). The insertion mutant strain, designated RW1bphB, was confirmed via PCR using the primers *Upfdx3*_F and *Dnfdx3*_R compared to the wild type RW1 strain.

Growth Curves.

For RW1 and the various RW1-derived strains cultures were grown on LB broth to stationary phase and then transferred twice on MSB with phenylalanine. Mid log phase MSB phenylalanine grown cells were subcultured into the desired aromatic compound

growth medium at a final OD 600 of 0.05. Amberlite XAD7HP resin (Sigma-Aldrich, St. Louis, MO) was added at 2 mg/ml for growth curves of strains for the ring cleavage analysis and Amberlite IRA-400 chloride resin (Sigma-Aldrich, St. Louis, MO) was added at 2 mg/ml for growth curves of strains for the hydrolase analysis. No resin was added for the growth curves of RW1 and RW1bphB.

Results

Effects of *bphB* on growth of *S. wittichii* RW1 on biphenyl

The *S. wittichii* RW1 wild type strain lacks the ability to grow on MSB containing biphenyl. We detected mutants of RW1 capable of growth on MSB agar with biphenyl after 4 to 5 weeks of incubation, confirming previously published observations by Wittich et al. (22). Subculture of these mutants showed very poor growth on biphenyl containing MSB plates (over four weeks to form colonies).

We hypothesized that all RW1 needed for growth on biphenyl is a functional biphenyl *cis*-dihydrodiol dehydrogenase (Figure 3). To test this hypothesis, we cloned the *S. yanoikuyae* B1 *bphB* gene into pRK415 downstream of the *lac* promoter. RW1 transconjugants containing pRK_bphB gained the ability to grow on biphenyl on both solid and liquid media. Since pRK415 is inherently unstable we permanently inserted the B1 *bphB* gene into the genome of *S. wittichii* RW1 downstream of the constitutively expressed *dxnA1A2BCfdx3* operon encoding some of the DXN/DBF pathway enzymes. The engineered strain RW1bphB grows on biphenyl with a doubling time of 3.2 hours revealing a hidden pathway for biphenyl degradation in *S. wittichii* RW1 (Figure 5). The

addition of *bphB* did not affect the ability of *S. wittichii* RW1 to grow on DXN and DBF (data not shown).

Identifying the genes involved in biphenyl degradation in *S. wittichii* RW1

The ability of RW1bphB to grow on biphenyl as the sole carbon source informs us that its genome possesses all the other enzymes required for the catabolic pathway. We (Chapter 2) and others (36) previously showed that the constitutively expressed DXN/DBF dioxygenase converts biphenyl to *cis*-biphenyl dihydrodiol so this enzyme is responsible for the first step in biphenyl degradation by RW1. Multiple ring cleavage enzymes and hydrolases are encoded by the RW1 genome (35) so the question remains as to which exact enzyme(s) are responsible for these two steps in the biphenyl catabolic pathway in RW1. Due to the large number of extradiol dioxygenases found in RW1 we first started with testing *dbfB1* and SWIT3046 that were previously found to function in the DBF and DXN pathways (82). For that purpose, pRK_bphB was introduced into RW1, RW1ΔdbfB, RW1ΔSWIT3046, and RW1ΔdbfBΔSWIT3046 and transconjugants were tested for their ability to grow on biphenyl. The data (Figure 6) shows that the deletion of either *dbfB1* or SWIT3046 alone did not prevent growth on biphenyl and that the highest effect was seen when both of these genes were deleted. These data show that either one of the two identified RW1 ring cleavage enzymes can function to utilize 2,3-dihydroxybiphenyl as a substrate to allow RW1 to grow on biphenyl. This latter fact is important in that while previous studies have measured 2,3-dihydroxybiphenyl ring cleavage activity in whole cells of RW1 (22) or with a purified enzyme (40) this is the first example showing that either of the two ring cleavage enzymes DbfB or SWIY3046 is physiologically capable of allowing RW1 to grow on biphenyl.

Three different hydrolases have been identified to function in the RW1 DXN and/or DBF catabolic pathways (82). In order to identify the exact hydrolase(s) involved in biphenyl degradation in RW1bphB, we introduced pRK_bphB in RW1ΔdxnB1, RW1ΔdxnB2, RW1ΔSWIT0910, RW1ΔdxnB1ΔdxnB2, RW1ΔdxnB1ΔSWIT0910, and RW1ΔdxnB2ΔSWIT0910. The use of these six different RW1 single and double hydrolase knockout strains enabled us to test the involvement of the three different hydrolases (DxnB1, DxnB2, and SWIT0910) in biphenyl degradation. The data (Figure 7) show that the three single knockout strains with pRK_bphB grow at the same rate and extent as the wild type RW1 strain with pRK_bphB on biphenyl. However, the double knockouts tell a different story. Two of the double knockouts with pRK_bphB grew the same as the wild type RW1(pRK_bphB) on biphenyl. However, RW1ΔdxnB1ΔdxnB2(pRK_bphB) was not able to grow on biphenyl. In combination, these data show that of the three hydrolases previously shown to be involved in RW1 DXN and/or DBF degradation only two function as HOPDA hydrolases to allow RW1 to grow on biphenyl. Their activity is substitutive and not additive, only one of the two enzymes is required. While one of these two hydrolase enzymes has been purified and studied in detail (44, 87, 88) this is the first example showing that one of two different hydrolases enzymes is physiologically capable of allowing RW1 to grow on biphenyl.

Discussion

Herein we report that the dioxin mineralizing bacterium *S. wittichii* RW1 contains all of the genes necessary to form a full pathway for biphenyl degradation except a biphenyl *cis*-dihydrodiol dehydrogenase. We engineered *S. wittichii* RW1 to grow on biphenyl by inserting *bphB*, a biphenyl *cis*-dihydrodiol dehydrogenase from *S.*

yanoikuyae B1. The B1 BphB dehydrogenase is responsible for dehydrogenation of the *cis*-dihydrodiols generated from the oxidation of biphenyl and many polycyclic aromatic hydrocarbons (31, 55). Stably inserting *bphB* in the RW1 genome under the control of the constitutive promotor of the *dxn* locus enabled RW1bphB to grow on biphenyl with the relatively high doubling time of 3.2 hours. The doubling time of RW1bphB on 3 mM biphenyl exceeded the doubling time for the wild type RW1 growing on 3 mM of either DBF (5 hour doubling time) or DXN (8 hour doubling time). Such an efficient doubling time reflects the efficiency of the enzymes in *S. wittichii* RW1 in metabolizing biphenyl and shows a proper metabolite flow in the pathway. Growth of *S. yanoikuyae* B1 on biphenyl is accompanied with the appearance of a bright yellow color due to HOPDA accumulation due to the different kinetic characteristics of the enzymes in the pathway or perhaps due to different regulation levels of the genes of the catabolic pathway. Unlike growth of *S. yanoikuyae* B1 on biphenyl, RW1bphB does not turn yellow while growing on biphenyl perhaps reflecting a more equal distribution of enzyme activity in the catabolic pathway. As expected, RW1bphB was not able to grow on naphthalene or phenanthrene and this is due to the lack of the ability of the RW1 angular dioxygenase to oxidize naphthalene and the fact that it oxidizes phenanthrene at the 9,10 position rather than the 3,4 position (Chapter 2).

No lag phase was noticed for growth of RW1bphB on biphenyl and growth was leveled off after 12 hours of incubation which is relatively fast compared with other biphenyl degraders. For instance, *Pseudomonas stutzeri* required 60 hours to level off when growing on 1 g/L biphenyl with particle size of 0.1-0.63 mm (equivalent to 6 mM) (89). *Burkholderia xenovorans* required around 25 hours to reach stationary phase when

grown on 20 mM biphenyl added as crystals (90). A different study on *Sphingobium fuliginis* HC3 showed that this strain required 24 hours to completely metabolize biphenyl when used at a concentration of 500 mg/L (3mM) (91). Due to the fact that the growth rate of biphenyl degraders varies according to the concentration of biphenyl and crystal size (89), we were unable to provide accurate comparison for growth of RW1bphB to other biphenyl degraders, but according to logical comparisons we considered this strain as one of the fastest biphenyl degraders.

Engineering bacteria to degrade toxic aromatic compounds are faced with multiple challenges such as: (i) availability of a transport system, (ii) toxicity of the compound or its metabolites, (iii) regulation of required genes, and (iv) physiological resistance to stress due to exposure to new toxic metabolites (76, 78). Introducing the *bphB* gene allowed *S. wittichii* RW1 to completely metabolize biphenyl which indicates the ability of this strain to overcome all such challenges. The constitutive expression of most of the genes involved in DXN and DBF degradation, the similarities in the backbone structure of biphenyl, DXN, and DBF, and the similarities of the DXN, DBF, and biphenyl metabolites are all factors that led to a successful engineered strain. Another example of successful engineering *S. wittichii* RW1 is the introduction of a set of genes encoding the formation of a superchannel responsible for alginate incorporation from *Sphingomonas* sp. A1. The superchannel led to a significant increase in the growth rate of *S. wittichii* RW1 on DBF and DXN due to more efficient diffusion of the large hydrocarbons from the culture medium to the interior of the cell (79).

S. wittichii RW1 encodes many different oxygenases, ring cleavage enzymes, and hydrolases in its genome (35). There have been very few studies on the physiological

role of these enzymes in the degradation of aromatic compounds by RW1. Our data show the involvement of two different ring-cleavage dioxygenases and two different hydrolases in RW1 biphenyl degradation. Previous studies by our laboratory showed that *dbfB* is involved only in DBF degradation while SWIT3046 is involved in both DBF and DXN degradation (82). Our work (Figure 6) showed that both enzymes participate equally in biphenyl degradation. A very slight amount of growth on biphenyl was seen even after both genes were deleted. This may be due to a low level of activity of another *meta*-cleavage dioxygenase in RW1. This agrees with what was noticed from the catechol 2,3-dioxygenase in *S. yanoikuyae* B1 which had maximal activity towards catechol but only 4.9% of that activity was detected against 2,3-dihydroxybiphenyl (84). Our recent work on *S. yanoikuyae* B1 showed that replacing its biphenyl dioxygenase genes with the angular dioxygenase system from *S. wittichii* RW1 led to growth of the resulting strain on DXN but not DBF and that the engineered strain uses the enzymes for the biphenyl pathway to metabolize DXN (Chapter 4). Such results enhance the hypothesis that genes for DXN metabolism evolved from genes for biphenyl degradation.

The importance of RW1bphB is not limited to extending the degradation ability of aromatic compounds but creates a biphenyl pathway in a strain that contains enzymes carrying the ability to transform different chlorinated dioxin congeners. Resting cells of *S. wittichii* RW1 grown on DBF were shown to be able to transform 2,7-dichlorodibenzo-*p*-dioxin, 1,2,3,4-tetrachlorodibenzo-*p*-dioxin, 1,2,3-trichlorodibenzo-*p*-dioxin, and 1,2,3,4,7,8-hexachlorodibenzo-*p*-dioxin (92, 93). Kinetic studies on purified 2,2',3-trihydroxybiphenyl dioxygenase, DbfB, from *S. wittichii* RW1 showed low activity of this enzyme to meta cleave 3,4-dihydroxybiphenyl besides 2,3-dihydroxybiphenyl and

2,2',3-trihydroxybiphenyl (40). Such ability is important in polychlorinated biphenyl degradation and was shown to be critical for the degradation of many PCB congeners by *Pseudomonas* sp. strain LB400 especially when such congeners carry chlorines on or near carbon 2 or 3 of the biphenyl backbone (57). More importantly, *S. wittichii* RW1 possesses a HOPDA hydrolase, DxnB2, which belongs to a phylogenetically divergent class of hydrolases capable of transforming 8-OH-HOPDA six times faster than HOPDA which makes it more specific for the degradation of DBF. DxnB2 was also found to be capable of cleaving 3-Cl-HOPDA and 4-OH-HOPDA with a 10-fold higher specificity compared to BphD from *Burkholderia* sp. strain LB400 and BphD from *Rhodococcus globerulus* P6 (44). The presence of multiple enzymes in *S. wittichii* RW1 carrying the ability to degrade different chlorinated dioxin congeners suggests the importance of our engineered strain in PCB degradation and creates a better candidate to be used for bioremediating sites contaminated with a mixture of chlorinated DXN, DBF, and biphenyl. Our work demonstrates that the enzymes in the upper pathway for DBF and DXN degradation have a wide substrate range with activity towards other aromatic hydrocarbons.

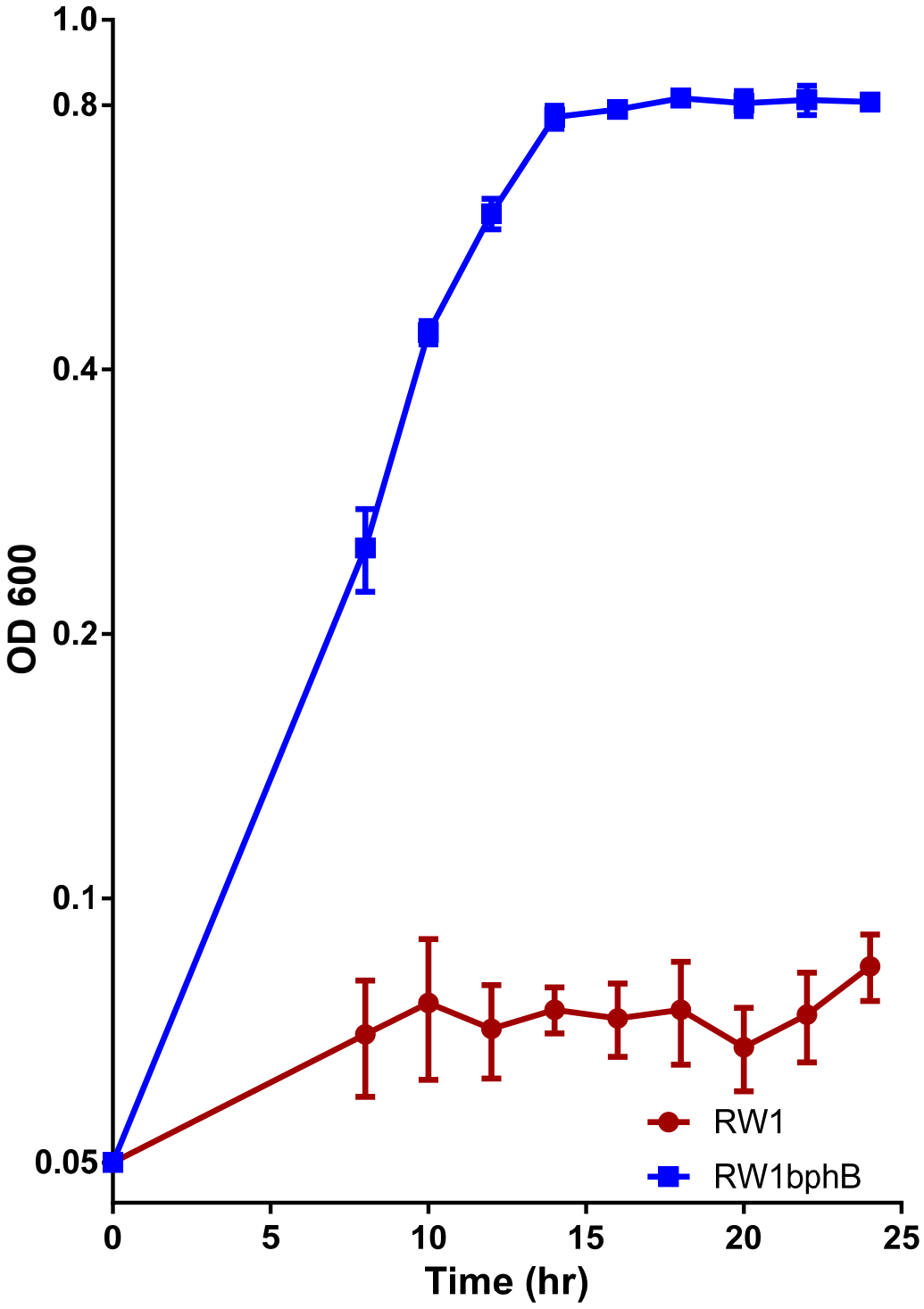

Figure 5. Growth of RW1 and RW1bphB on biphenyl.

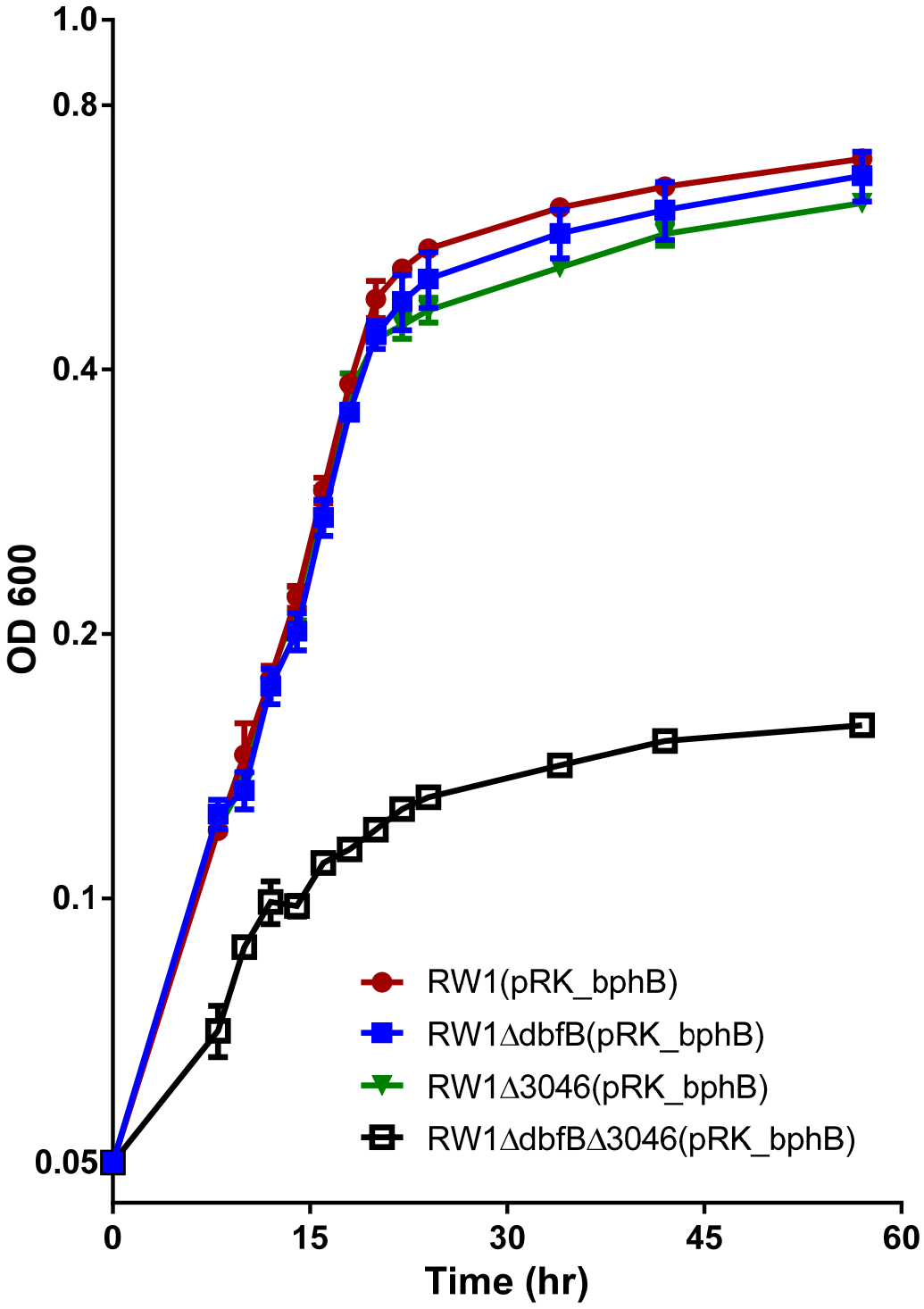

Figure 6. Role of two extradiol dioxygenases, DbfB and SWIT3046, in biphenyl degradation by RW1(pRK_bphB).

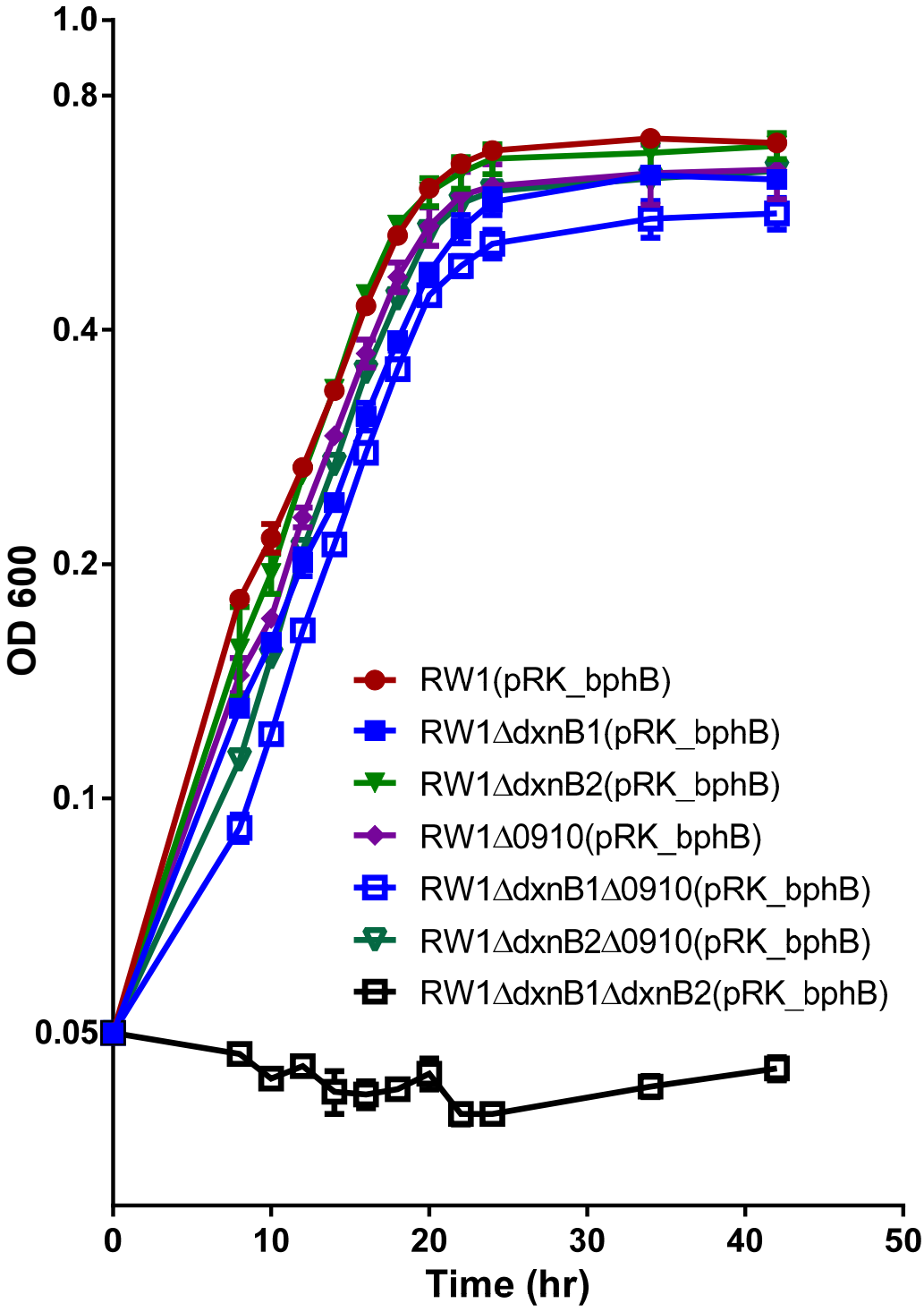

Figure 7. Role of three different hydrolases in the metabolism of biphenyl by RW1(pRK_bphB).

Chapter 4: Genes for biphenyl degradation in *Sphingobium yanoikuyae* B1 function on dibenzo-*p*-dioxin but not dibenzofuran

Introduction

Sphingobium yanoikuyae B1 is well known for its ability to utilize a wide variety of polycyclic aromatic hydrocarbons (PAHs) including biphenyl, naphthalene, anthracene, and phenanthrene as sole sources for carbon and energy. In addition, this strain can completely metabolize monocyclic hydrocarbons such as toluene, *m*-, and *p*-xylene as well as transform a wide variety of PAHs to their corresponding *cis*-dihydrodiols (31, 64). Analysis of the B1 genome referred this extraordinary degradation ability to the presence of 35 putative ring-oxidizing and ring-cleaving dioxygenases (94). The majority of the genes responsible for monocyclic and polycyclic aromatic hydrocarbon degradation are located in multiple operons on a 39 kb segment of the *S. yanoikuyae* B1 chromosome (64, 95). The genes encoding the alpha and beta subunits of the oxygenase component of the initial biphenyl (and PAH) dioxygenase are located elsewhere in the chromosome (96). The biphenyl dioxygenase system in *S. yanoikuyae* B1 is a three component enzyme system composed of a two subunit dioxygenase (BphA1f and BphA2f) arranged as a heterotrimer ($\alpha 3\beta 3$) , a 43.2 kDa reductase (BphA4); and a ferredoxin (BphA3) (54). Heterologous expression of all three components of the biphenyl dioxygenase system in *E. coli* showed the ability of this enzyme to oxygenate biphenyl and naphthalene and covert indole to indigo while no catalytic activity was observed when the oxygenase was expressed alone without its electron supply system (96).

S. yanoikuyae B1 grows on the three ring compounds anthracene and phenazine (97) but not on the oxygen containing three ring compounds dibenzo-*p*-dioxin (DXN) and dibenzofuran (DBF). Biotransformation studies using the B1 mutant strain B8/36 blocked in the dihydrodiol dehydrogenase step showed that dibenzo-*p*-dioxin (DXN) and dibenzofuran (DBF) are transformed by the initial dioxygenase to *cis*-1 2-dihydroxy-1,2-dihydrodibenzo-*p*-dioxin and 2,3-dihydroxy-2,3-dihydrodibenzofuran, respectively (56, 98). In addition, 1,2-dihydroxydibenzo-*p*-dioxin accumulated in resting cells of *S. yanoikuyae* B1 previously grown on succinate and biphenyl demonstrating that the compound is not ring cleaved by either of the two biphenyl pathway meta ring cleavage enzymes (56). Interestingly, 1,2-dihydroxydibenzo-*p*-dioxin acts as a mixed type inhibitor against both 2,3-dihydroxybiphenyl dioxygenase and 2,3-catechol dioxygenase (56). When strain B1 grows on phenazine the compound is initially oxidized by biphenyl oxygenase to 1,2-dihydroxy-1,2-dihydrophenzime (phenazine *cis*-dihydrodiol) which then spontaneously dehydrates to 1,2-dihydroxyphenazine (97). Interestingly the 2,3-dihydroxybiphenyl ring cleavage dioxygenase encoded by *bphC* in B1 does not cleave 1,2-dihydroxyphenazine (97) just as it does not cleave the analogous dihydroxylated intermediates formed from DXN and DBF (56).

Growth on DXN and DBF as the sole sources of carbon and energy by *Sphingomonas wittichii* RW1 requires an angular dioxygenase which possibly explains why *S. yanoikuyae* B1, which encodes a lateral DXN and DBF dioxygenase, does not. *S. wittichii* RW1 is the only known DXN degrader that has been genetically characterized (25, 37-39, 45). The dibenzofuran-4,4a-dioxygenase (DBFDO) in this strain is a three component enzyme system that catalyzes angular dioxygenation of several aromatics

including DXN and DBF, *cis*-dihydroxylation of several aromatics including biphenyl, and monooxygenation of the sulfur heteroatom in dibenzothiophene and the benzylic methylenic group in fluorene (Chapter 2). Following angular dioxygenation of DXN and DBF, the products 2,2',3-trihydroxydiphenylether and 2,2',3-trihydroxybiphenyl (respectively) undergo ring cleavage and a hydrolytic enzymatic step to produce catechol or salicylate, respectively.

Comparison of all the many ring cleavage and hydrolytic enzymes from *S. yanoikuyae* B1 and *S. wittichii* RW1 shows very little amino acid sequence identity even though the two strains metabolize the similar intermediates 2,3-dihydroxybiphenyl, 2,2',3-trihydroxybiphenyl, and 2,2',3-trihydroxydiphenylether. Our previous work showed that the RW1 angular dioxygenase can oxidize biphenyl in a lateral fashion to *cis*-2,3-dihydroxy-2,3-dihydrobiphenyl (Chapter 2). We hypothesize that replacing the B1 lateral oxidizing biphenyl dioxygenase with the RW1 angular oxidizing dioxygenase will still allow growth of B1 on biphenyl. The engineered strain will then enable us to test the ability of B1 to metabolize DXN and DBF since the dead end laterally oxidized intermediate will no longer be formed.

Materials and Methods

Bacterial strains, plasmids, and growth conditions

S. yanoikuyae B1 is the wild type strain capable of growth on biphenyl but not DXN and DBF (81). *S. wittichii* RW1 is the wild type strain capable of growing on DXN and DBF but not biphenyl (22). *Escherichia coli* DH5α [F^-φ80*lac*ZΔM15 Δ(*lac*ZYA-*arg*F) U169 *rec*A1 *end*A1 *hsd*R17 (r_k^- , m_k^+) *pho*A *sup*E44 thi-1 *gyr*A96 *rel*A1 λ^-] was

obtained from Invitrogen (Waltham, Massachusetts) and used as a recipient in transformation experiments. PCR amplicons were cloned into the pGEM-T easy vector (Promega, Madison, WI) while pRK415 (83) was used as an unstable low copy number vector to prepare all the constructs used to insert or knockout genes in *S. yanoikuyae* B1. *E. coli* HB101 carrying the helper plasmid pRK2013 was used as a helper strain in all triparental mating experiments to mobilize pRK415 constructs into *S. yanoikuyae* B1 (85). Mineral salts basal (MSB) was used as minimal media to test growth of wild type and engineered strains on aromatic compounds (86). Aromatics were added as crystals to the plate lid while 3 mM of each aromatics was added as crystals to liquid cultures in growth curve experiments. MSB plates containing tetracycline (15 µg/ml) and supplemented with 20 mM phenylalanine were used to select for *S. yanoikuyae* B1 transconjugants. Luria-Bertani (LB) broth and agar were used as a complete medium for *E. coli* growth. Kanamycin (50 µg/ml), gentamycin (10 µg/ml), and tetracycline (15 µg/ml) were added when needed. *S. yanoikuyae* B1 and *S. wittichii* RW1 were incubated at 30°C while 37°C was used for *E. coli*.

DNA manipulations and molecular techniques

Genomic DNA was extracted from pure colonies of *S. wittichii* RW1 and *S. yanoikuyae* B1 using the Ultraclean microbial DNA isolation kit and following the recommendations of the manufacturer (MoBio, Carlsbad, CA). Plasmid DNA was isolated from *E. coli* DH5α cells harboring constructs for gene insertion/deletion using Nucleospin plasmid purification kit (Macherey-Nagel, Germany) and following the protocol supplied. Restriction enzyme digestion, ligation, transformation and gel electrophoresis were performed using standard methods (68). Phusion high fidelity PCR

kit (New England Biolabs) was used to amplify all DNA fragments used in this study and Geneclean III kit (MP Biomedicals, Ohio, USA) was used to purify DNA fragments from PCR solutions or agarose gels. Sequencing was done through Genewiz sequencing company (North Plainfield, New Jersey, USA). Sequence analysis was performed using the DNAStar Lasergene program (DNASTAR, Madison, WI).

Dioxygenase replacement and construction of insertional mutants

The biphenyl dioxygenase (*bphA1fA2f*) genes of *S. yanoikuyae* B1 were replaced by the angular dioxygenase system (*dxnA1A2*, *fxd3*, *redA2*) from *S. wittichii* RW1 by taking advantage of homologous recombination and an unstable delivery vehicle as previously used by us in B1 (64). This was accomplished as follows: approximately 1 kb upstream of *bphA1fA2f* was amplified from *S. yanoikuyae* B1 using the primers Up*bphA*-F: GGAAGCTTACCATGTGATAGGTTTCAAGTCTC and Up*bphA*-R: CCTCTAGAGGCTCTCTCCGGTTTTCACGAACT that were designed to introduce *Hind*III and *Xba*I sites, respectively. The PCR product was cloned via TA cloning into the pGEM-T easy vector and sequenced (pGEM_Up*bphA*). Primers to amplify the kanamycin3 cassette (99) and the downstream sequence of *bphA1fA2f* (Dn*bphA*) were designed to allow ligation of both fragments via overlap extension PCR (100). The kanamycin3 cassette was amplified from p34S-Km3 (99) using the primers *km3*-F: GGTCTAGAAGATCTCAAAGCCACGTTGTGTCTCAAAAT and *km3*-R: ATCGCGCGTTAAGCTCTTAGAAAAACTCAT which introduced both *Xba*I and *Bgl*II restriction sites at the 5' end while its 3' end contained homologous sequences from the 5' end of Dn*bphA*. The *bphA1fA2f* downstream region was amplified from B1 genomic DNA using the forward primer Dn*bphA*-F:

TCTAAGAGCTTAACGCGCGATTGCCAAAA that introduced homologous sequences to the 3'end of Km3 cassette and the reverse primer Dn*bphA*-R: CCGGTACCCGTACCGCCGCCGGTCATCGCGAC that introduces a *Kpn*I restriction site to the 3' end of the PCR product. PCR products from both fragments were mixed (0.5 ng/µL of each PCR product) in a single PCR reaction without primers for 15 cycles. Then the primers km3-F and Dn*bphA*-R were added and PCR was continued for 30 cycles. The PCR product from overlap extension PCR was ran on 0.8% agarose gel and the band corresponding to the correct size of the Km3 resistant gene and the downstream sequence of *bphA1fA2f* (Km-Dn*bphA*) was excised, purified, cloned via TA cloning, and sequenced. Both fragments, Up*bphA* and Km-Dn*bphA*, were digested from their corresponding vectors with appropriate enzymes and cloned into the *Hind*III-*Kpn*I sites of pRK415 (pRKUpKmDn*bphA*). Finally, the *Xba*I-*Bgl*II fragment carrying the genes for the angular dioxygenase system of *S. wittichii* RW1 (*dxnA1dxnA2*, *fdx3*, and *redA2*), was digested from pET-DBFDOS (Chapter 2) and cloned into the *Xba*I-*Bgl*II sites of pRK_UpKmDnbphA to form the dioxygenase replacement clone (pRK_DR). The final clone pRK_DR was delivered to *S. yanoikuyae* B1 via triparental mating using pRK2013 as the helper plasmid. Transconjugants were selected for tetracycline resistance on MSB plates supplemented with 20 mM succinate. A single colony was transferred to 5 mL LB broth without antibiotics and subcultures were screened for colonies resistant to kanamycin and sensitive to tetracycline as described elsewhere (64). PCR using the primers B1DR-F: GGGCAGACGACAACCGCAGTTC and B1DR-R: CCCCATGCATATTCTCCCGGGT was conducted on colonies of *S. yanoikuyae* B1 that

possessed the dioxygenase replacement (B1DR) to confirm that a homologous substitution recombination event occurred.

B1DR was used as recipients for the insertion of two different ring cleavage dioxygenases from *S. wittichii* RW1, *dbfB* and SWIT3046. Genomic DNA of *S. wittichii* RW1 was used as a template to amplify *dbfB* using the primers *dbfB1*-F: GGAGATCTAAGGAGAGTTATCGTCATGT and *dbfB1*-R: GGTCTAGACTCAATGCGCCGGCAACTGCA that introduces *Bgl*II and *Xba*I sites, respectively. Genomic DNA from *S. yanoikuyae* B1 was used as a template to amplify the downstream sequence with the primers Dn*dxnA*-F: GGTCTAGACGCGCGATTGCCAAAAACCC and Dn*dxnA*-R: GGAAGCTTACCGCCGCCGGTCATCGCGA that introduces *Xba*I and *Hin*dIII sites, respectively. Both PCR fragments were cloned into pGEM-T and verified by sequencing. The two PCR fragments were then cloned along with the *Kpn*I-*Bgl*II fragment from pET-DBFDOS to the *Kpn*I-*Hind*III sites of pRK415. An *Xba*I digested gentamycin cassette was introduced into the *Xba*I site of this construct leading to the formation of pRK_DRB1. This construct was delivered to the B1DR strain as described above. PCR was used to confirm insertional mutants (B1DRB1) that were gentamycin resistant and both kanamycin and tetracycline sensitive. To insert SWIT3046 downstream of the angular dioxygenase genes in B1DR, pRK_DRB1 was digested with *Xba*l and *Bgl*II to remove *dbfB* and the gentamycin cassette. Genomic DNA from *S. wittichii* RW1 was used to amplify SWIT3046 using the primers *dbfB2*-F: GGAGATCTATCCATGGTGACGATCCTGA and *dbfB2*-R: GGTCTAGATCAATGCGCGTGCGCGTGTC that introduces *Xba*I and *Bgl*II sites,

respectively. The amplified product was then cloned along with the *Xba*I digested gentamycin cassette to the *Xba*I-*Bgl*II sites of pRK_DRB1. This construct was delivered to the B1DR strain and insertional mutants of SWIT3046 (B1DRB2) were identified as described above. All fragments amplified were first cloned into pGEM-T and sequenced. To insert *dxnB* downstream of *dbfB* in B1DRB1, the following steps were conducted: *dxnB* was amplified from the genomic DNA of *S. wittichii* RW1 using the primers *dxnB*-F: GGTCTAGAGTGAGGATAGAAATGACCCA and *dxnB*-R: CGTGGCTTTGGCATGCTAGAATTTCCGAGC which were designed to connect this fragment to the kanamycin resistance cassette amplified by the primers km3OLE-F: TCTAGCATGCCAAAGCCACGTTGTGTCTCA and km3OLE-R: CCGAGCTCTTAGAAAAACTCATCGA via overlap extension PCR. Primers used for the amplification of the overlap extension product generated *XbaI* and *Sac*I sites. The downstream sequence of *dbfB* was amplified from genomic DNA of B1DRB1 using the primers Dn*dbfB*-F: GGGAGCTCACGCGCGATTGCCAAAAACC and Dn*dbfB*-R: GGCTGCAGCCGTTCCCCATTCGCCAGGG that introduce restriction sites for *Sac*I and *Pst*I, respectively. Both fragments were cloned along with the *Eco*RI-*Xba*I fragment from pRK_DRB1 to the *Eco*RI- *Pst*I sites of pRK415, generating pRK_DRB1B1. This construct was delivered to the B1DRB1 strain and insertional mutants (B1DRB1B1) were detected by PCR for colonies that were kanamycin resistant and both gentamycin and tetracycline sensitive. To insert *dxnB* downstream SWIT3046, pRK_DRB1B1 was digested with *Xba*I and *Bgl*II removing *dbfB*. The PCR fragment of SWIT3046 amplified with the primers *dbfB2*-F and *dbfB2*-R was cloned into the *Xba*I-*Bgl*II sites generated from pRK_DRB1B1 after removal of *dbfB1*. The final construct, pRK_DRB2B1, was

delivered to B1DRB2 and insertional mutations (B1DRB2B1) were identified via PCR for colonies resistant to kanamycin and sensitive to both gentamycin and tetracycline.

Gene knockout of B1 *bphC* and *bphD*

The 2,3-dihydroxybiphenyl dioxygenase, *bphC*, was deleted from *S. yanoikuyae* B1, B1DR, B1DRB1, B1DRB2, B1DRB1B1, and B1DRB2B1 to identify its role in the degradation of biphenyl, DXN, and DBF. A construct in pRK415 was designed for that purpose as following: *bphC* and its upstream region was amplified from B1 genomic DNA using the primers Up*bphC*-F: GGAAGCTTCGAGTGATGATGACGGGCGT and Up*bphC*-R: GGTCTAGACGATTCCTTCCGATCCGGTC that introduces *Hind*III and *Xba*I sites, respectively. A second PCR fragment containing part of *bphC* with its downstream region was amplified by the primers Dn*bphC*-F: GGTCTAGAGGCATTGCATCCTGCGTCAG and Dn*bphC*-R: GGGGTACCGAATCCATGTTTCGCTCGAA that introduces *Xba*I and *Kpn*I sites, respectively. Both fragments were cloned into the *Hin*dIII-*Kpn*I sites of pRK415. An *Xba*I digested kanamycin and gentamycin cassette were cloned separately to the *Xba*I site of this construct. Depending on the antibiotic resistance, an appropriate construct was introduced to each strain of *S. yanoikuyae* B1 via triparental mating. Knockouts were confirmed via PCR as mentioned earlier. The role of *bphD*, the HOPDA hydrolase for the biphenyl degradation pathway in *S. yanoikuyae* B1, was deleted in a similar manner in *S. yanoikuyae* B1, B1DR, B1DRB1B1, and B1DRB2B1 to determine its role in the biphenyl, DXN, and DBF degradation pathways. For that purpose, a pRK415 construct was designed to disrupt the function of *bphD* in the four strains mentioned above. A 2kb fragment containing *bphD* and its flanking region was amplified from *S. yanoikuyae* B1

using the primers *bphD*-F: AAGCTTATCGCTCCAGGCTCGCCC and *bphD*-R: GGATCCCCGCAGGACGTCGAACAC that introduces *Hind*III and *Bam*HI restriction sites, respectively. This fragment was cloned into the *Hind*III-*Bam*HI sites of pRK415. A *Pst*I digested gentamycin cassette was cloned into the *Pst*I site of this clone which cleaves inside the *bphD* gene. The final clone was transferred to *S. yanoikuyae* B1, B1DR, B1DRB1B1, and B1DRB2B1 via triparental mating. Knockouts were verified by PCR and examined for their ability to grow on biphenyl, DXN, and DBF.

Growth Curves.

For B1 and the various B1-derived strains were grown on LB broth to late log phase and then subcultured directly into the desired aromatic compound growth medium at a final OD 600 of 0.05. Amberlite XAD7HP resin (Sigma-Aldrich, St. Louis, MO) was added at 2 mg/ml for growth curves of strains for the ring cleavage analysis and Amberlite IRA-400 chloride resin (Sigma-Aldrich, St. Louis, MO) was added at 2 mg/ml for growth curves of strains for the hydrolase analysis.

Results

Replacement of *S. yanoikuyae* B1 biphenyl dioxygenase with *S. wittichii* RW1 DXN/DBF dioxygenase

S. yanoikuyae B1 grows on biphenyl and many other PAHs as the sole source of carbon and energy through lateral dioxygenation of these aromatics by its biphenyl dioxygenase. Unfortunately, B1 also oxidizes DXN and DBF at the lateral position to eventually generate dihydroxylated dead end products. In order to test whether the *S. yanoikuyae* B1 biphenyl pathway can metabolize the bicyclic biphenyl-like intermediates

of the angular degradation pathway for DXN and DBF metabolism, the B1 biphenyl dioxygenase *bphA1fA2f* genes were replaced with the genes *dxnA1A2fdx3redA2* coding for the RW1 angular dioxygenase system as explained in Materials and Methods. The gene replacement strain B1DR containing the DXN/DBF dioxygenase grew at the same rate and extent as the wild type B1 strain (Figure 8). No accumulation of any intermediates was observed from growth of B1DR on biphenyl, unlike B1 that turns yellow during growth on biphenyl due to accumulation of the yellow HOPDA intermediate. Interestingly, the B1DR strain is also able to grow on DXN as the sole source of carbon and energy (Figure 9). The B1DR strain did not grow on DBF and resting cells accumulated a brown intermediate identified as 2,2',3-trihydroxybiphenyl. As expected, the B1DR strain lost the ability to metabolize naphthalene and phenanthrene.

Addition of two different RW1 ring cleavage dioxygenases

In order to determine if a different ring cleavage dioxygenase will allow B1DR to grow on DBF and to examine the effect of a different enzyme on biphenyl and DXN degradation in B1DR, two different ring cleavage dioxygenases were selected from *S. wittichii* RW1 and added to the genome of B1DR. The 2,2',3-trihydroxybiphenyl dioxygenase, DbfB, and the recently identified 2, 2',3-trihydroxydiphenylether dioxygenase, SWIT3046, were inserted one at a time downstream of the DXN/DBF dioxygenase genes in B1DR leading to the construction of two new strains designated B1DRB1 and B1DRB2, respectively. The data show that addition of either enzyme did not improve the degradation capability of B1DR on biphenyl (Figure 10) or DXN (Figure 11). B1DRB1 and B1DRB2 still were not able to grow on DBF, nevertheless, resting

cells of these cultures accumulated a yellow intermediate, signifying that DBF is cleaved to some extent. The inability of B1DR and the ability of B1DRB1 and B1DRB2 to convert 2,2',3-trihydroxybiphenyl to the ring cleavage product shows that both RW1 ring cleavage enzymes are functioning to some extent in the engineered strains and that *S. yanoikuyae* B1 lacks both a ring cleavage dioxygenase and a hydrolase that functions on DBF metabolites.

Effect of adding a RW1 hydrolase

To determine whether *S. yanoikuyae* B1 lacks a specific hydrolase for the DBF ring cleavage product, the RW1 DxnB1 hydrolase was inserted downstream of *dbfB* and SWIT3046 in strains B1DRB1 and B1DRB2, respectively. This led to the generation of the strains B1DRB1B1 and B1DRB2B1 that were tested for their ability to grow on DBF as well as determine the effect of this hydrolase to enhance the degradation capability of these strains on biphenyl and DXN. The data showed the ability of both strains, B1DRB1B1 and B1DRB2B1 to grow on DBF at a rate and extent similar to that seen for growth on biphenyl (Figure 12). The addition of *dxnB* to the strains B1DRB1 and B1DRB2 did not enhance their ability to grow on biphenyl and DXN (data not shown). Collectively, our data demonstrate that *S. yanoikuyae* B1 does not naturally have the ability to grow on dibenzofuran but can grow when genes encoding the first three catabolic steps are added.

Role of B1 *bphC* and *bphD* in dibenzo-*p*-dioxin degradation

The data mentioned above indicates the importance of ring cleavage dioxygenases and hydrolases already present in *S. yanoikuyae* B1 in the degradation of DXN. Due to

the lack of known dioxin degrading pure cultures it is important to identify the exact genes involved in this engineered pathway. For that purpose, the 2, 3-dihydroxybiphenyl 1,2-dioxygenase (*bphC*) was deleted from *S. yanoikuyae* B1, B1DR, B1DRB1, B1DRB2, B1DRB1B1, and B1DRB2B1. These knockout strains were then tested for growth on biphenyl, DXN, and DBF. The data show that all *bphC* knockout strains retained the ability to grow on biphenyl at the same rate and extent as the wild type strain indicating that other meta ring cleavage enzymes in the genome of B1 can take the place of BphC (Figure 13). On the other hand, deletion of *bphC* abolished growth of B1DR on DXN (Figure 14) indicating the importance of this enzyme in DXN degradation and that no other B1 ring cleavage dioxygenase can substitute unlike what was seen for biphenyl degradation. Deletion of *bphC* from B1DRB2 and B1DRB2B1 did not affect growth of these strains on DXN while the deletion abolished growth of B1DRB1 and B1DRB1B1 on DXN. This shows the ability of SWIT3046 but not *dbfB* to replace *bphC* in DXN degradation (Figure 14). Deletion of *bphC* had no effect on growth of B1DRB1B1 and B1DRB2B1 on DBF (Figure 15) confirming that both DbfB and SWIT3046 function as ring cleavage enzymes in the DBF catabolic pathway.

To determine the B1 hydrolase involved in DXN degradation in the B1 engineered strains, the biphenyl pathway HOPDA hydrolase *bphD* was deleted from B1, B1DR, B1DRB1B1, and B1DRB2B1. The knockout mutants were tested for their ability to grow on biphenyl, DXN, and DBF. Deletion of *bphD* from B1 abolished growth of the wild type strain on biphenyl showing that *bphD* is absolutely required for B1 to grow on biphenyl and that no other hydrolases in the B1 genome can take its place (Figure 16). Deletion of *bphD* from B1DR also abolished growth of this strain on DXN identifying

bphD as playing a role in DXN degradation by B1 (Figure 17). Deletion of *bphD* from engineered strains carrying the RW1 *dxnB* hydrolase, B1DRB1B1 and B1DRB2B1, had no effect on the ability of these two strains to grow on biphenyl (Figure 16), DXN (Figure 17), and DBF (Figure 18) indicating that *dxnB* functions on metabolites from all three pathways.

Discussion

Enhancing the degradation ability of microorganisms through genetic manipulations has been conducted in many biphenyl degrading bacteria to improve degradation ability of chlorinated dioxin congeners or to modify regiospecificity of initial dioxygenases. Such genetic manipulations include DNA shuffling for the large subunit of biphenyl dioxygenases (101), changing of amino acids in the active sites (102), or modifying the regulation system of degradation genes by replacing an inducible promoter with a constitutive promoter (103). In this study the biphenyl dioxygenase in *S. yanoikuyae* B1 was replaced with the angular dioxygenase system from *S. wittichii* RW1 via double reciprocal homologous recombination to engineer a dioxin degrading microorganism and to identify genes functional on dioxin metabolites. Our data show addition of the RW1 angular dioxygenase to B1 (strain B1DR) created a strain that retained its ability to grow on biphenyl and gained the ability to grow on dibenzo-*p*-dioxin. The ability of this strain to degrade biphenyl was expected due to the ability of DBFDO to perform *cis*-dihydroxylation of biphenyl leading to the formation of *cis*-2, 3-dihydro-2,3-dihydroxybiphenyl which is the same intermediate in the normal B1 biphenyl pathway (Figure 3)(104). Similar growth rates for *S. yanoikuyae* B1 and B1DR were seen on 3 mM biphenyl crystals which demonstrates the ability of the RW1 DBFDO

substituted for the B1 biphenyl dioxygenase to oxidize biphenyl at a rate allowing physiological growth on biphenyl similar to the wild type. Liquid cultures of B1 growing on 3 mM biphenyl turn the media yellow a few hours after inoculation. This is most likely due to the high catalytic rate of the B1 biphenyl dioxygenase, dihydrodiol dehydrogenase, and ring cleavage dioxygenase leading to the accumulation of the ring cleavage product and indicating that the hydrolase step is a bottle neck in biphenyl degradation. Unlike what was seen in the wild type strain B1, the engineered strain B1DR showed similar growth on biphenyl without accumulation of the ring cleavage product. We hypothesize that DBFDO has less activity toward biphenyl than the normal B1 biphenyl dioxygenase of *S. yanoikuyae* B1 but still supplies enough activity for optimum growth on biphenyl.

Interestingly, replacement of the B1 biphenyl dioxygenase with the RW1 angular dioxygenase created a strain (B1DR) capable of growth on DXN. This indicates that B1 contains the enzymes for both the upper pathway for dioxin metabolism to the common aromatic pathway intermediate catechol. It is interesting to note here that wild type B1 metabolizes DXN to the unproductive product 1,2-dihydroxydibenzo-*p*-dioxin which has an inhibitory effect on the ring cleavage dioxygenases XylE and BphC in the strain (56). Replacing the B1 biphenyl dioxygenase with the angular dioxygenase DBFDO allows B1 to retain the ability to grow on biphenyl while now oxidizing DXN to 2,2',3-trihydroxydiphenylether. This latter compound is efficiently metabolized by the B1 biphenyl pathway enzymes to allow growth on DXN.

The B1DR strain does not grow on DBF but the strain metabolizes DBF to a brown colored product identified as 2,2',3-trihydroxybiphenyl. This fact indicates that the

2,3-dihydroxybiphenyl 1,2-dioxygenase BphC is incapable of accepting 2,2',3-trihydroxybiphenyl as a substrate, indicating the inhibitory effect of the extra hydroxyl group in the uncleaved ring. The B1DRB1 and B1DRB2 strains are incapable of growth on DBF but both strains accumulate a yellow intermediate that is likely the ring cleavage metabolite from DBF degradation. These results indicate that the two RW1 meta cleavage dioxygenases added are expressed in both strains and are capable of converting 2,2',3-trihydroxybiphenyl to its ring cleaved intermediate. These results agree with the kinetic activity results for DbfB1 (40) and with the fact that both DbfB and SWIT3046 function in RW1 DBF degradation (82). Eltis and Bolin (105) suggested that the ability of the RW1 DbfB ring cleavage oxygenase to accommodate the extra hydroxyl group in the trihydroxy substrate may be due to the enzyme's unique structure compared with all other known ring cleavage enzymes.

The B1DRB1 and B1DRB2 strains are incapable of growth on DBF and both strains accumulate a yellow intermediate that is the ring cleavage metabolite from DBF degradation. When *dxnB* was inserted downstream of *dbfB* and SWIT3046 in B1DRB1 and B1DRB2 the resulting strains B1DRB1B1 and B1DRB2B1, respectively, were able to grow on DBF. This demonstrates that while the only enzyme needed for B1 growth on DXN is the initial ring oxidizing dioxygenase, B1 growth on DBF requires enzymes catalyzing the three steps for the conversion of DBF to salicylate. These results agree with the hypothesis that suggests that the enzymes involved in DXN degradation are different from those involved in DBF degradation (24) and additionally suggests that the dioxin degradation genes evolved from the biphenyl degradation genes. In fact, random priming recombinational mutagenesis of the *P. pseudoalcaligenes* KF707 biphenyl

dioxygenase evolved an enzyme with new capabilities in aromatic oxygenation, most notably gaining the ability to perform angular dioxygenation of DBF and DXN (52).

In vivo knockout of *bphC* from B1 showed that this *meta* cleavage dioxygenase involved in biphenyl and PAH degradation is the only B1 meta cleavage enzyme involved in DXN metabolism. Deletion of *bphC* from B1DR accumulated 2,2',3-trihydroxydiphenylether and blocked growth of this strain on DXN while it grew normally on biphenyl. This identifies the role of a second *meta* cleavage dioxygenase for 2,3-dihydroxybiphenyl that has no activity towards 2,2',3-trihydroxydiphenylether. Studies with *S. yanoikuyae* B1 identified two *meta* cleavage dioxygenases involved in biphenyl and *m*-xylene degradation. Genes for these enzymes are located in separate operons and transcribed in opposite directions. Analysis of both enzymes showed that *bphC* was more specific for 2,3-dihydroxybiphenyl while *xylE* was more specific for catechol (84). Due to the activity of XylE against 2,3-dihydroxybiphenyl this enzyme is most likely taking the place of BphC for biphenyl degradation in the *bphC* knockout and that this meta cleavage dioxygenase has no activity toward 2,2',3-trihydroxydiphenylether.

B1DRB1Δ*bphC* lost the ability to grow on DXN while B1DRB2Δ*bphC* retained the ability to grow on DXN with a similar growth rate as the B1DR strain. These data show the ability of SWIT3046 but not *dbfB* to complement the role of *bphC* in those strains and agrees with recent work from our laboratory (82). These results also explain the failure of purified DbfB to efficiently cleave 2,2',3-trihydroxydiphenylether (40). Similar growth rates for B1DRB2Δ*bphC* and B1DR indirectly show that the activity of BphC is equal to the activity of its counterpart SWIT3046 from *S. wittichii* RW1.

Data obtained from deletion of *bphD* from *S. yanoikuyae* B1 suggests that BphD is the only enzyme responsible for *meta* cleavage product hydrolysis in the biphenyl degradation pathway. Complementation of B1Δ*bphD* with *bphD* restored growth of the knockout mutant on biphenyl indicating no polar effect on downstream genes. Lack of growth of B1DRΔ*bphD* on DXN indicates the role of this enzyme in the hydrolysis of the *meta* cleavage product from 2,2',3-trihydroxydiphenyl ether from the DXN pathway. The ability of BphD to cleave 2-hydroxy-6-oxo-6-phenyl-hexa 2,4-dienoate (HOPDA) and not 8-OH-HOPDA shows the inhibitory effect of the 2' hydroxyl group to this enzyme. These results collectively suggest the relatedness of DXN pathway enzymes to biphenyl pathway enzymes and shows that enzymes that function on DXN metabolites do not necessarily have to function on DBF metabolites.

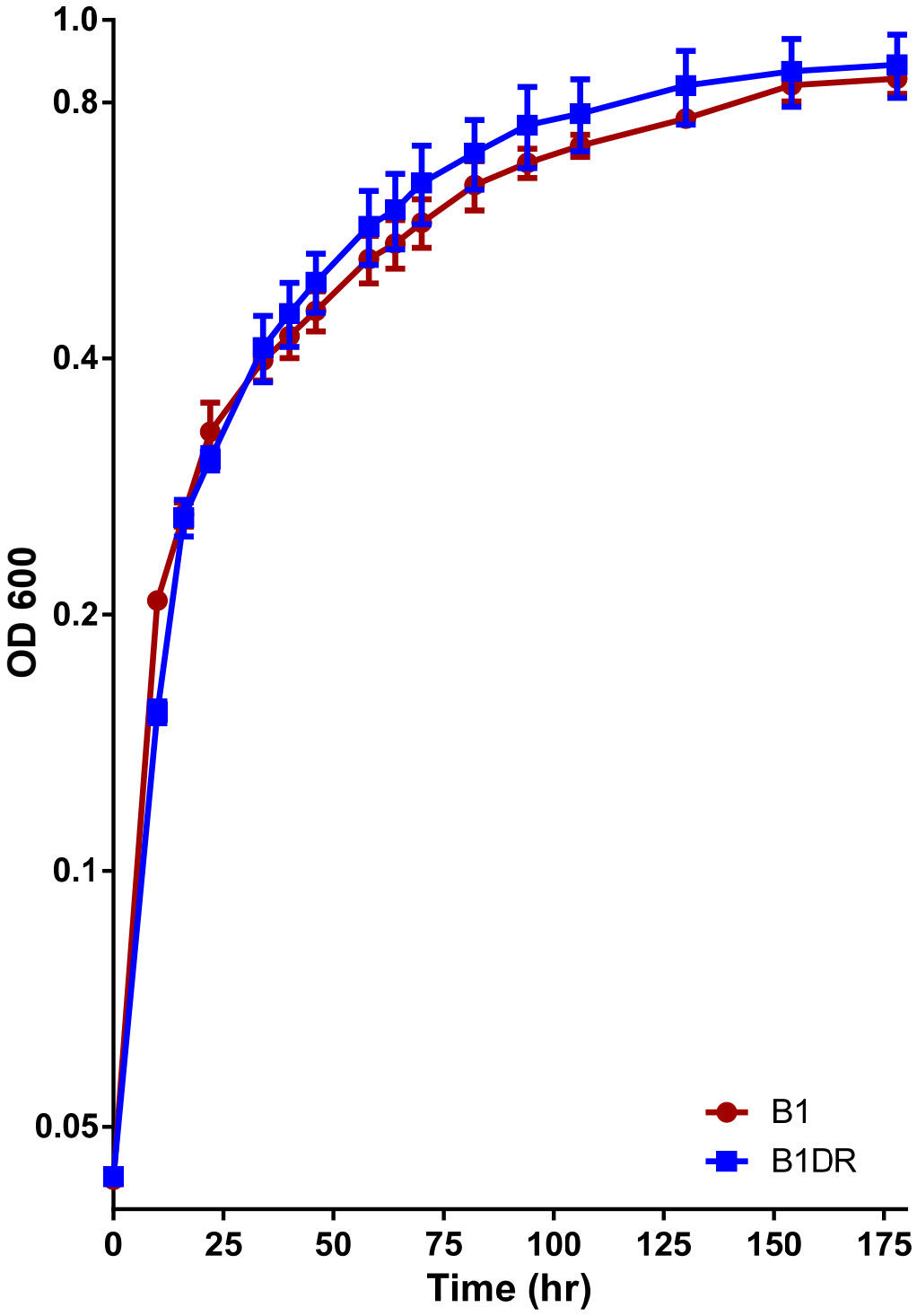

Figure 8. Growth of B1 and B1DR on biphenyl.

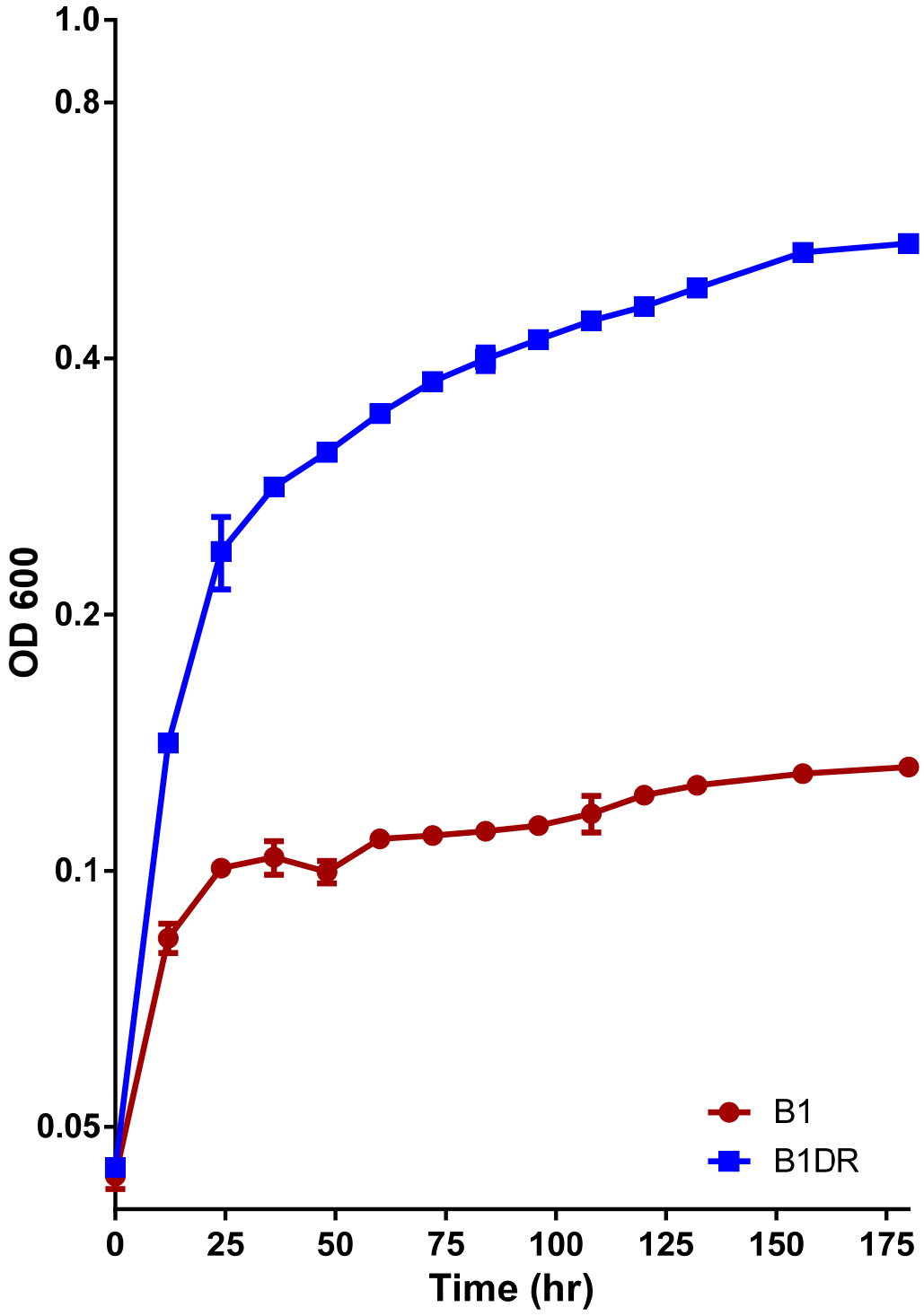

Figure 9. Growth of B1 and B1DR on dibenzo-*p*-dioxin.

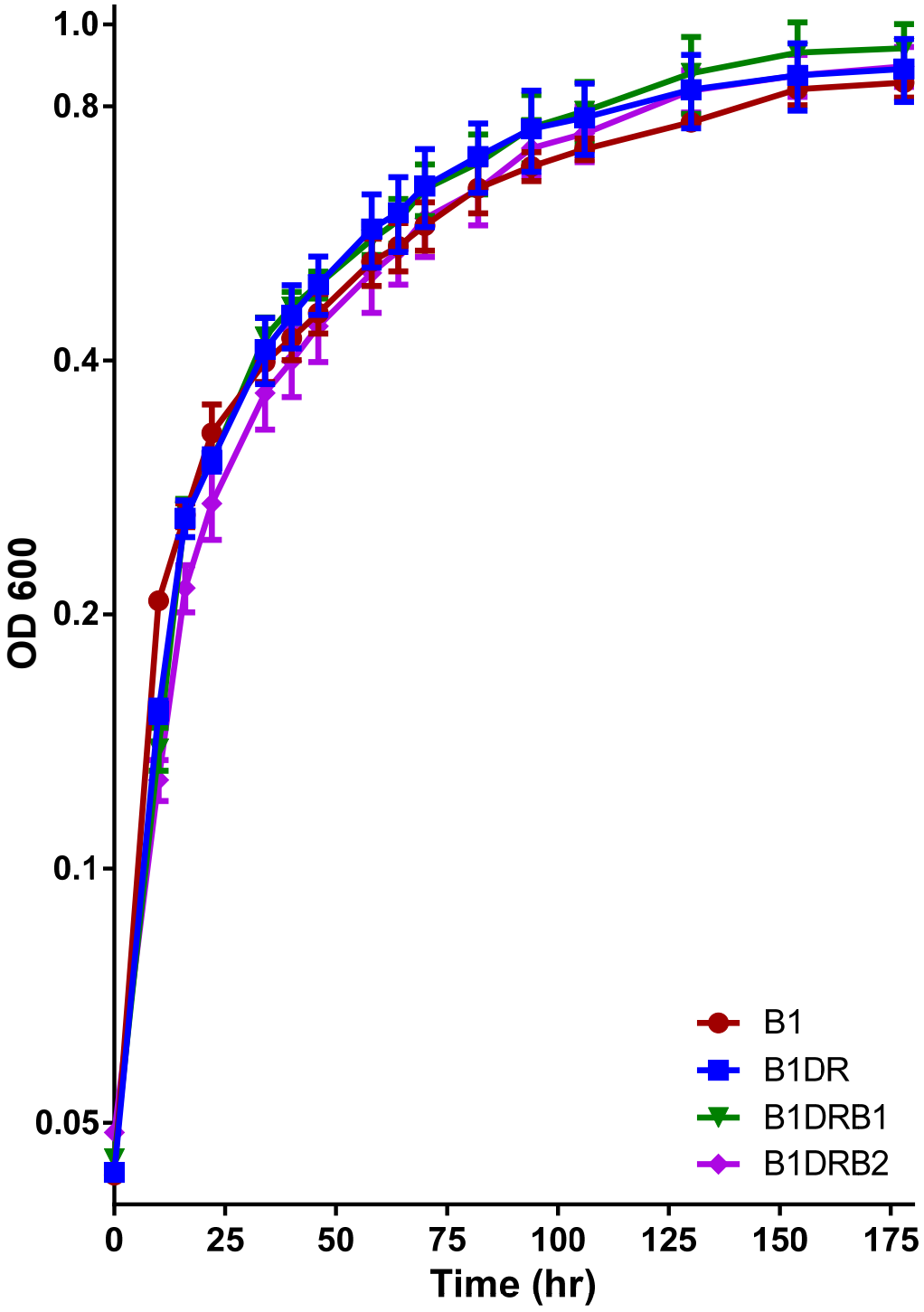

Figure 10. Effect of adding *dbfB* (B1) and SWIT3046 (B2) on growth of B1DR on biphenyl.

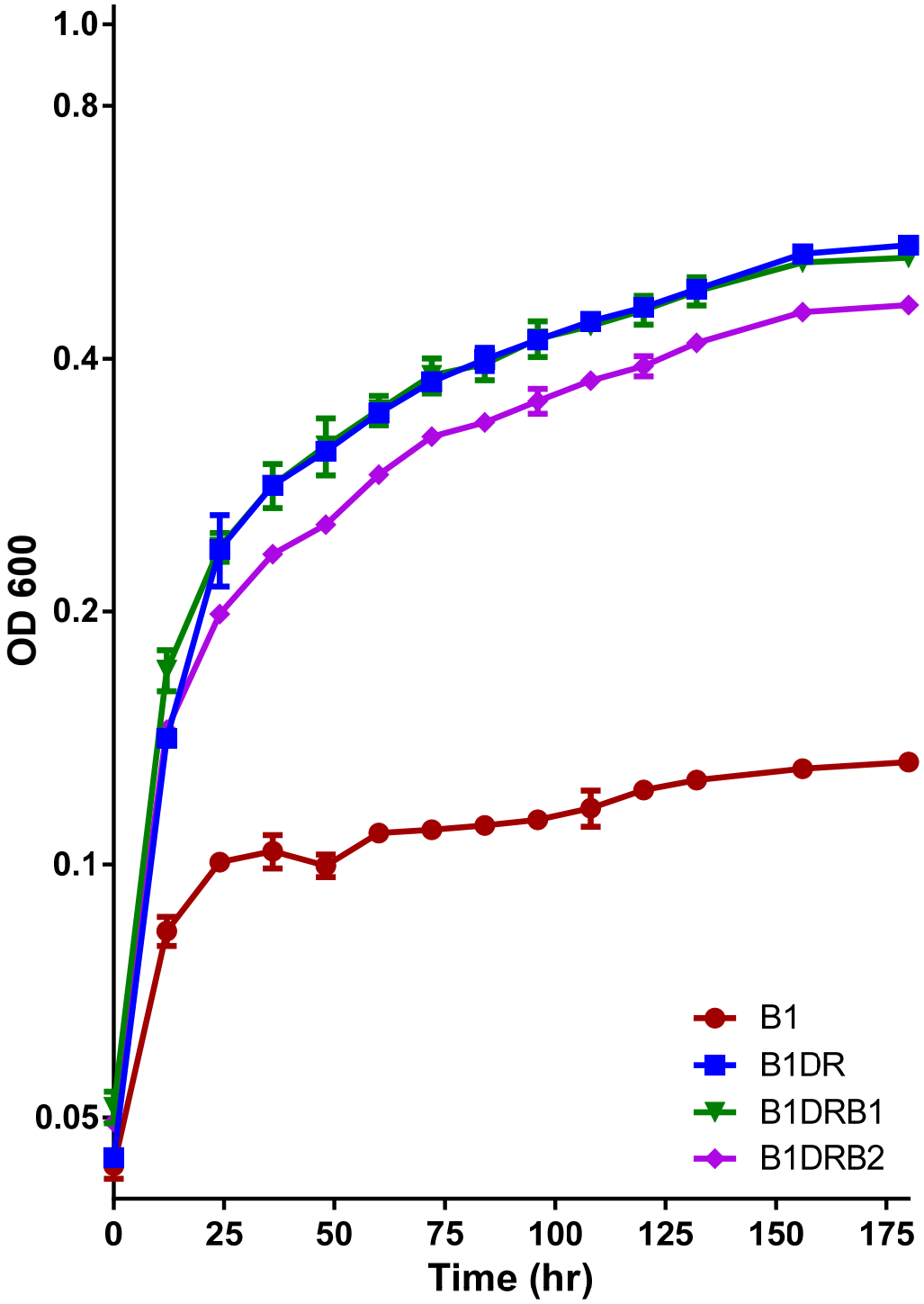

Figure 11. Effect of adding dbfB (B1) and SWIT3046 (B2) on growth of B1DR on dibenzo-*p*-dioxin

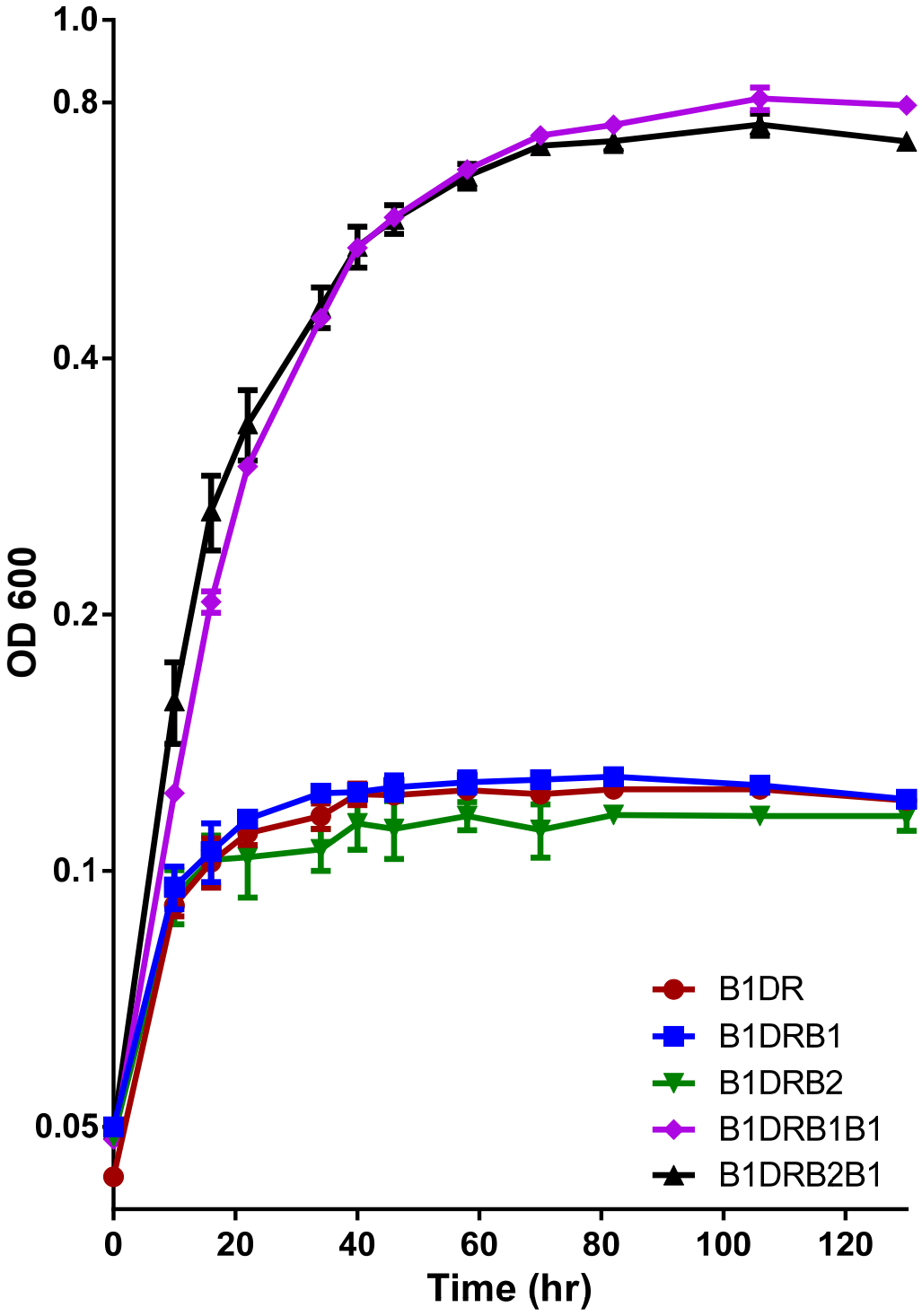

Figure 12. Effect of adding *dxnB* on growth of B1DRB1 and B1DRB2 on dibenzofuran.

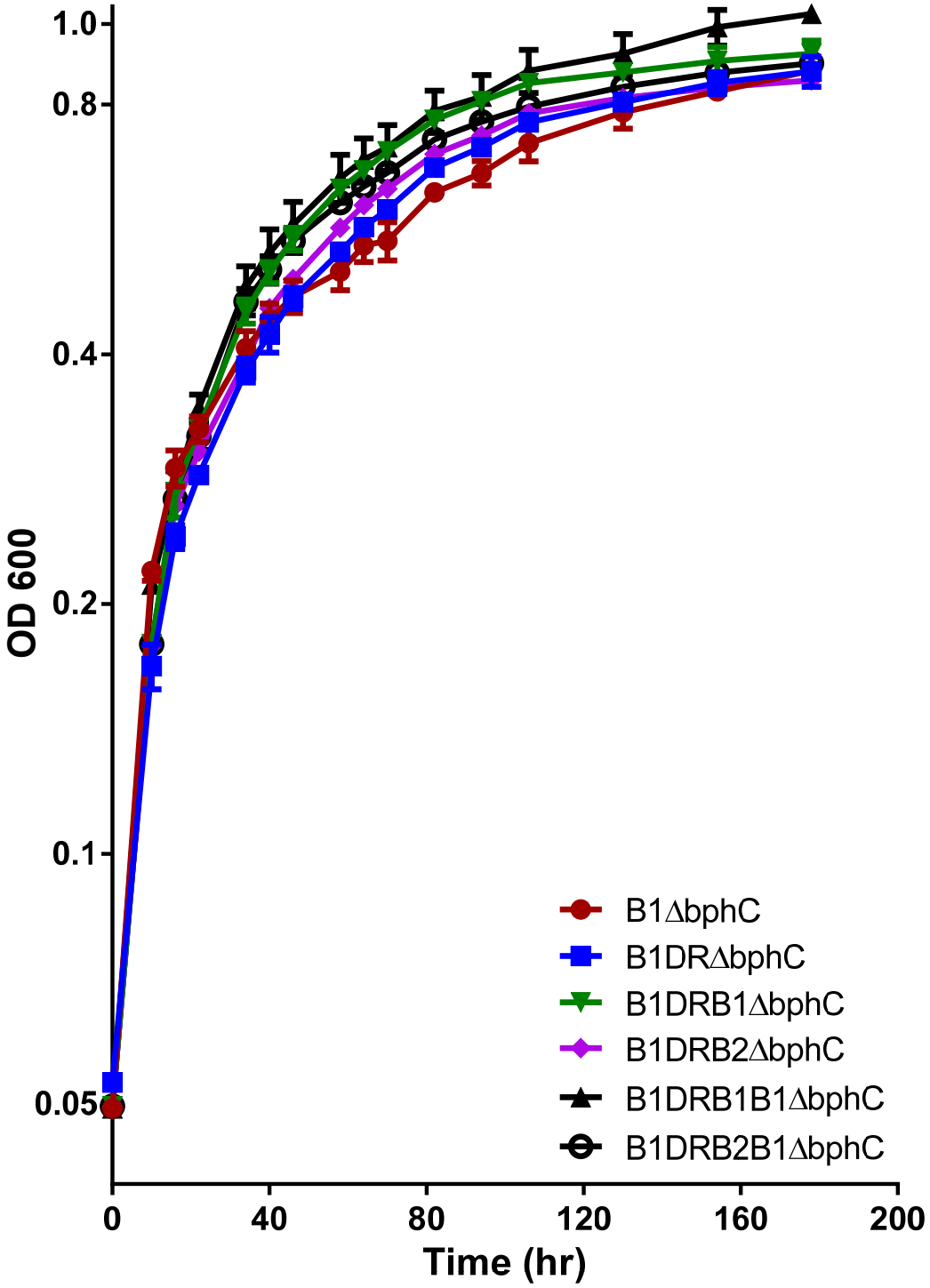

Figure 13. Effect of *bphC* deletion on growth of *S. yanoikuyae* B1 and its engineered strains on biphenyl.

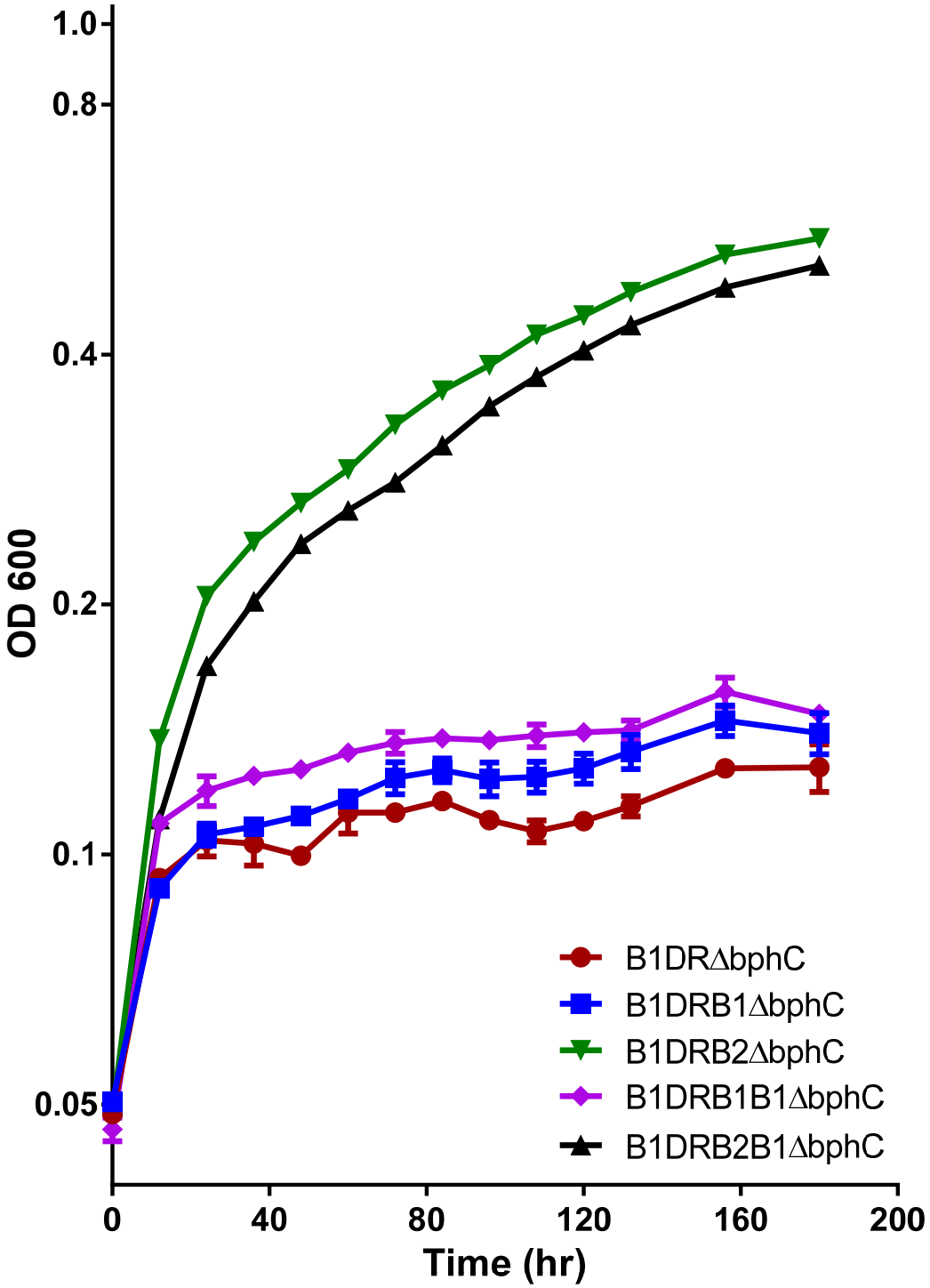

Figure 14. Effect of *bphC* deletion on growth of *S. yanoikuyae* B1 and its engineered strains on dibenzo-*p*-dioxin.

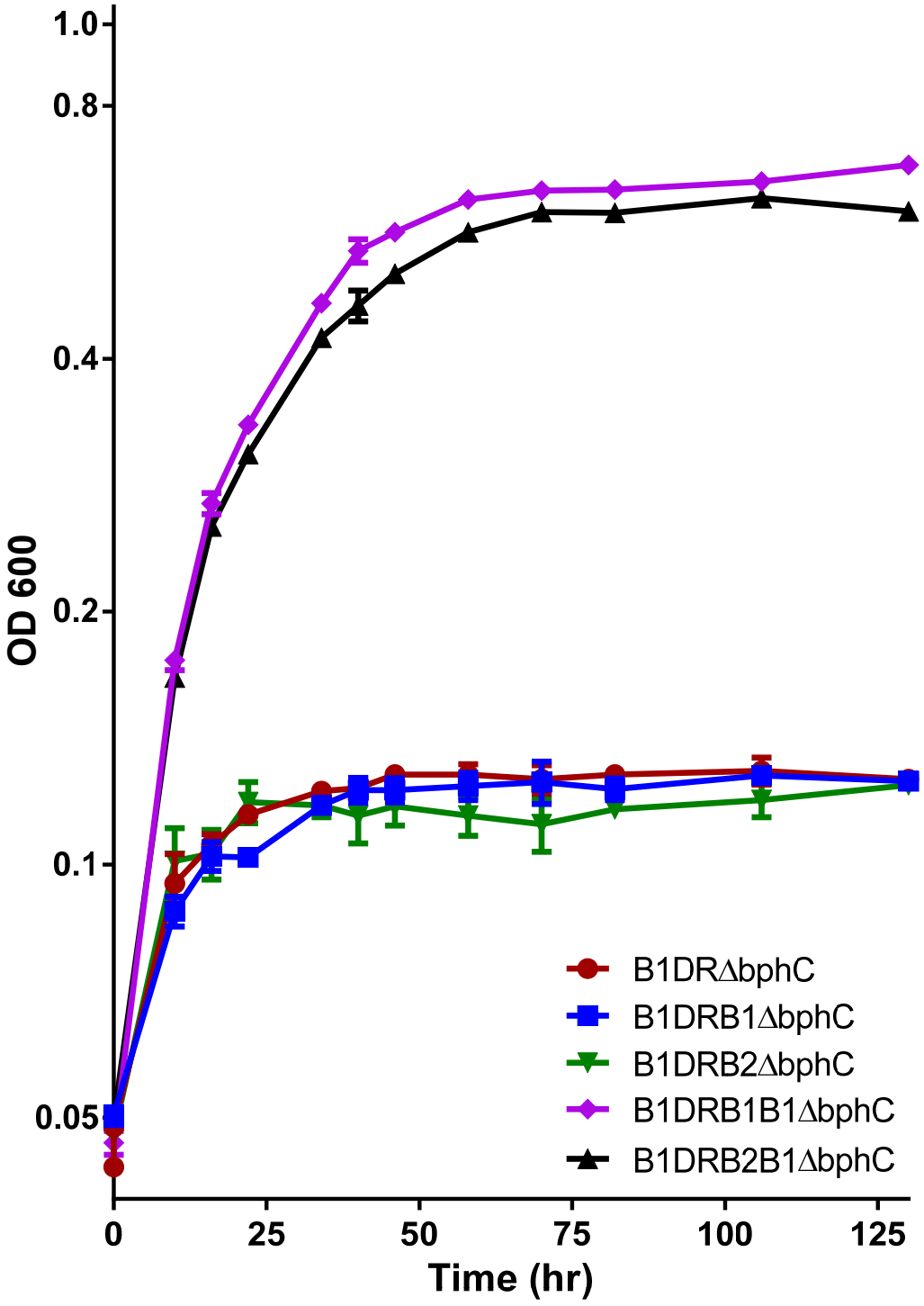

Figure 15. Effect of *bphC* deletion on growth of *S. yanoikuyae* B1 and its engineered strains on dibenzofuran.

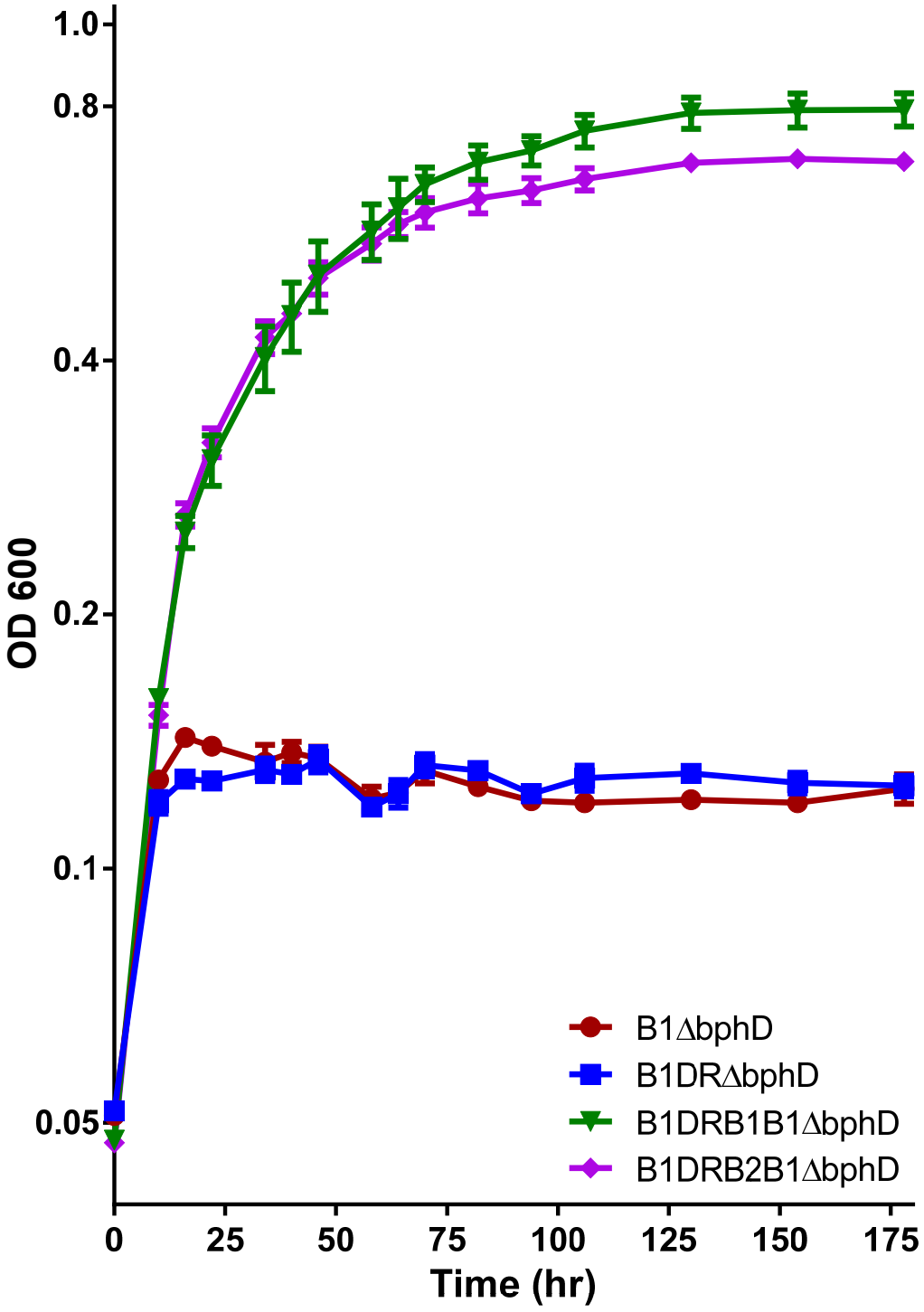

Figure 16. Effect of *bphD* deletion on growth of *S. yanoikuyae* B1 and its engineered strain on biphenyl.

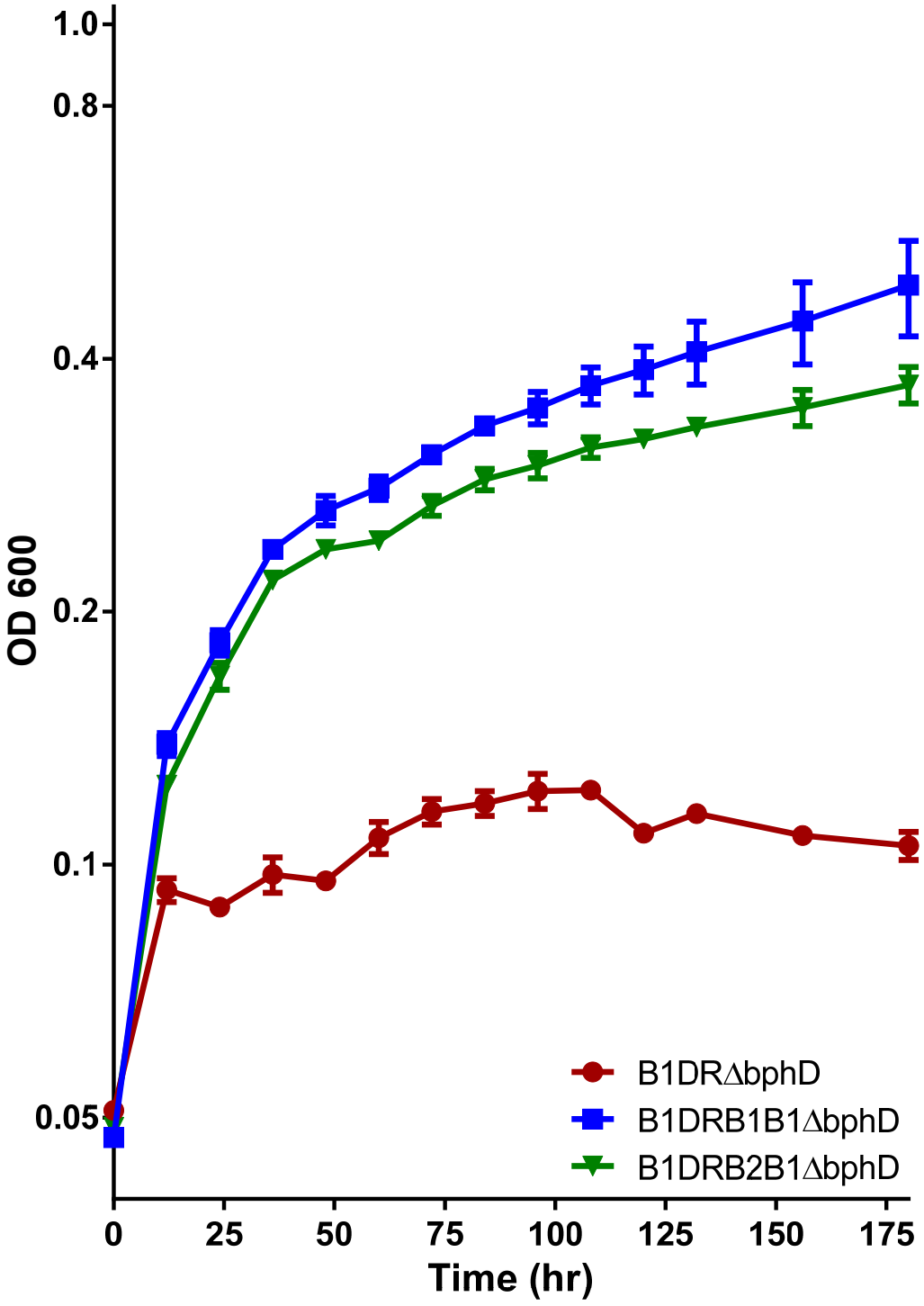

Figure 17. Effect of *bphD* deletion on growth of *S. yanoikuyae* B1 and its engineered strain on dibenzo-*p*-dioxin.

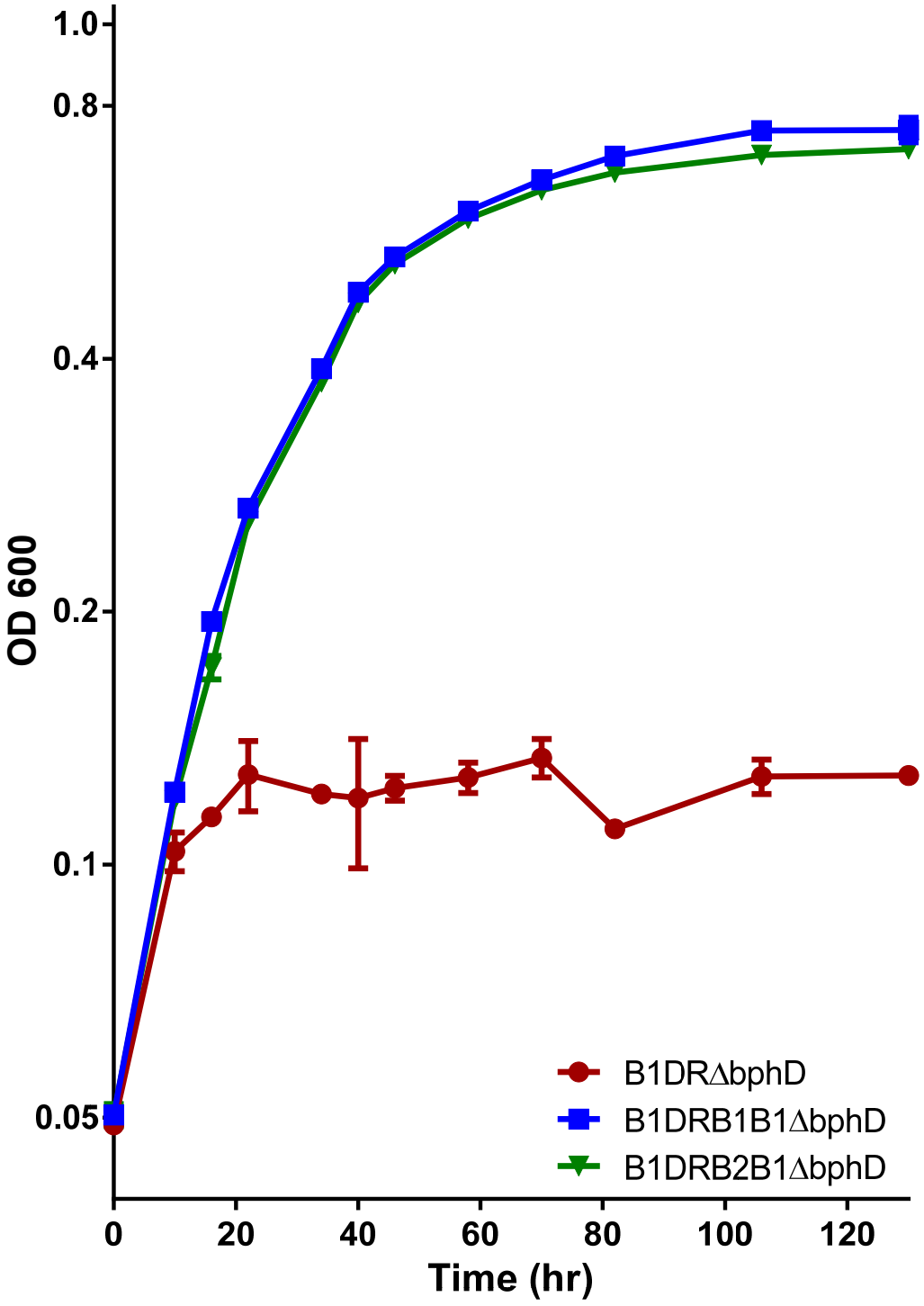

Figure 18. Effect of *bphD* deletion on growth of *S. yanoikuyae* B1 and its engineered strain on dibenzofuran.

Appendices

Appendix A: High Performance Liquid Chromatography Data

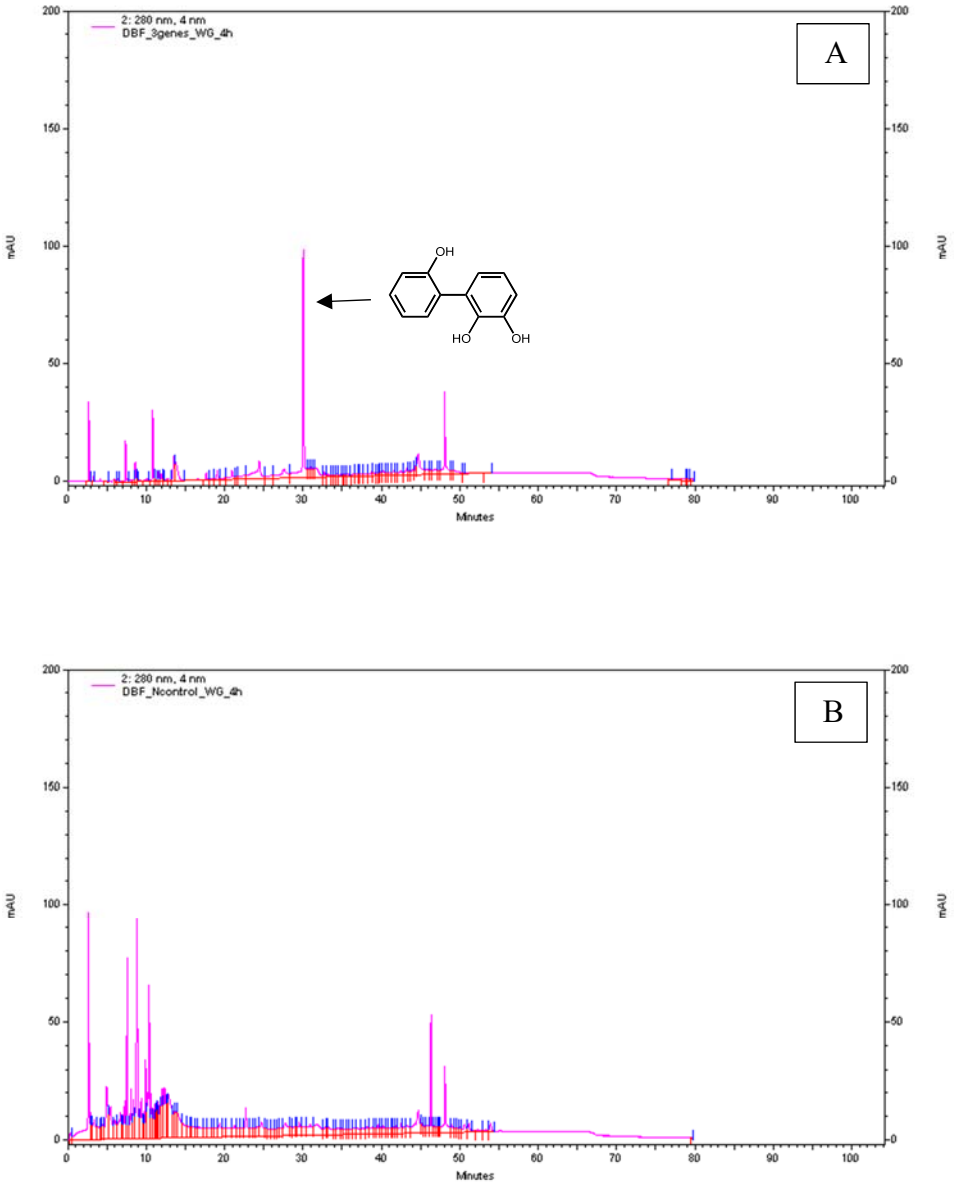

Figure (A.1): HPLC analysis of supernatant from induced cultures of (A) BL21/pET-DBFDOS (B) BL21/pET-30a (control) incubated with DBF for 4 hours. Chromatograms were recorded at a wavelength of 280nm.

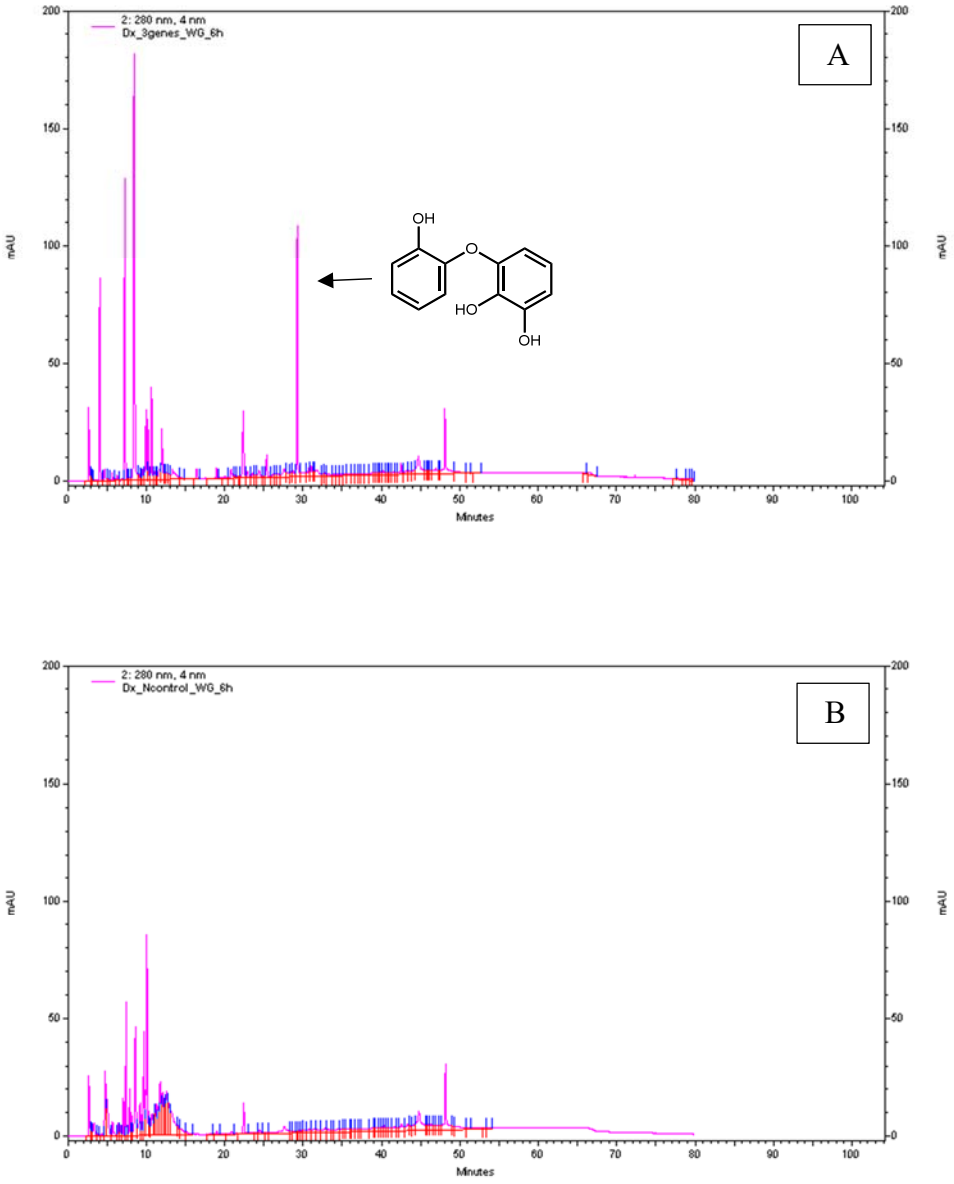

Figure (A.2): HPLC analysis of supernatant from induced cultures of (A) BL21/pET-DBFDOS (B) BL21/pET-30a (control) incubated with DD for 6 hours. Chromatograms were recorded at a wavelength of 280nm.

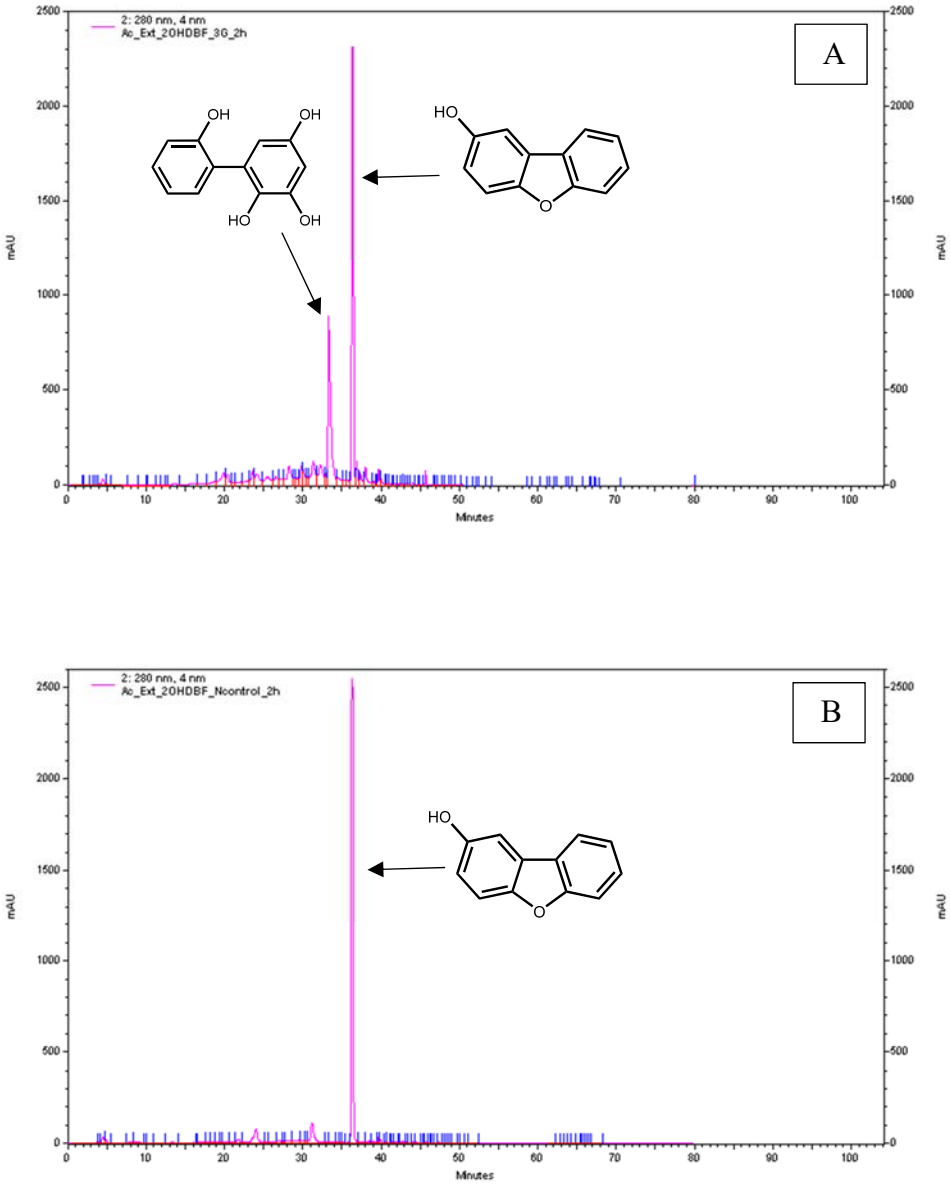

Figure (A.3): HPLC analysis of supernatant from induced cultures of (A) BL21/pET-DBFDOS (B) BL21/pET-30a (control) incubated with 2-hydroxyDBF for 2 hours. Chromatograms were recorded at a wavelength of 280nm.

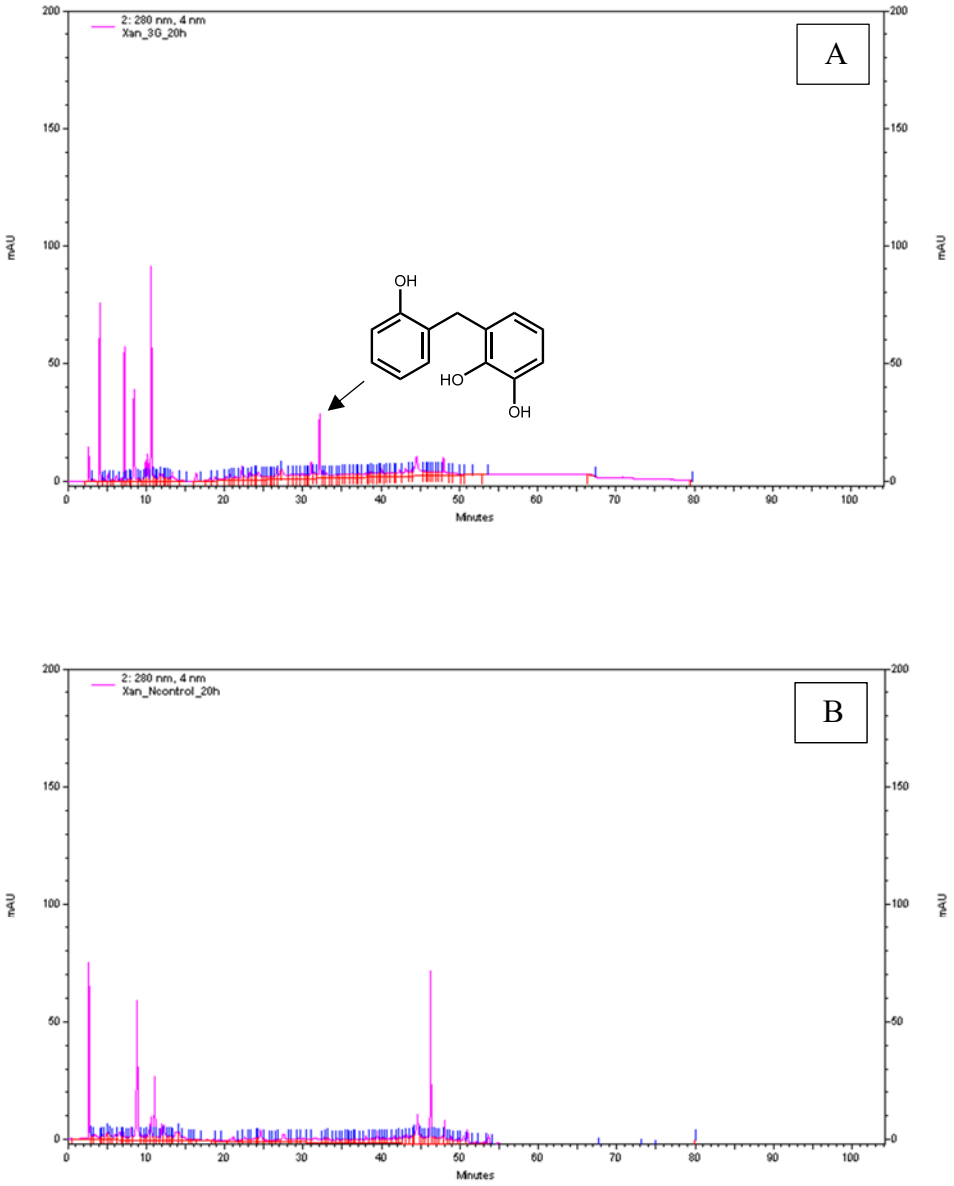

Figure (A.4): HPLC analysis of supernatant from induced cultures of (A) BL21/pET-DBFDOS (B) BL21/pET-30a (control) incubated with xanthene for 20 hours. Chromatograms were recorded at a wavelength of 280nm.

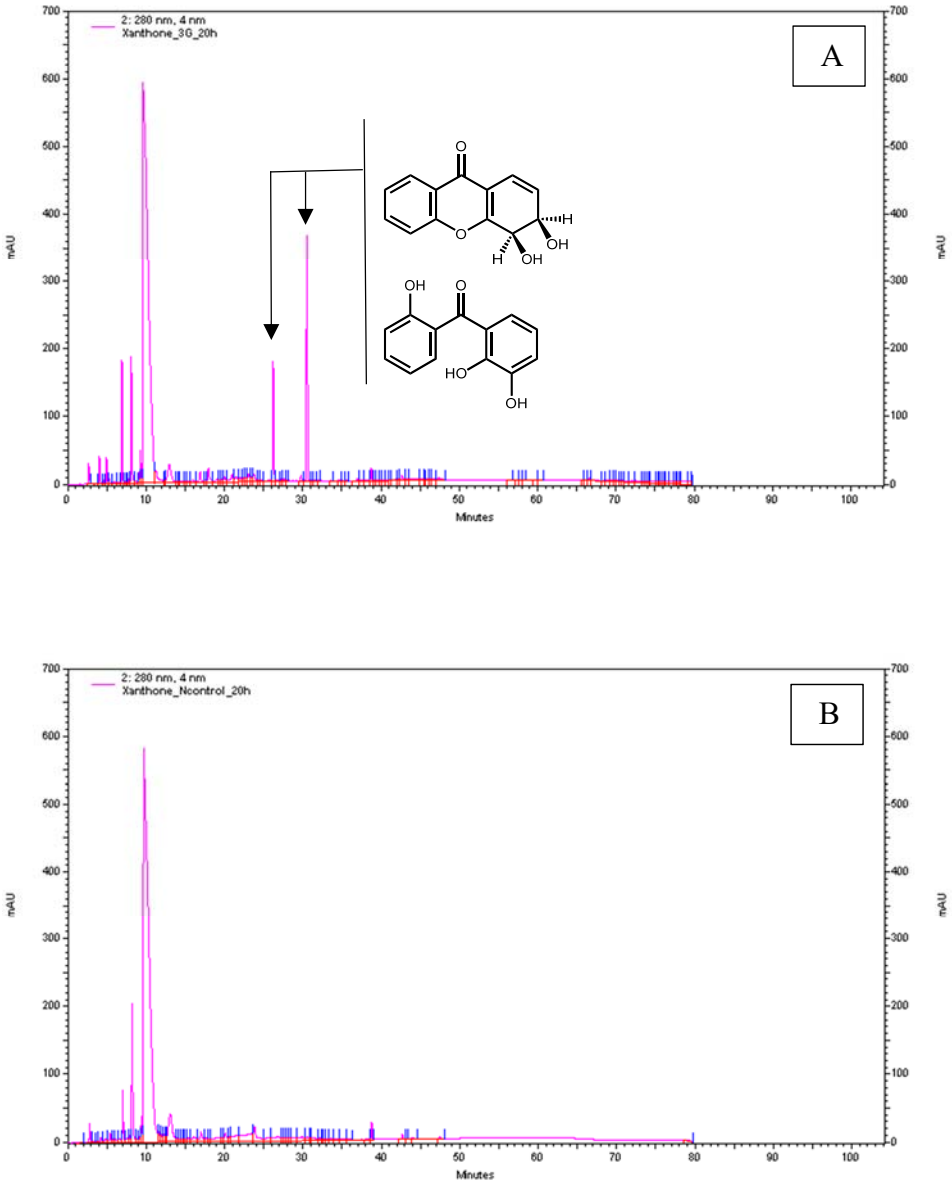

Figure (A.5): HPLC analysis of supernatant from induced cultures of (A) BL21/pET-DBFDOS (B) BL21/pET-30a (control) incubated with xanthone for 20 hours. Chromatograms were recorded at a wavelength of 280nm.

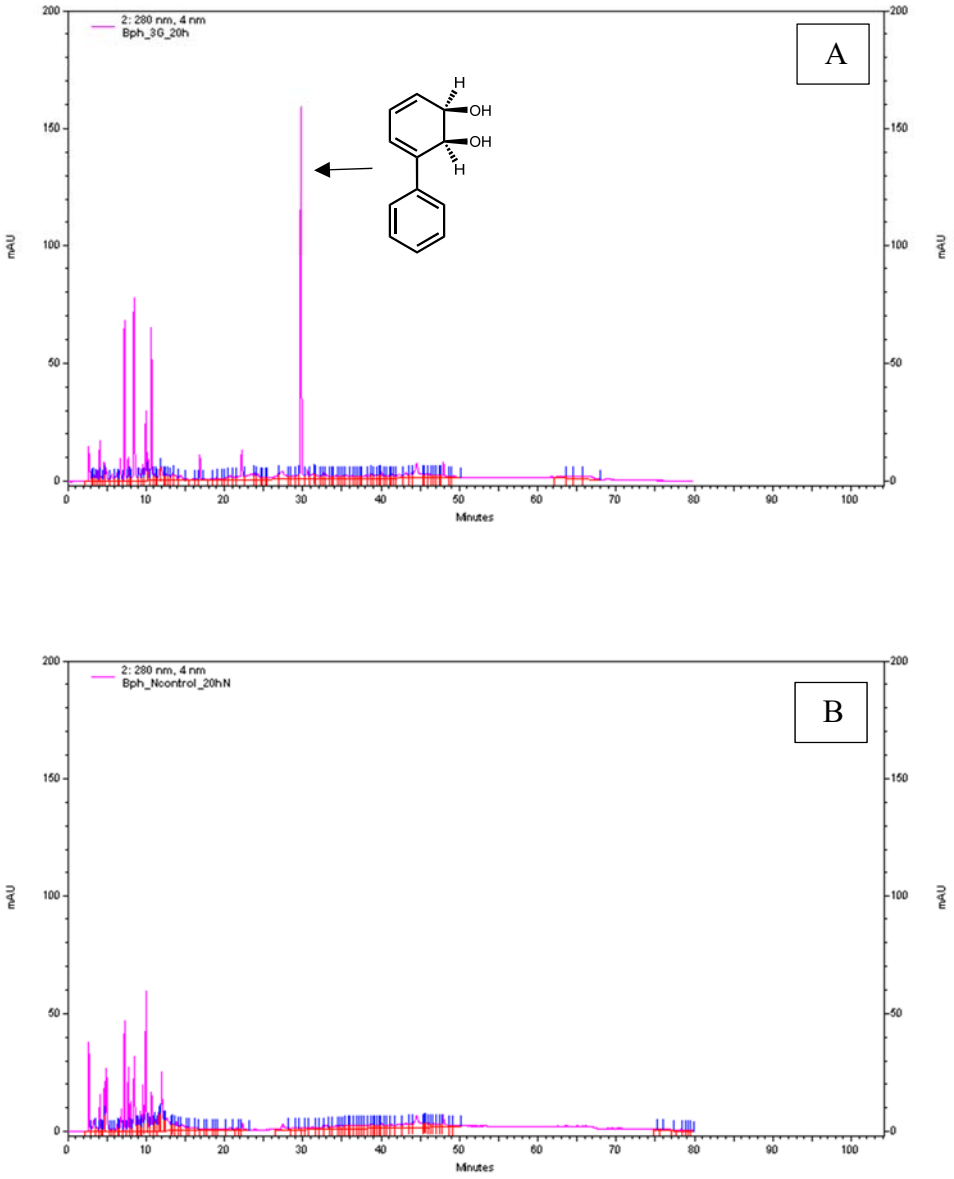

Figure (A.6): HPLC analysis of supernatant from induced cultures of (A) BL21/pET-DBFDOS (B) BL21/pET-30a (control) incubated with biphenyl for 20 hours. Chromatograms were recorded at a wavelength of 280nm.

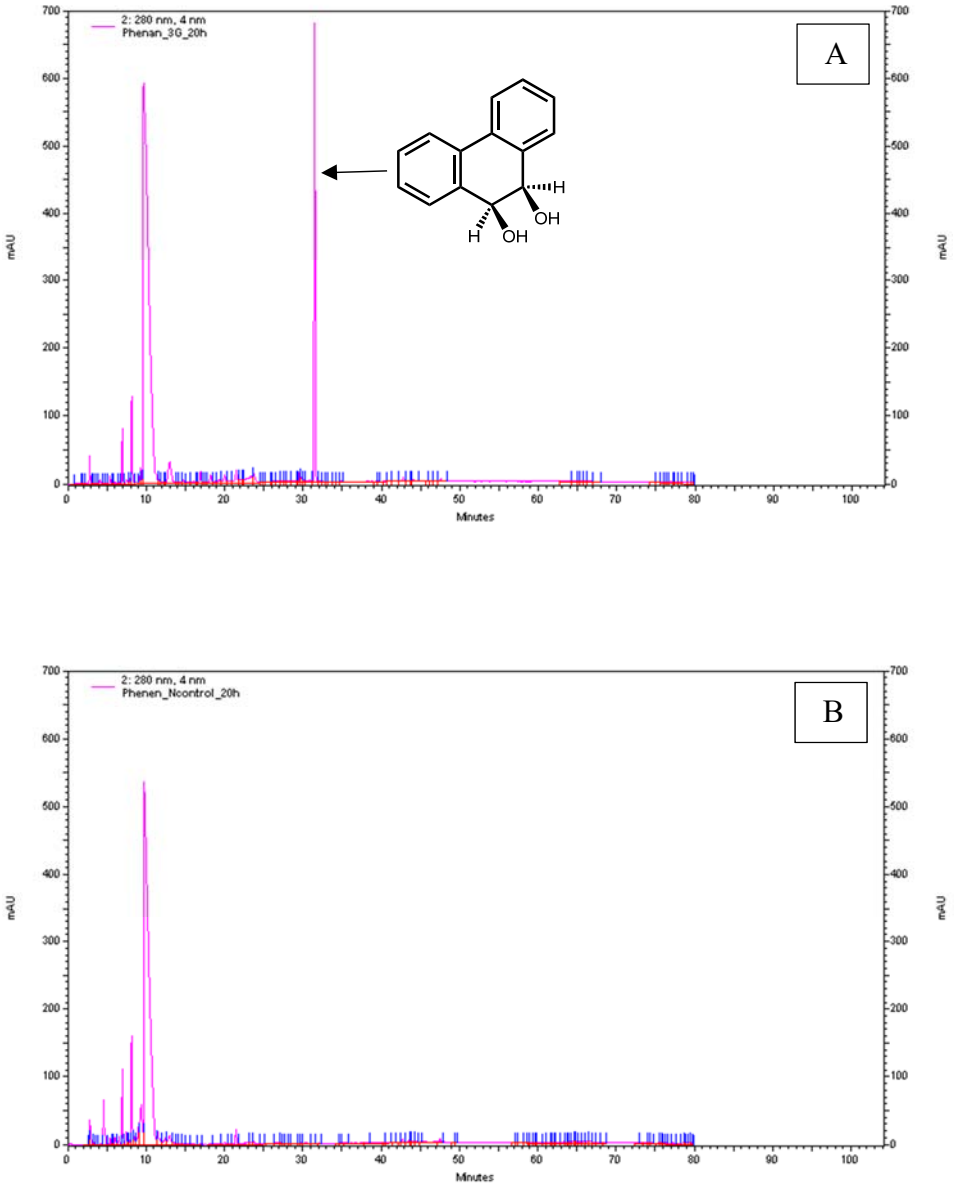

Figure (A.7): HPLC analysis of supernatant from induced cultures of (A) BL21/pET-DBFDOS (B) BL21/pET-30a (control) incubated with phenanthrene for 20 hours. Chromatograms were recorded at a wavelength of 280nm.

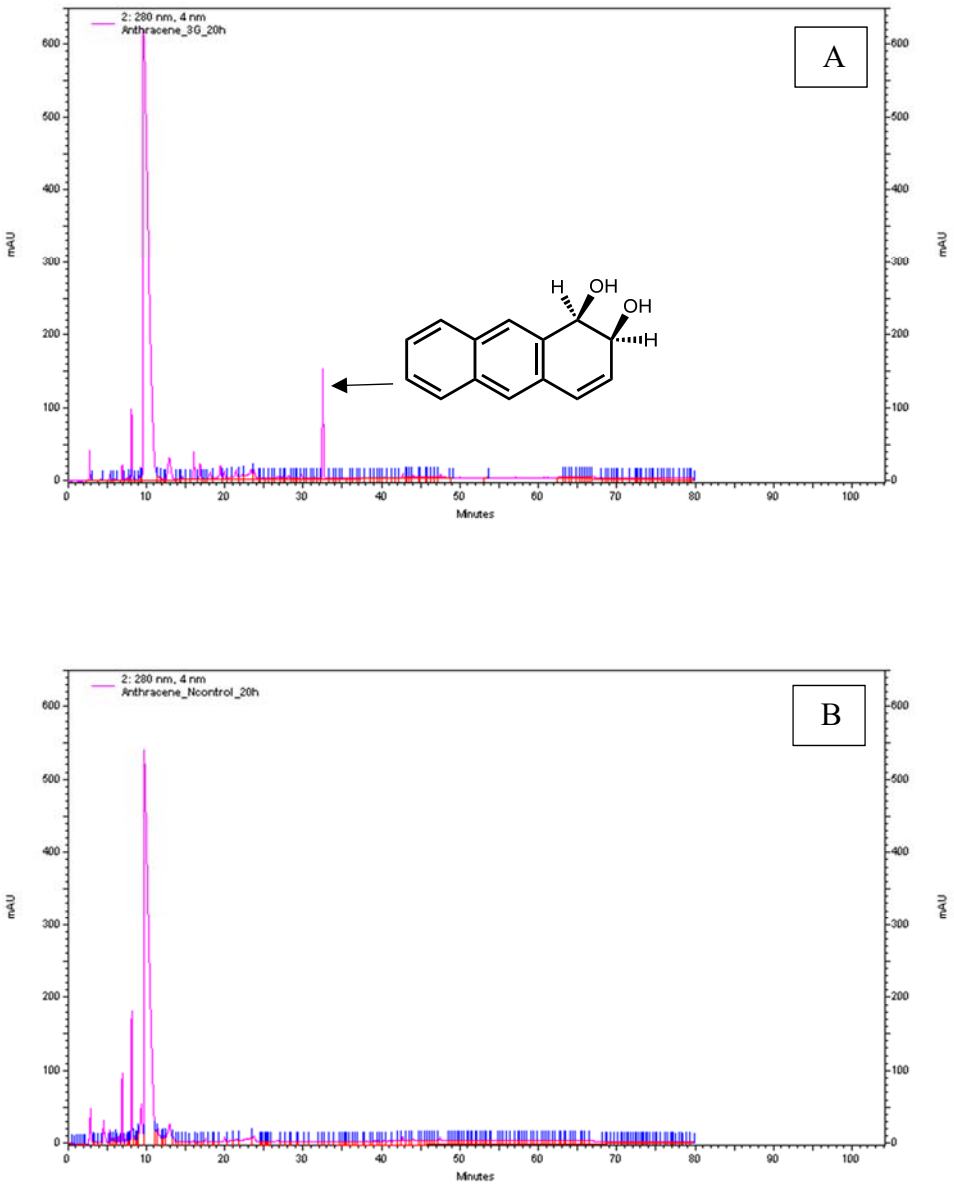

Figure (A.8): HPLC analysis of supernatant from induced cultures of (A) BL21/pET-DBFDOS (B) BL21/pET-30a (control) incubated with anthracene for 20 hours. Chromatograms were recorded at a wavelength of 280nm.

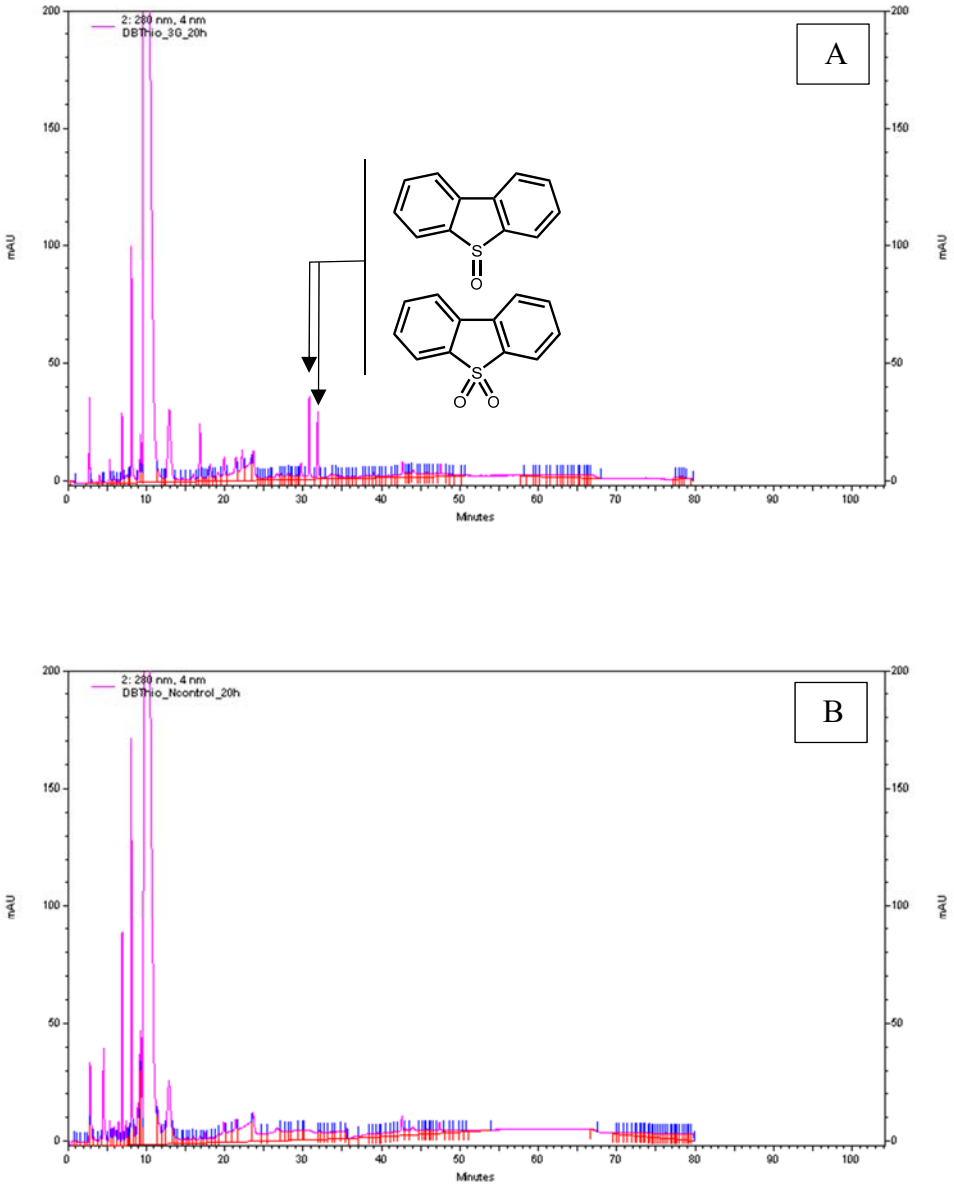

Figure (A.9): HPLC analysis of supernatant from induced cultures of (A) BL21/pET-DBFDOS (B) BL21/pET-30a (control) incubated with dibenzothiopene for 20 hours. Chromatograms were recorded at a wavelength of 280nm.

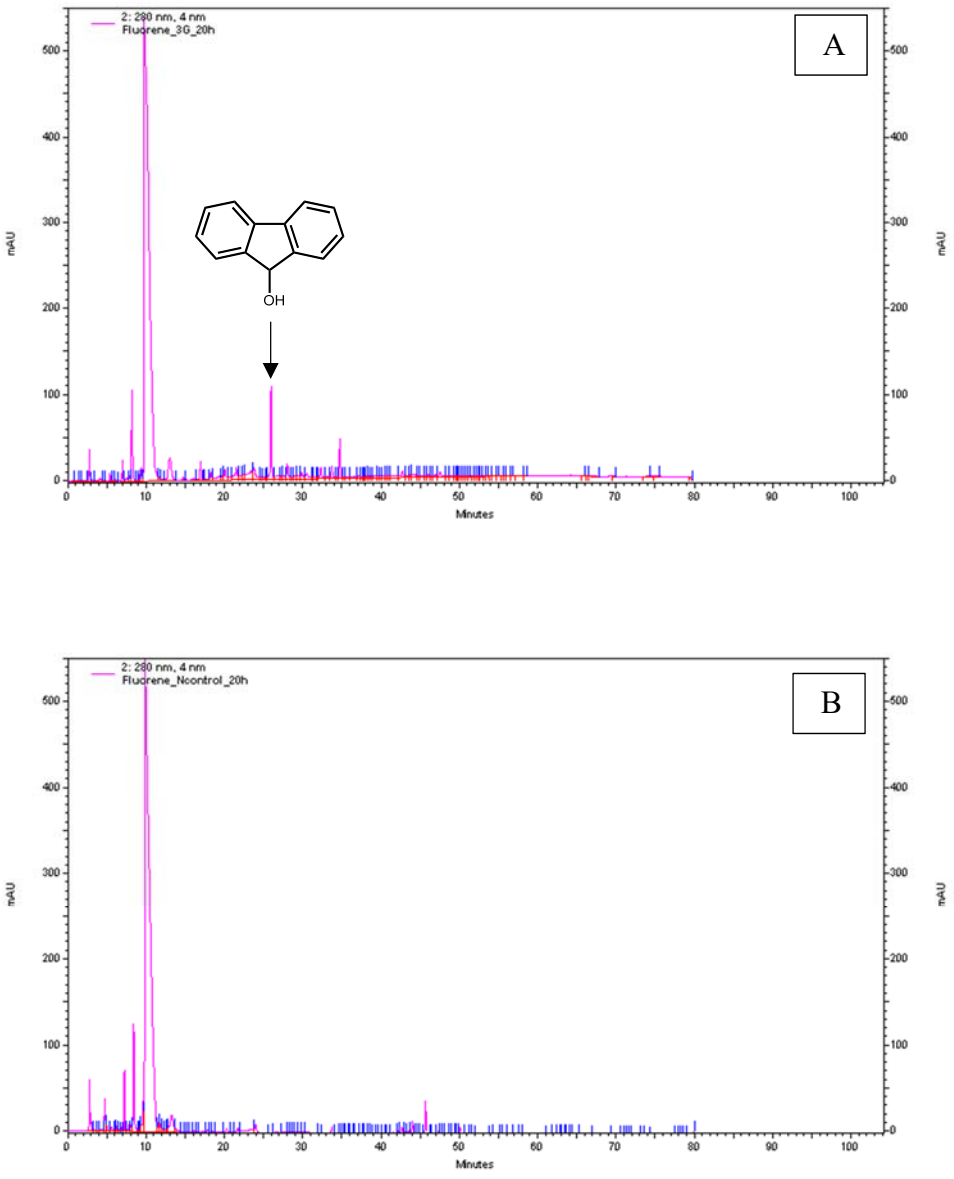

Figure (A.10): HPLC analysis of supernatant from induced cultures of (A) BL21/pET-DBFDOS (B) BL21/pET-30a (control) incubated with fluorene for 20 hours. Chromatograms were recorded at a wavelength of 280nm.

Appendix B: Gas Chromatography - Mass Spectrometry Data

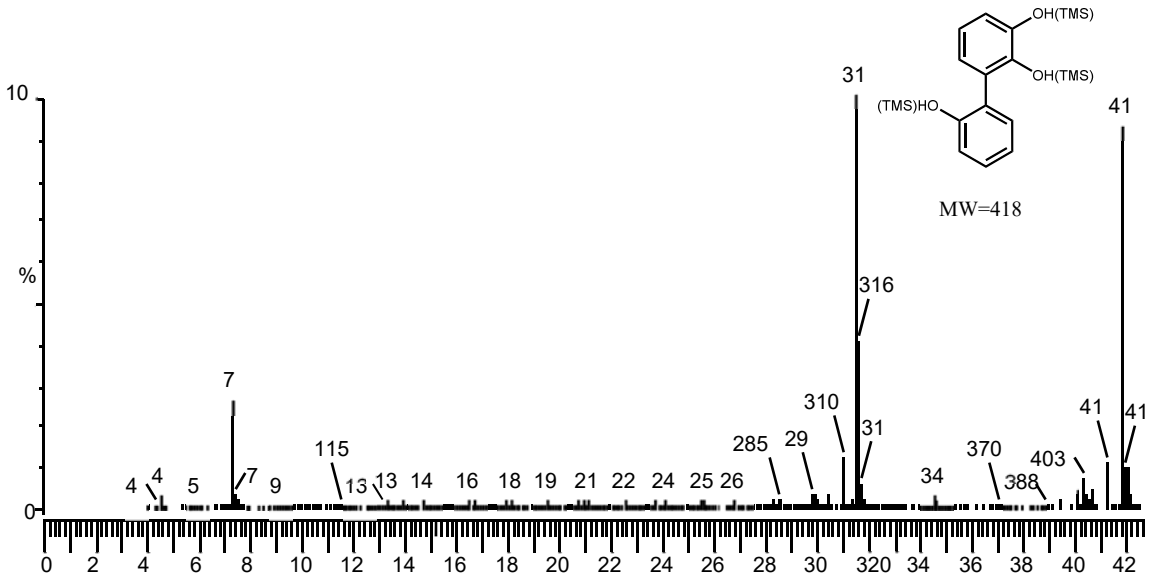

Fig (B.1): GC-MS of 2,2',3-trihydroxybiphenyl. The x axis represents the retention time and the y axis is the relative abundance.

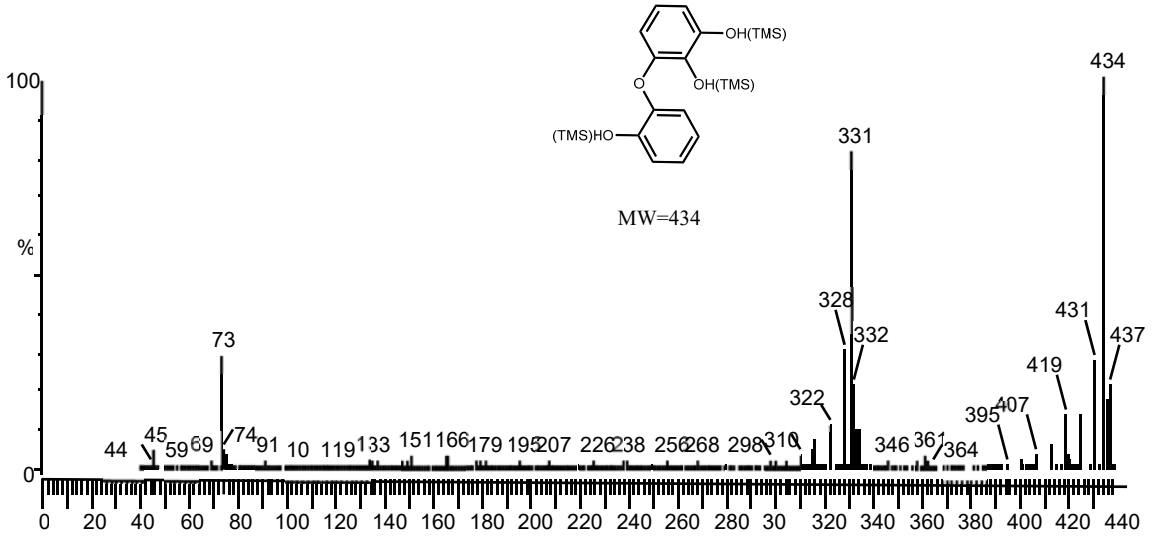

Fig (B.2): GC-MS of 2,2',3-trihydroxydiphenylether. The x axis represents the retention time and the y axis is the relative abundance.

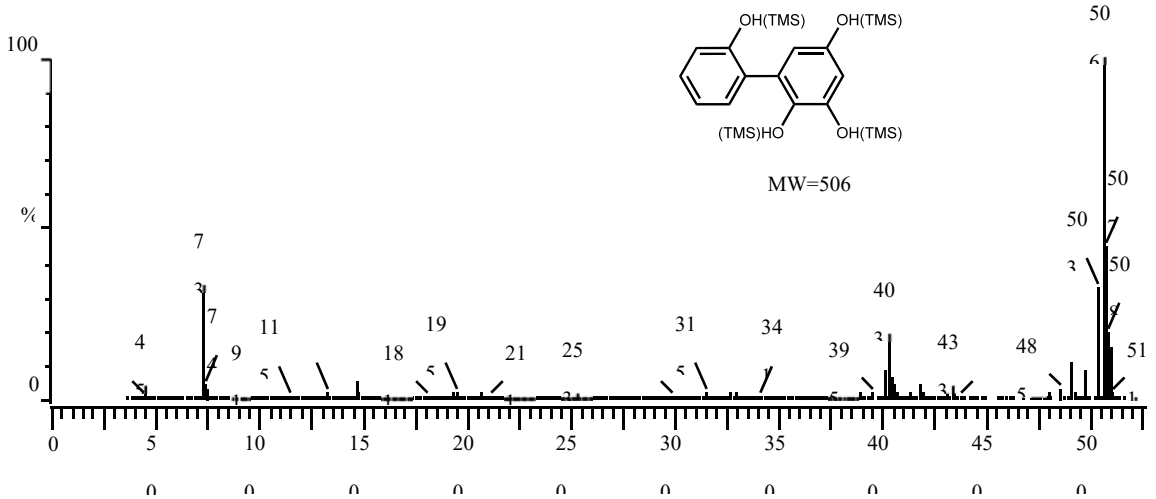

Fig (B.3): GC-MS of 2,2',3,5-tetrahydroxybiphenyl. The x axis represents the retention time and the y axis is the relative abundance.

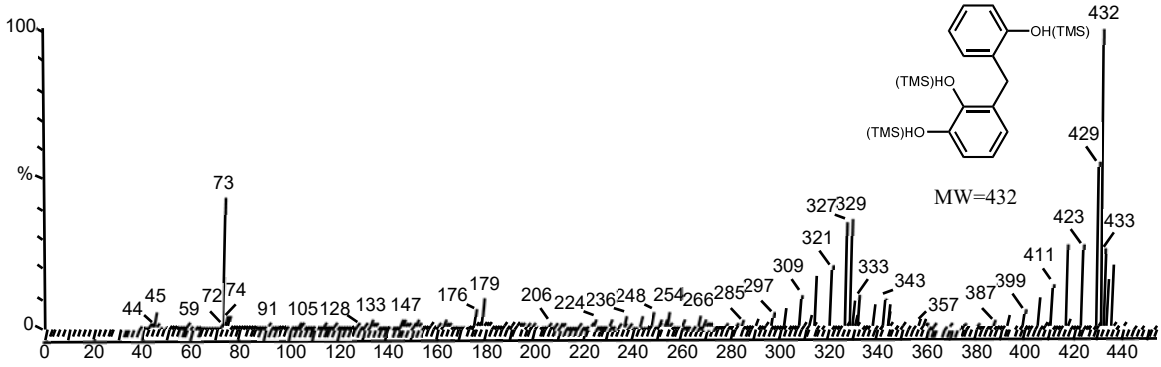

Fig (B.4): GC-MS of 2,2',3-trihydroxydiphenylmethane. The x axis represents the retention time and the y axis is the relative abundance.

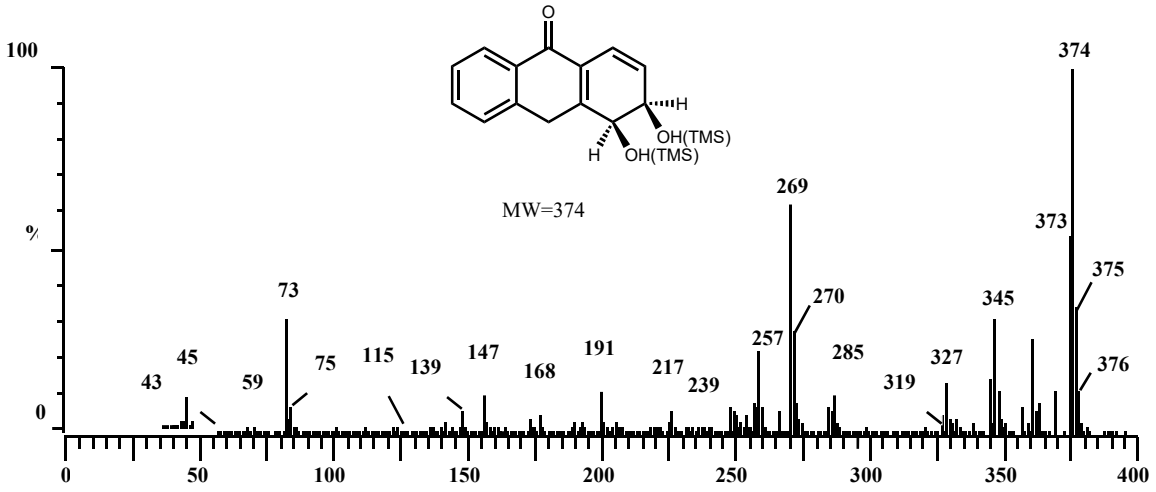

Fig (B.5): GC-MS of *cis*-3,4-dihydro-3,4-dihydroxyxanthone. The x axis represents the retention time and the y axis is the relative abundance.

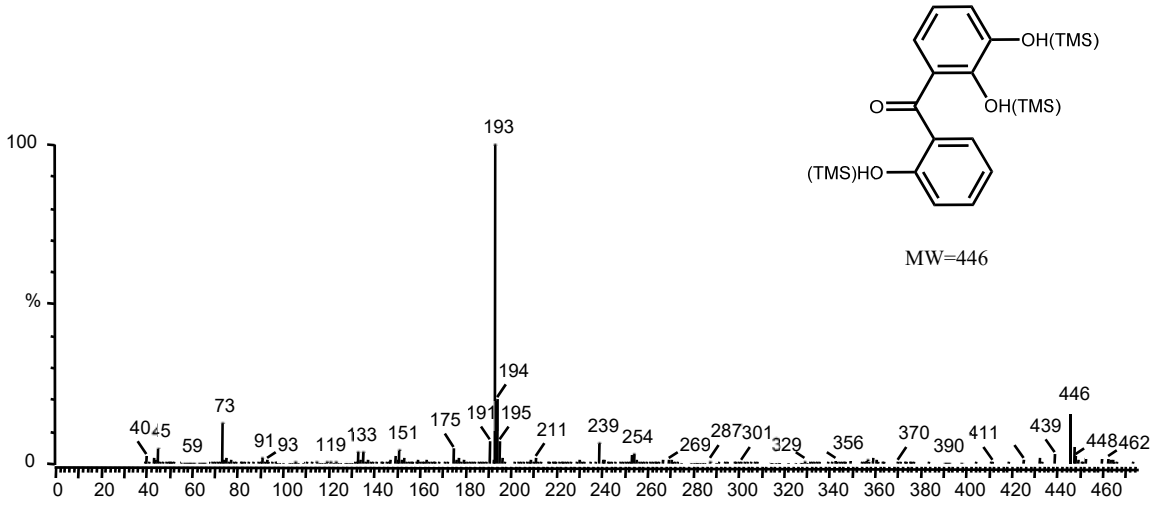

Fig (B.6): GC-MS of 2,2',3-trihydroxybenzophenone. The x axis represents the retention time and the y axis is the relative abundance.

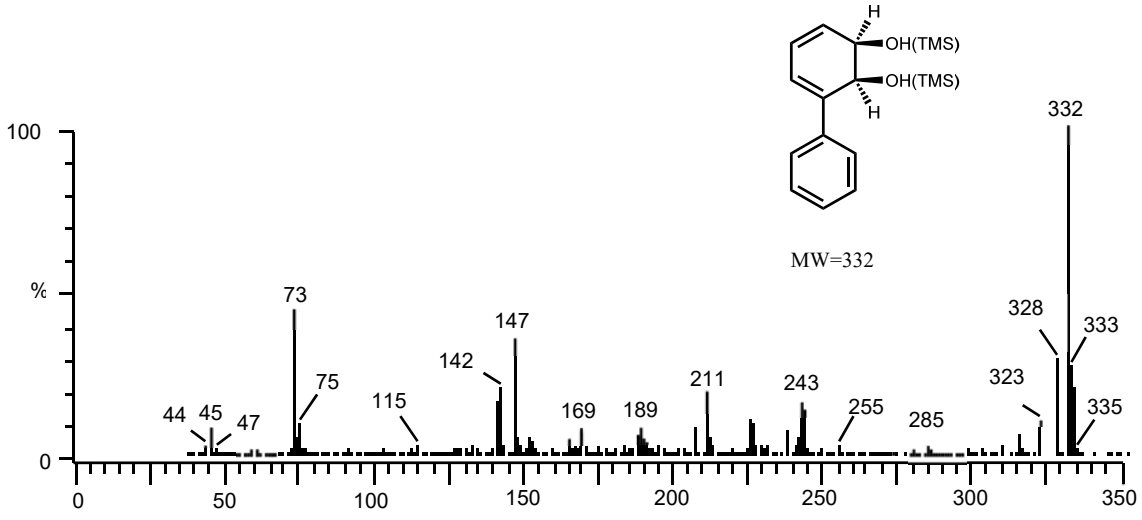

Fig (B.7): GC-MS of *cis*-2,3-dihydro-2,3-dihydroxybiphenyl. The x axis represents the retention time and the y axis is the relative abundance.

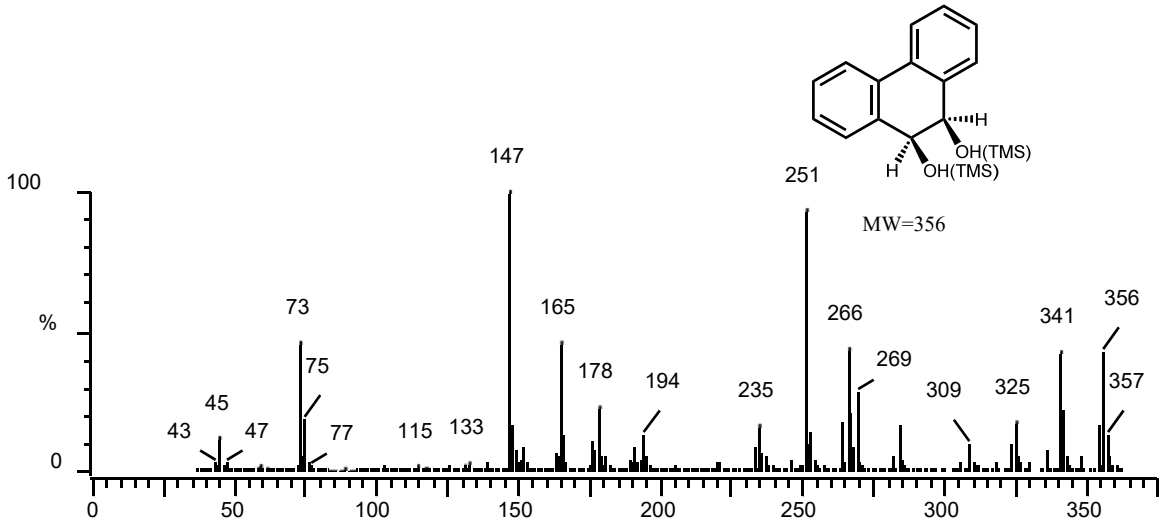

Fig (B.8): GC-MS of *cis*-9,10-dihydro-9,10-dihydroxyphenanthrene. The x axis represents the retention time and the y axis is the relative abundance.

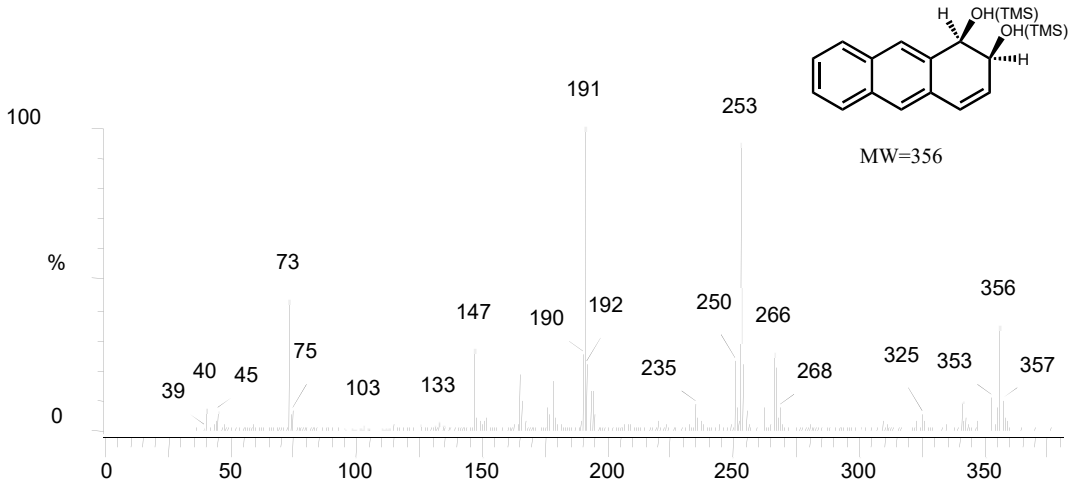

Fig (B.9): GC-MS of *cis*-1,2-dihydro-1,2-dihydroxy-anthracene. The x axis represents the retention time and the y axis is the relative abundance.

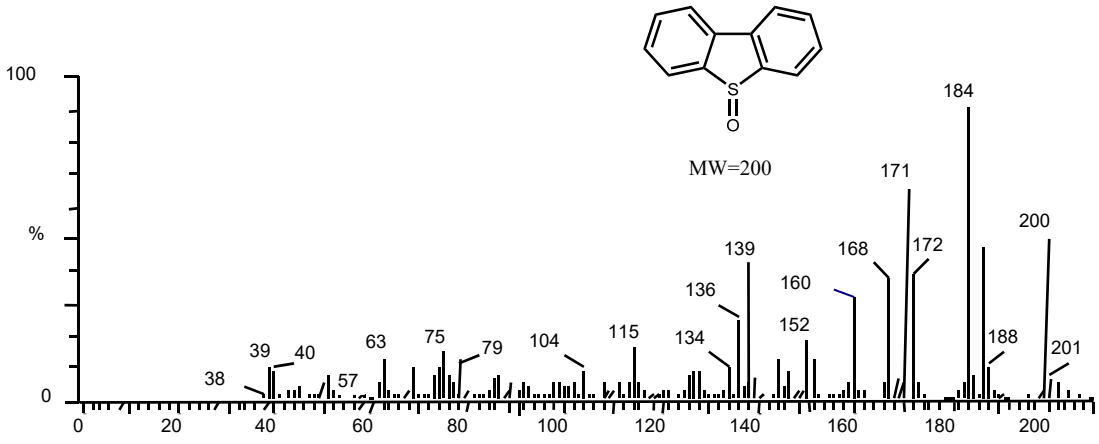

Fig (B.10): GC-MS of dibenzothiopene sulfoxide. The x axis represents the retention time and the y axis is the relative abundance.

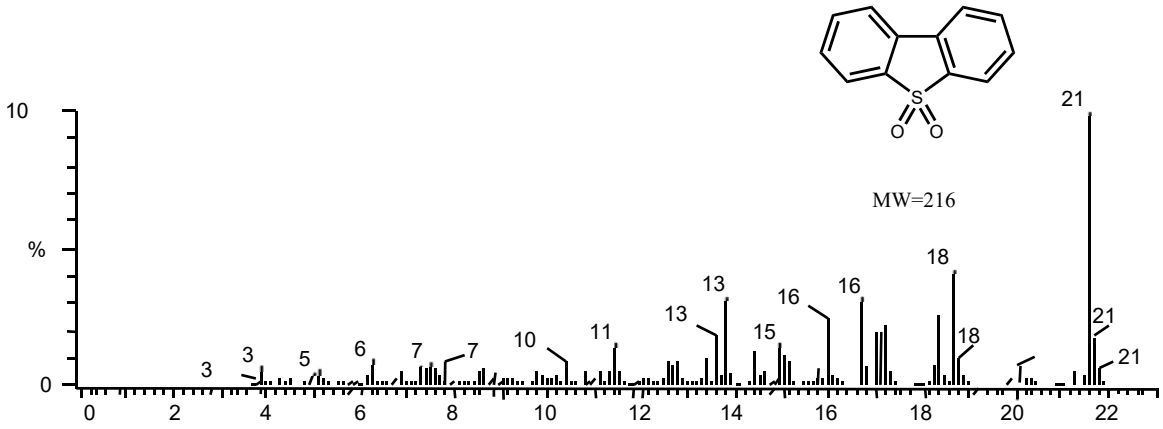

Fig (B.11): GC-MS of dibenzothiopene sulfone. The x axis represents the retention time and the y axis is the relative abundance.

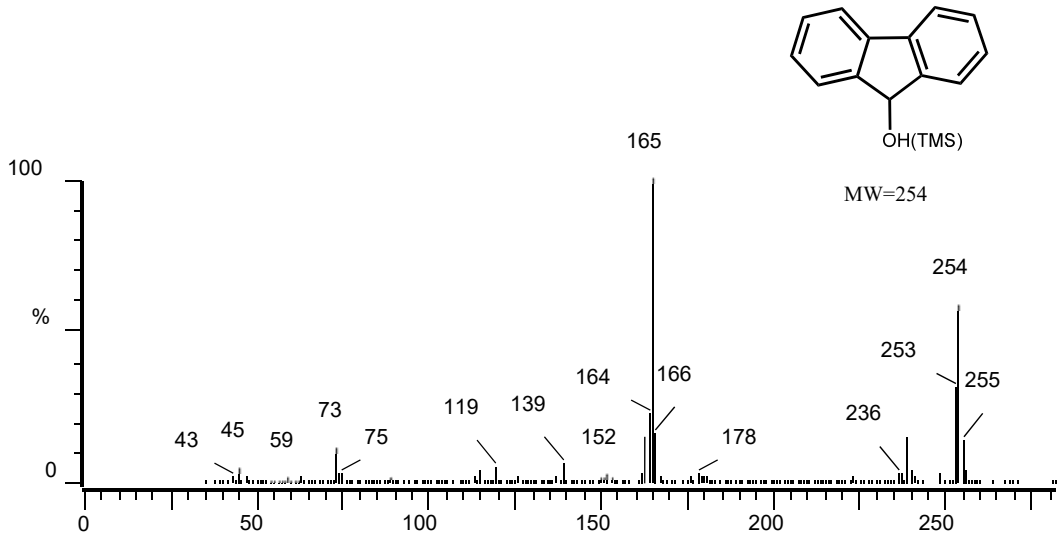

Fig (B.12): GC-MS of 9-hydroxyfluorene. The x axis represents the retention time and the y axis is the relative abundance.

Appendix C: Nuclear Magnetic Resonance Data

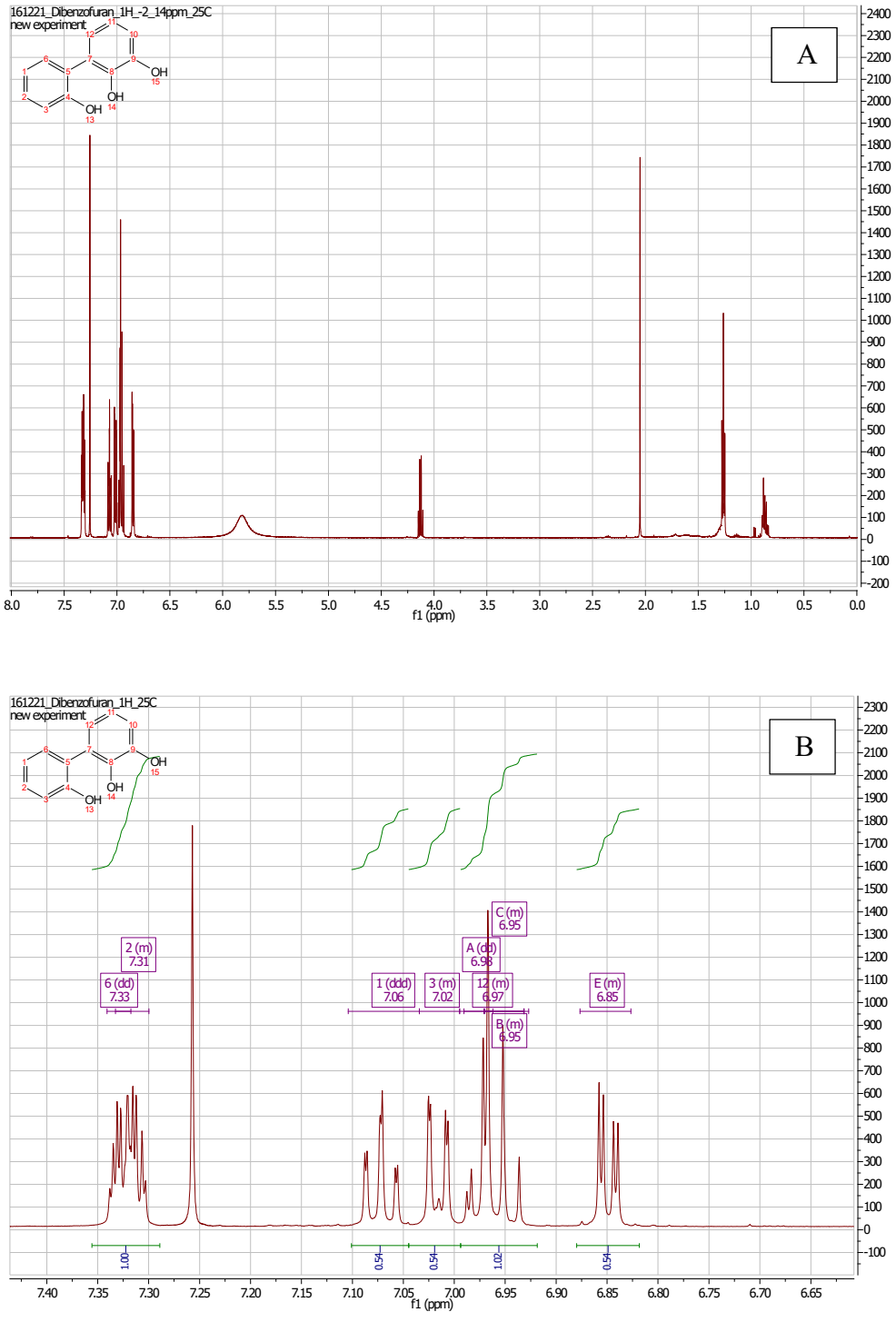

Figure (C.1): ^{1}H NMR spectrum for 2,2',3-trihydroxybiphenyl. (A) whole ^{1}H spectrum (B) expanded aromatic region of the spectrum

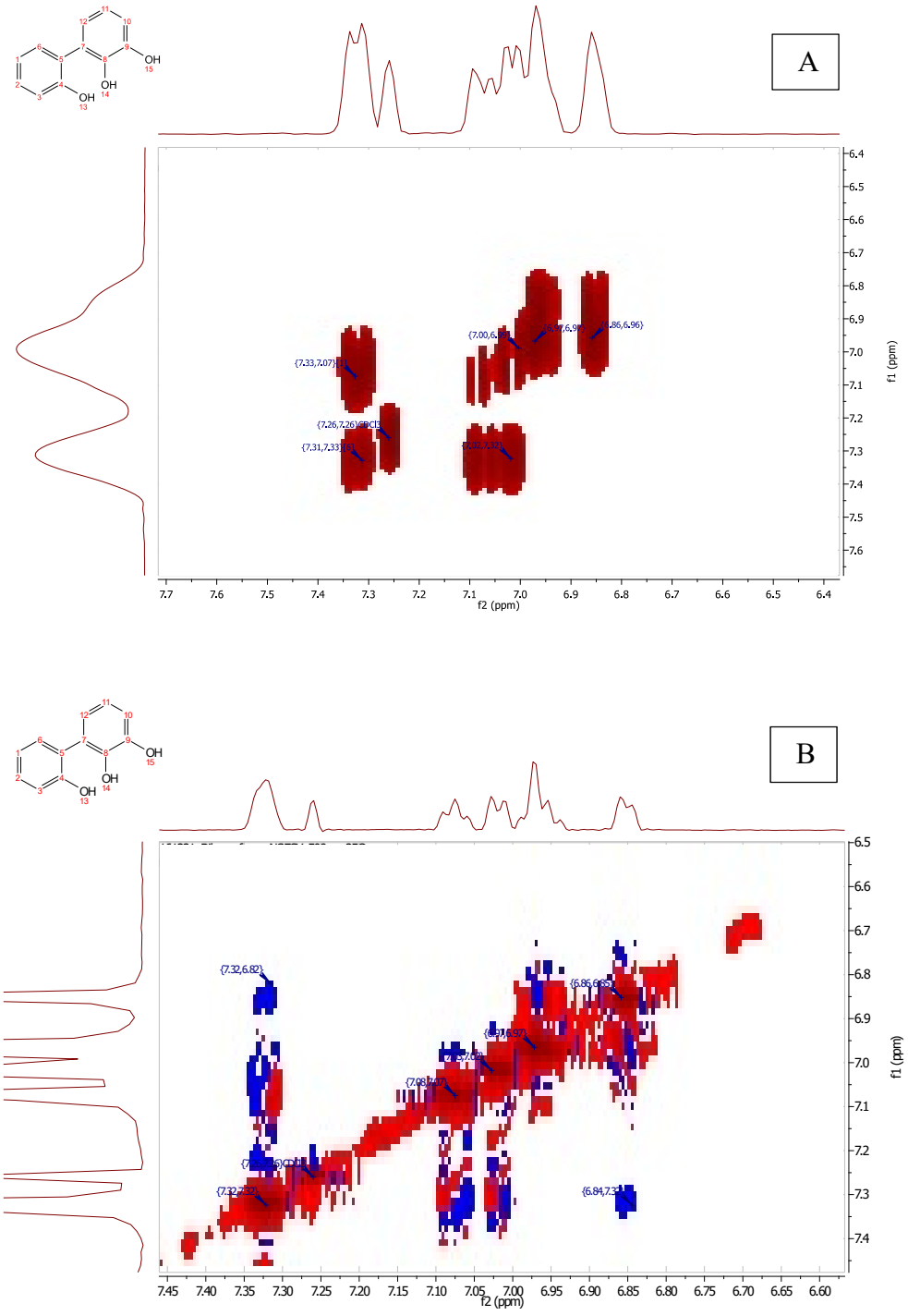

Figure (C.2): Expanded aromatic region for 2,2’,3-trihydroxybiphenyl of (A) COSY spectrum (B) NOESY spectrum

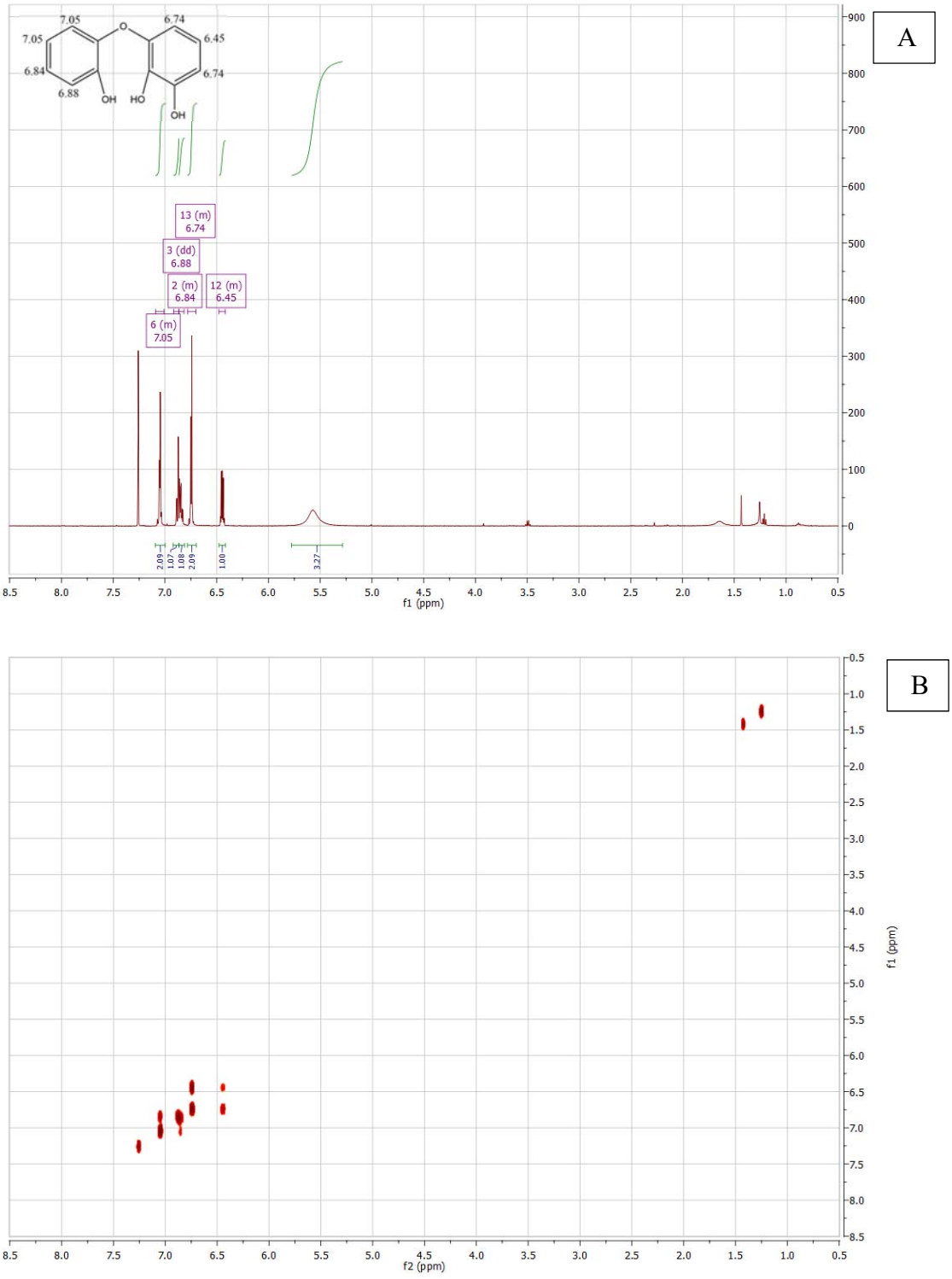

Figure (C.3): ^{1}H NMR spectrum for 2,2',3-trihydroxydiphenylether. (A) whole ^{1}H spectrum (B) gradient enhanced COSY spectrum

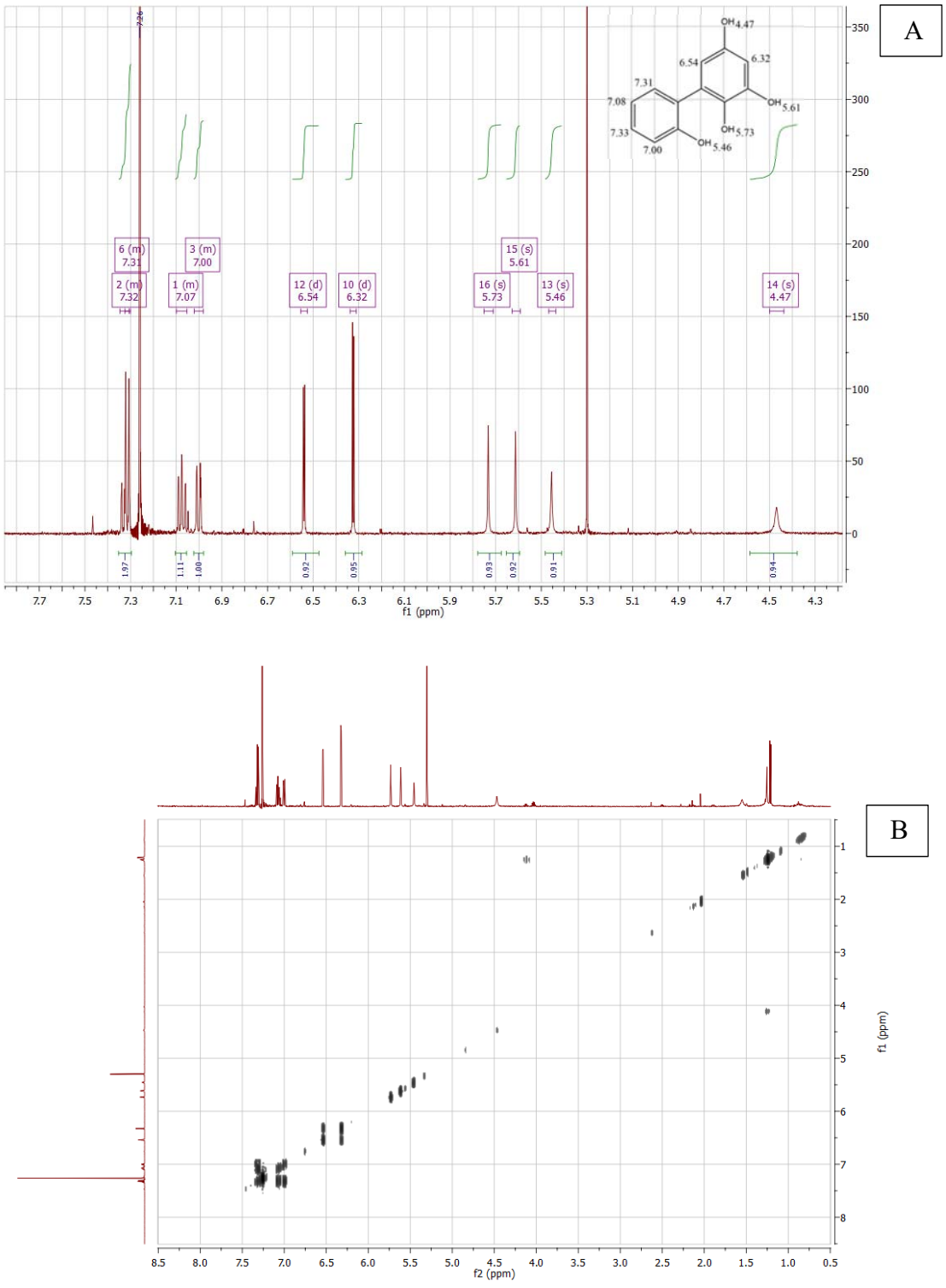

Figure (C.4):[1]H NMR spectrum for 2,2',3,5-tetrahydroxybiphenyl (A) expanded aromatic region (B) gCOSY spectrum

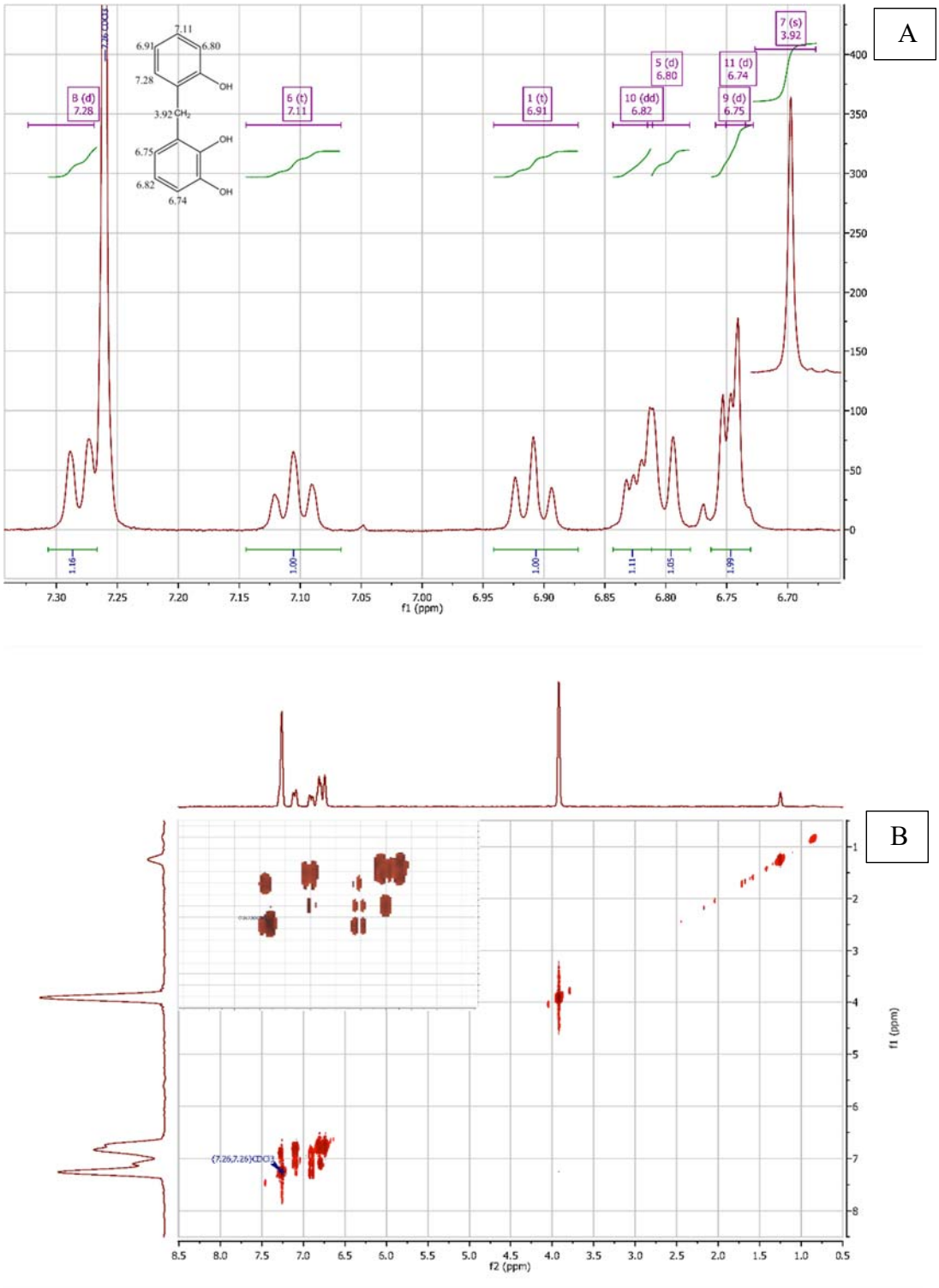

Figure (C.5):NMR spectrum of 2,2',3-trihydroxydiphenylmethane (A) ^{1}H NMR expanded aromatic region, isolated CH2 peaks at 3.92ppm are shown on the right (B) Gradient enhanced COSY spectrum, insert shows the expanded aromatic region.

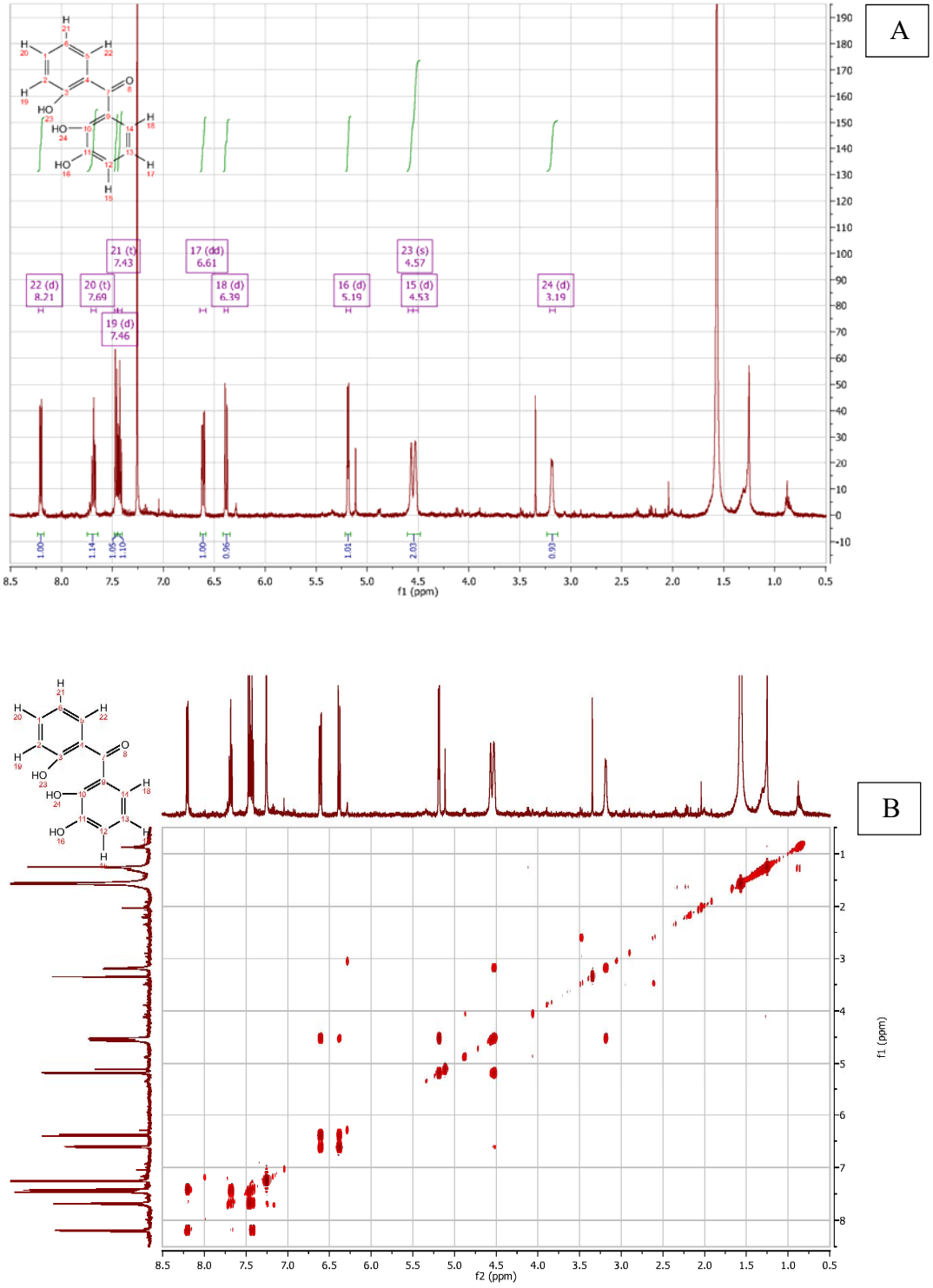

Figure (C.6):NMR spectrum of 2,2',3-trihydroxybenzophenone (A) ^{1}H NMR Expanded aromatic region (B) Gradient enhanced COSY spectrum.

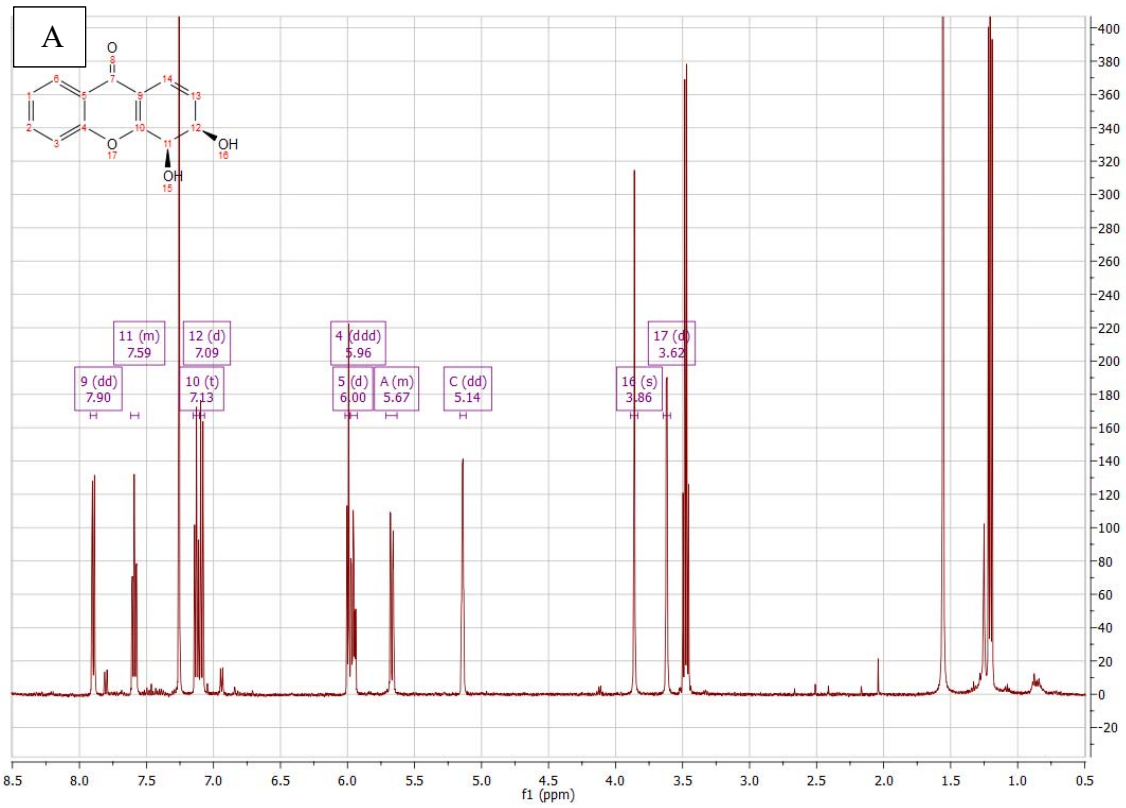

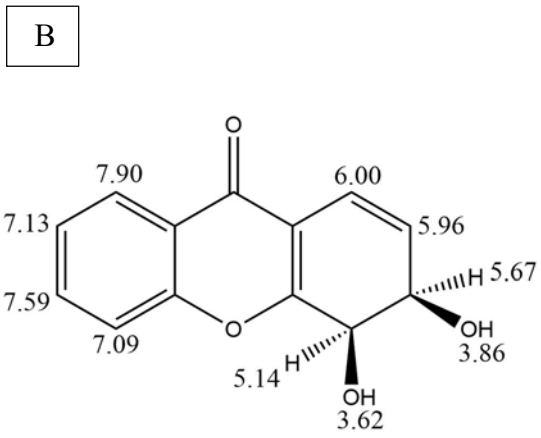

Figure (C.7): (A) ^{1}H NMR spectrum for the expanded aromatic region of *cis*-3,4-dihydro-3,4-dihydroxyxanthone (B) resonance assignment of the product.

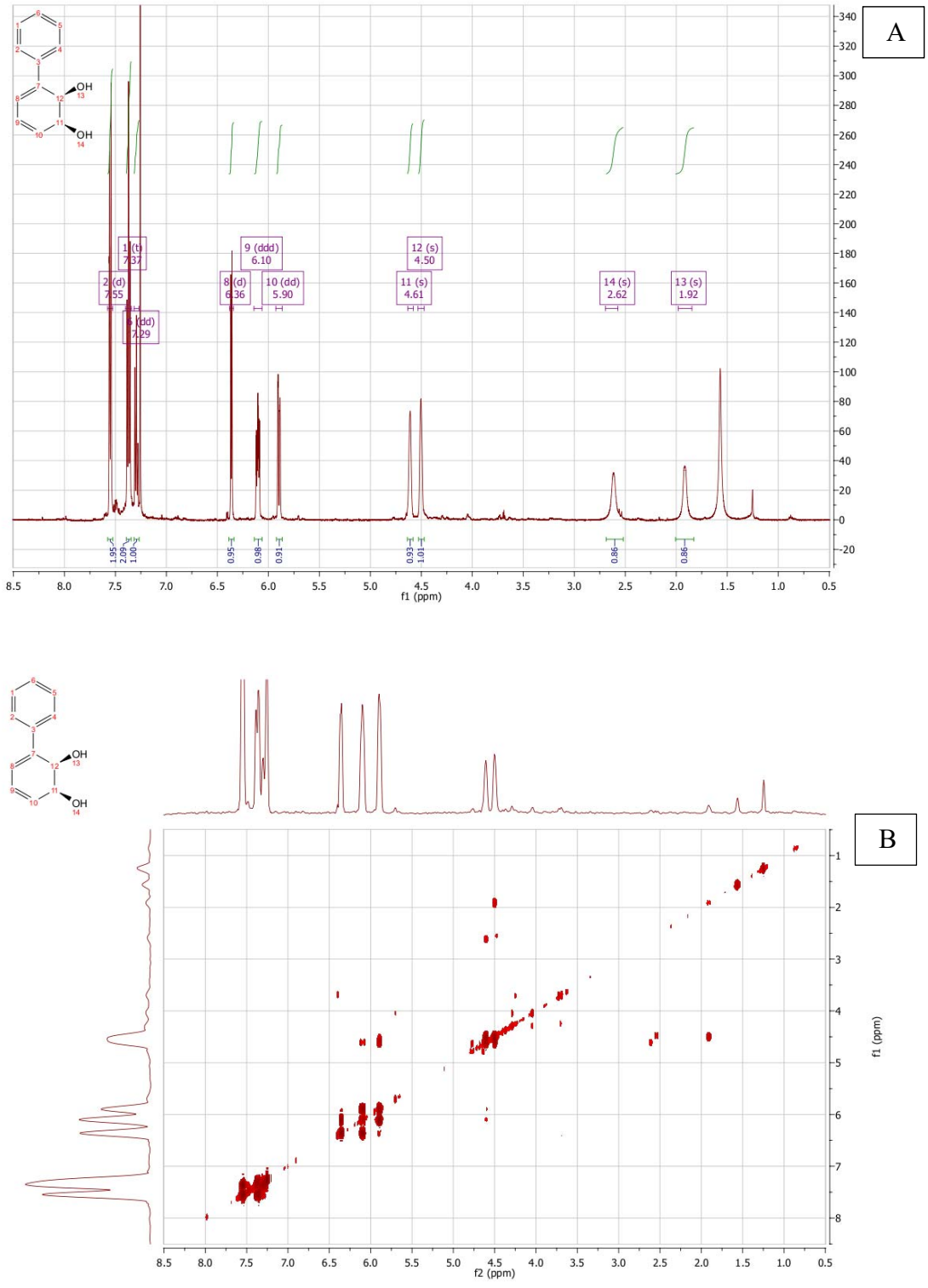

Figure (C.8):NMR spectrum of *cis*-2,3-dihydro-2,3-dihydroxybiphenyl (A) ^{1}H NMR Expanded aromatic region (B) Gradient enhanced COSY spectrum.

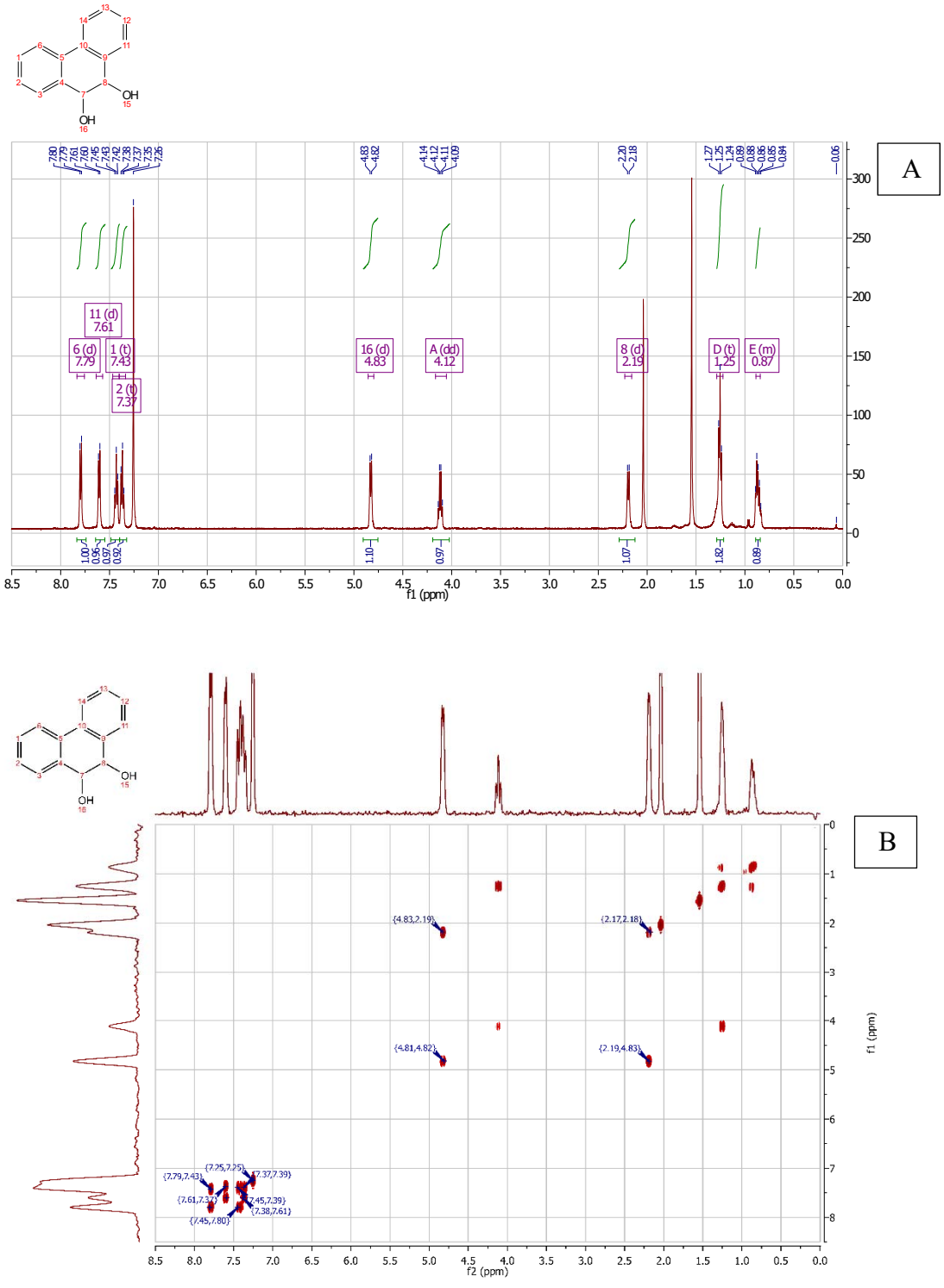

Figure (C.9):NMR spectrum of *cis*-9,10-dihydro-9,10-dihydroxyphenanthrene (A) ^{1}H NMR Expanded aromatic region (B) Gradient enhanced COSY spectrum.

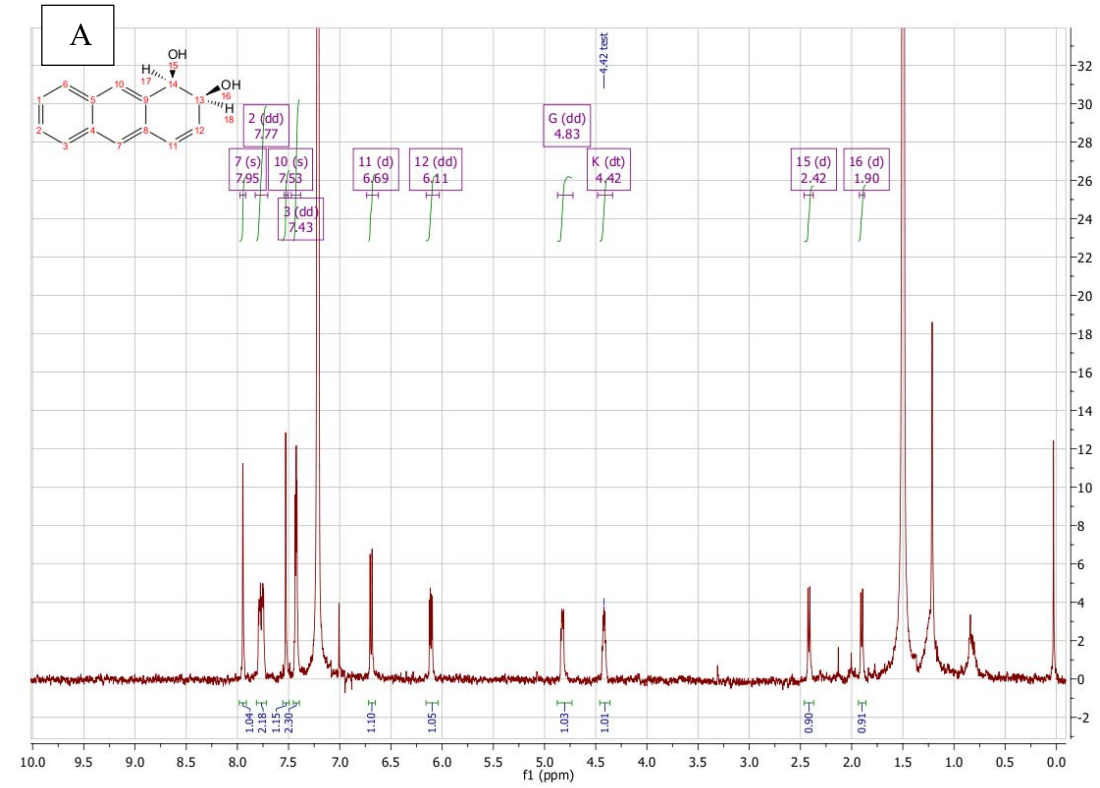

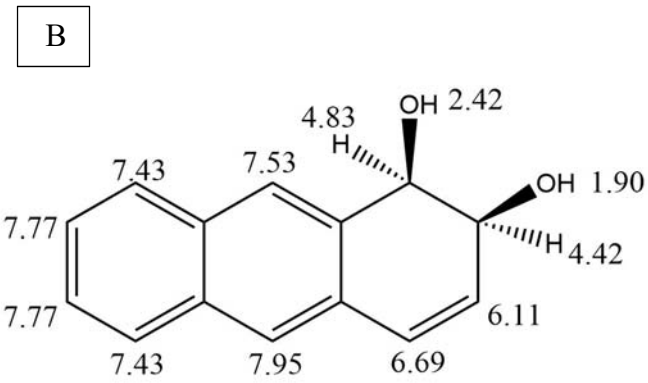

Figure (C.10): (A) ^{1}H NMR spectrum for the expanded aromatic region of *cis*-1,2-dihydro-1,2-dihydroxyanthracene (B) resonance assignment of the product.

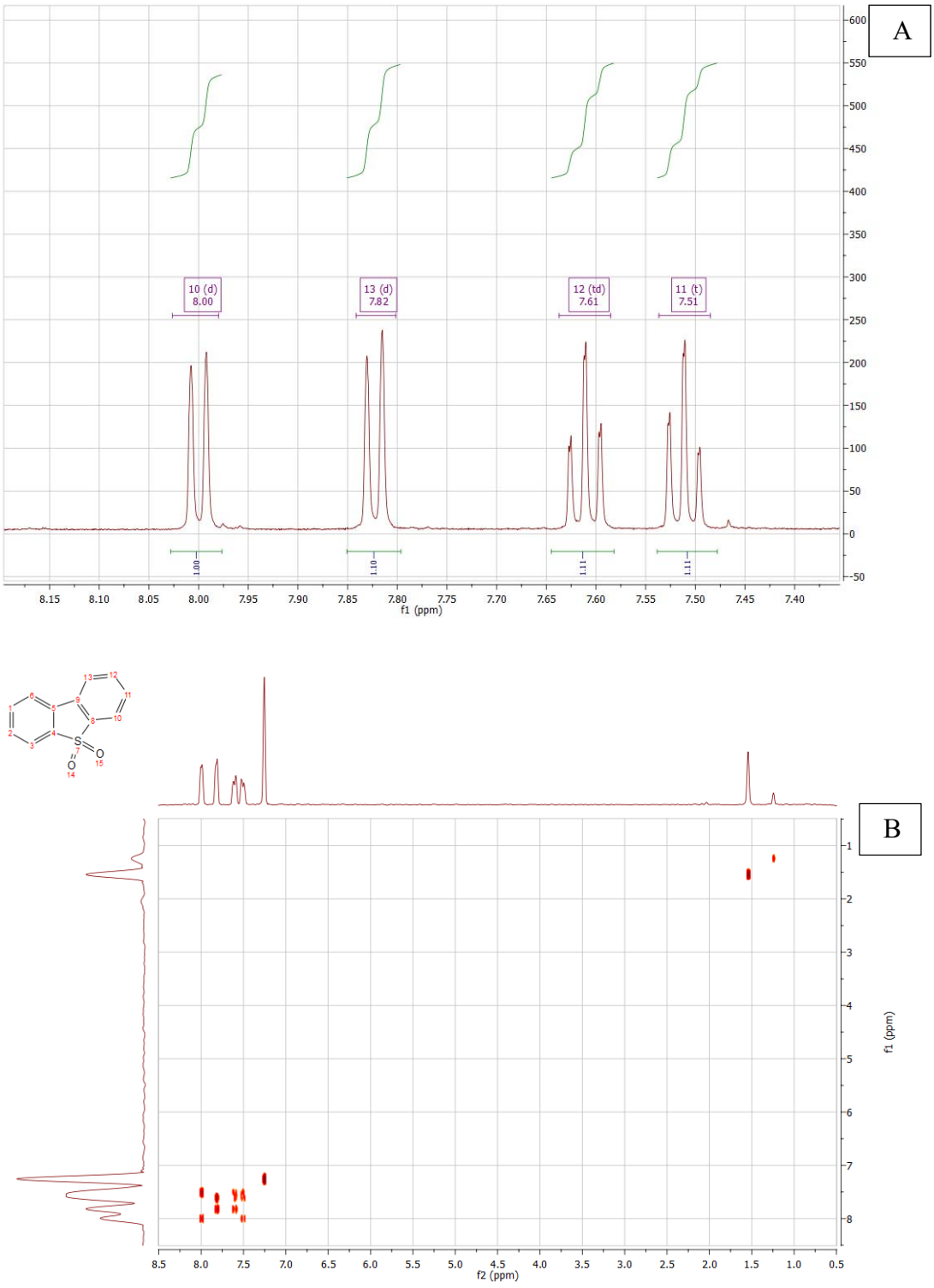

Figure (C.11):NMR spectrum of dibenzothiopene sulfone (A) ^{1}H NMR Expanded aromatic region (B) Gradient enhanced COSY spectrum.

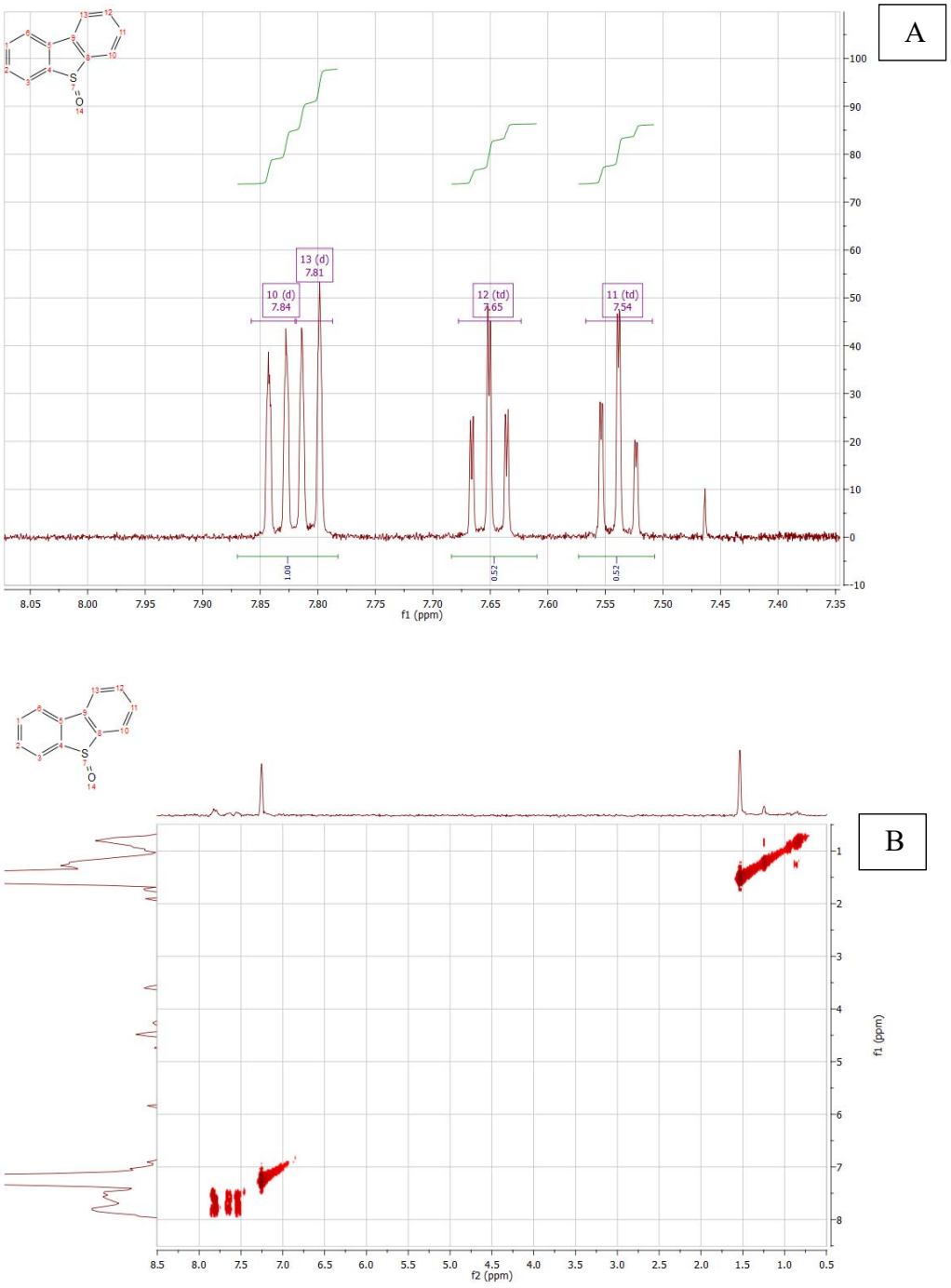

Figure (C.12):NMR spectrum of dibenzothiopene sulfoxide (A) ^{1}H NMR Expanded aromatic region (B) Gradient enhanced COSY spectrum.

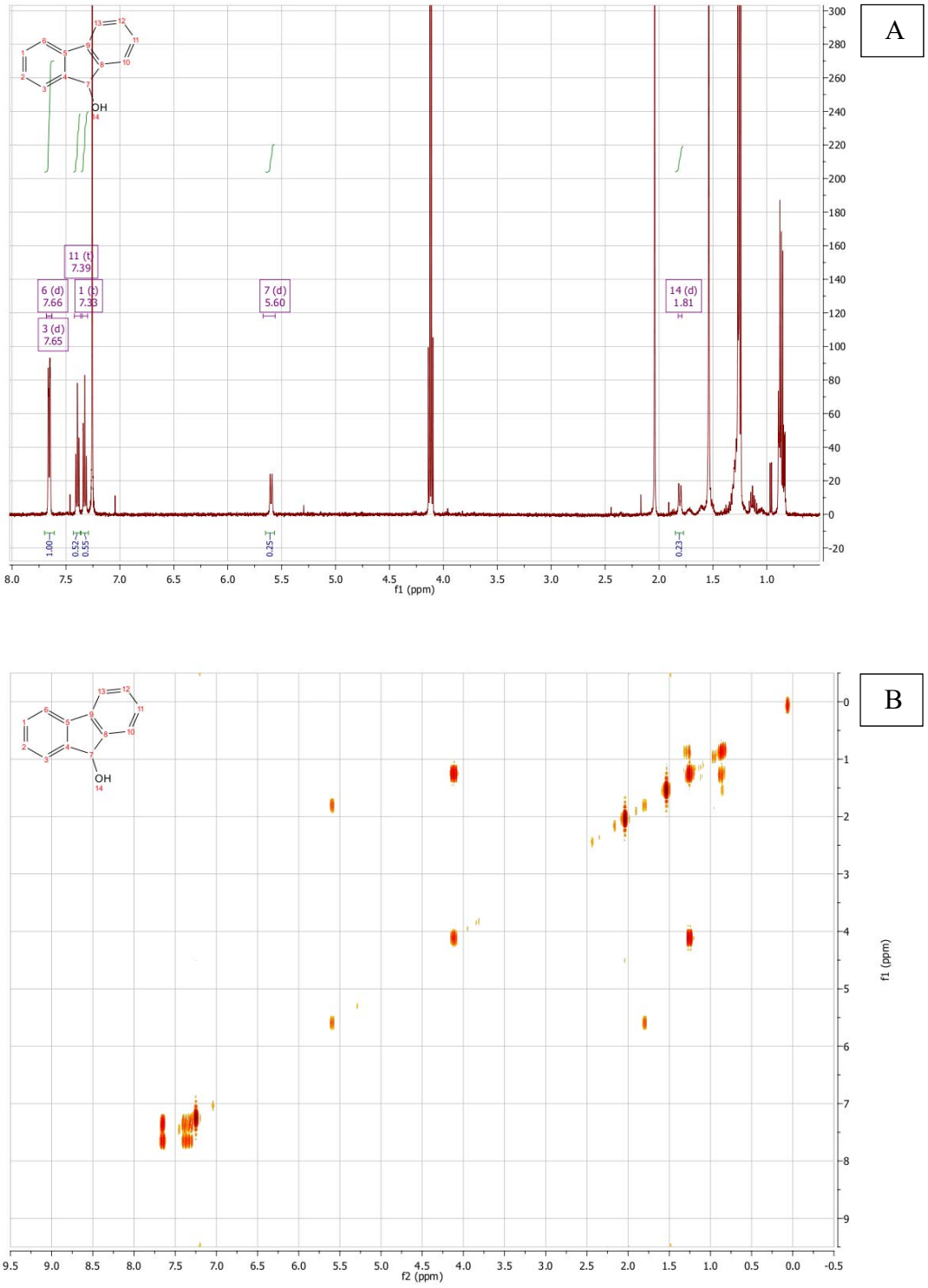

Figure (C.13):NMR spectrum of 9-hydroxyfluorene (A) ^{1}H NMR Expanded aromatic region (B) Gradient enhanced COSY spectrum.

Bibliography

1. Kim KH, Jahan SA, Kabir E, Brown RJ. 2013. A review of airborne polycyclic aromatic hydrocarbons (PAHs) and their human health effects. Environ Int 60:71-80.

2. Haritash AK, Kaushik CP. 2009. Biodegradation aspects of polycyclic aromatic hydrocarbons (PAHs): a review. J Hazard Mater 169:1-15.

3. Abdel-Shafy HI, Mansour MSM. 2016. A review on polycyclic aromatic hydrocarbons: Source, environmental impact, effect on human health and remediation. Egypt J Petrol 25:107-123.

4. Ravindra K, Sokhi R, Vangrieken R. 2008. Atmospheric polycyclic aromatic hydrocarbons: Source attribution, emission factors and regulation. Atmos Environ 42:2895-2921.

5. Wilcke W. 2000. SYNOPSIS Polycyclic Aromatic Hydrocarbons (PAHs) in Soil — a Review. J Plant Nutr Soil Sc 163:229-248.

6. Ball A, Truskewycz A. 2013. Polyaromatic hydrocarbon exposure: an ecological impact ambiguity. Environ Sci Pollut Res Int 20:4311-26.

7. Boffetta P, Jourenkova N, Gustavsson P. 1997. Cancer risk from occupational and environmental exposure to polycyclic aromatic hydrocarbons. Cancer Causes Control 8:444-72.

8. Chen SC, Liao CM. 2006. Health risk assessment on human exposed to environmental polycyclic aromatic hydrocarbons pollution sources. Sci Total Environ 366:112-23.

9. Moorthy B, Chu C, Carlin DJ. 2015. Polycyclic aromatic hydrocarbons: from metabolism to lung cancer. Toxicol Sci 145:5-15.

10. Perera FP, Jedrychowski W, Rauh V, Whyatt RM. 1999. Molecular epidemiologic research on the effects of environmental pollutants on the fetus. Environ Health Perspect 107 Suppl 3:451-60.

11. Wormley DD, Ramesh A, Hood DB. 2004. Environmental contaminant-mixture effects on CNS development, plasticity, and behavior. Toxicol Appl Pharmacol 197:49-65.

12. Uemura H, Arisawa K, Hiyoshi M, Kitayama A, Takami H, Sawachika F, Dakeshita S, Nii K, Satoh H, Sumiyoshi Y, Morinaga K, Kodama K, Suzuki T, Nagai M, Suzuki T. 2009. Prevalence of metabolic syndrome associated with body burden levels of dioxin and related compounds among Japan's general population. Environ Health Perspect 117:568-73.

13. Fries GF. 1995. A review of the significance of animal food products as potential pathways of human exposures to dioxins. J Anim Sci 73:1639-50.

14. Orban JE, Stanley JS, Schwemberger JG, Remmers JC. 1994. Dioxins and dibenzofurans in adipose tissue of the general US population and selected subpopulations. Am J Public Health 84:439-45.

15. Field JA, Sierra-Alvarez R. 2008. Microbial degradation of chlorinated dioxins. Chemosphere 71:1005-18.

16. Kulkarni PS, Crespo JG, Afonso CA. 2008. Dioxins sources and current remediation technologies--a review. Environ Int 34:139-53.

17. Bertazzi A, Pesatori AC, Consonni D, Tironi A, Landi MT, Zocchetti C. 1993. Cancer incidence in a population accidentally exposed to 2,3,7,8-tetrachlorodibenzo-para-dioxin. Epidemiology 4:398-406.

18. Bertazzi PA, Consonni D, Bachetti S, Rubagotti M, Baccarelli A, Zocchetti C, Pesatori AC. 2001. Health effects of dioxin exposure: a 20-year mortality study. Am J Epidemiol 153:1031-44.

19. Habe H, Chung JS, Lee JH, Kasuga K, Yoshida T, Nojiri H, Omori T. 2001. Degradation of chlorinated dibenzofurans and dibenzo-*p*-dioxins by two types of bacteria having angular dioxygenases with different features. Appl Environ Microbiol 67:3610-7.

20. Kimura N, Urushigawa Y. 2001. Metabolism of dibenzo-*p*-dioxin and chlorinated dibenzo-*p*-dioxin by a gram-positive bacterium, *Rhodococcus opacus* SAO101. J Biosci Bioeng 92:138-43.

21. Hong HB, Nam IH, Murugesan K, Kim YM, Chang YS. 2004. Biodegradation of dibenzo-*p*-dioxin, dibenzofuran, and chlorodibenzo-p-dioxins by *Pseudomonas veronii* PH-03. Biodegradation 15:303-13.

22. Wittich RM, Wilkes H, Sinnwell V, Francke W, Fortnagel P. 1992. Metabolism of dibenzo-*p*-dioxin by *Sphingomonas* sp. strain RW1. Appl Environ Microbiol 58:1005-10.

23. Coronado E, Roggo C, Johnson DR, van der Meer JR. 2012. Genome-wide analysis of salicylate and dibenzofuran metabolism in *Sphingomonas wittichii* RW1. Front Microbiol 3:300.

24. Chai B, Tsoi TV, Iwai S, Liu C, Fish JA, Gu C, Johnson TA, Zylstra G, Teppen BJ, Li H, Hashsham SA, Boyd SA, Cole JR, Tiedje JM. 2016. *Sphingomonas wittichii* strain RW1 genome-wide gene expression shifts in response to dioxins and clay. PLoS One 11:e0157008.

25. Armengaud J, Happe B, Timmis KN. 1998. Genetic analysis of dioxin dioxygenase of *Sphingomonas* sp. strain RW1: catabolic genes dispersed on the genome. J Bacteriol 180:3954-66.

26. Halden RU, Halden BG, Dwyer DF. 1999. Removal of dibenzofuran, dibenzo-*p*-dioxin, and 2-chlorodibenzo-*p*-dioxin from soils inoculated with *Sphingomonas* sp. strain RW1. Appl Environ Microbiol 65:2246-9.

27. Hong HB, Chang YS, Nam IH, Fortnagel P, Schmidt S. 2002. Biotransformation of 2,7-dichloro- and 1,2,3,4-tetrachlorodibenzo-*p*-dioxin by S*phingomonas wittichii* RW1. Appl Environ Microbiol 68:2584-8.

28. Yabuuchi E, Yamamoto H, Terakubo S, Okamura N, Naka T, Fujiwara N, Kobayashi K, Kosako Y, Hiraishi A. 2001. Proposal of *Sphingomonas wittichii* sp. nov. for strain RW1^{T}, known as a dibenzo-*p*-dioxin metabolizer. Int J Syst Evol Microbiol 51:281-92.

29. Busse HJ, Kampfer P, Denner EB. 1999. Chemotaxonomic characterisation of *Sphingomonas*. J Ind Microbiol Biotechnol 23:242-251.

30. Muller TA, Byrde SM, Werlen C, van der Meer JR, Kohler HP. 2004. Genetic analysis of phenoxyalkanoic acid degradation in *Sphingomonas herbicidovorans* MH. Appl Environ Microbiol 70:6066-75.

31. Zylstra GJ, Kim E. 1997. Aromatic hydrocarbon degradation by *Sphingomonas yanoikuyae* B1. J Ind Microbiol Biotechnol 19:408-14.

32. Keck A, Rau J, Reemtsma T, Mattes R, Stolz A, Klein J. 2002. Identification of quinoide redox mediators that are formed during the degradation of naphthalene-2-sulfonate by *Sphingomonas xenophag*a BN6. Appl Environ Microbiol 68:4341-9.

33. Yang CF, Lee CM, Wang CC. 2006. Isolation and physiological characterization of the pentachlorophenol degrading bacterium *Sphingomonas chlorophenolica*. Chemosphere 62:709-14.

34. Jaiswal PK, Thakur IS. 2007. Isolation and characterization of dibenzofuran-degrading *Serratia marcescens* from alkalophilic bacterial consortium of the chemostat. Curr Microbiol 55:447-54.

35. Miller TR, Delcher AL, Salzberg SL, Saunders E, Detter JC, Halden RU. 2010. Genome sequence of the dioxin-mineralizing bacterium *Sphingomonas wittichii* RW1. J Bacteriol 192:6101-2.

36. Bunz PV, Cook AM. 1993. Dibenzofuran 4,4a-dioxygenase from *Sphingomonas* sp. strain RW1: angular dioxygenation by a three-component enzyme system. J Bacteriol 175:6467-75.

37. Armengaud J, Timmis KN. 1998. The reductase RedA2 of the multi-component dioxin dioxygenase system of *Sphingomonas* sp. RW1 is related to class-I cytochrome P450-type reductases. Eur J Biochem 253:437-44.

38. Armengaud J, Timmis KN. 1997. Molecular characterization of Fdx1, a putidaredoxin-type [2Fe-2S] ferredoxin able to transfer electrons to the dioxin dioxygenase of *Sphingomonas* sp. RW1. Eur J Biochem 247:833-42.

39. Armengaud J, Gaillard J, Timmis KN. 2000. A second [2Fe-2S] ferredoxin from *Sphingomonas* sp. strain RW1 can function as an electron donor for the dioxin dioxygenase. J Bacteriol 182:2238-44.

40. Happe B, Eltis LD, Poth H, Hedderich R, Timmis KN. 1993. Characterization of 2,2',3-trihydroxybiphenyl dioxygenase, an extradiol dioxygenase from the dibenzofuran- and dibenzo-*p*-dioxin-degrading bacterium *Sphingomonas* sp. strain RW1. J Bacteriol 175:7313-20.

41. Hartmann EM, Armengaud J. 2014. Shotgun proteomics suggests involvement of additional enzymes in dioxin degradation by *Sphingomonas wittichii* RW1. Environ Microbiol 16:162-76.

42. Colquhoun DR, Hartmann EM, Halden RU. 2012. Proteomic profiling of the dioxin-degrading bacterium *Sphingomonas wittichii* RW1. J Biomed Biotechnol 2012:408690.

43. Bunz PV, Falchetto R, Cook AM. 1993. Purification of two isofunctional hydrolases (EC 3.7.1.8) in the degradative pathway for dibenzofuran in *Sphingomonas* sp. strain RW1. Biodegradation 4:171-8.

44. Seah SY, Ke J, Denis G, Horsman GP, Fortin PD, Whiting CJ, Eltis LD. 2007. Characterization of a C-C bond hydrolase from *Sphingomonas wittichii* RW1 with novel specificities towards polychlorinated biphenyl metabolites. J Bacteriol 189:4038-45.

45. Armengaud J, Timmis KN, Wittich RM. 1999. A functional 4-hydroxysalicylate/hydroxyquinol degradative pathway gene cluster is linked to the initial dibenzo-*p*-dioxin pathway genes in *Sphingomonas* sp. strain RW1. J Bacteriol 181:3452-61.

46. Camara B, Bielecki P, Kaminski F, dos Santos VM, Plumeier I, Nikodem P, Pieper DH. 2007. A gene cluster involved in degradation of substituted salicylates via ortho cleavage in *Pseudomonas* sp. strain MT1 encodes enzymes specifically adapted for transformation of 4-methylcatechol and 3-methylmuconate. J Bacteriol 189:1664-74.

47. Bosch R, Moore ER, Garcia-Valdes E, Pieper DH. 1999. NahW, a novel, inducible salicylate hydroxylase involved in mineralization of naphthalene by *Pseudomonas stutzeri* AN10. J Bacteriol 181:2315-22.

48. Ishiyama D, Vujaklija D, Davies J. 2004. Novel pathway of salicylate degradation by *Streptomyces* sp. strain WA46. Appl Environ Microbiol 70:1297-306.

49. Rehmann L, Daugulis AJ. 2006. Biphenyl degradation kinetics by *Burkholderia xenovorans* LB400 in two-phase partitioning bioreactors. Chemosphere 63:972-9.

50. Sha'arani S, Hara H, Araie H, Suzuki I, Mohd Noor MJM, Akhir FNM, Othman N, Zakaria Z. 2019. Whole gene transcriptomic analysis of PCB/biphenyl degrading *Rhodococcus jostii* RHA1. J Gen Appl Microbiol doi:10.2323/jgam.2018.08.003.

51. Pham TT, Sylvestre M. 2013. Has the bacterial biphenyl catabolic pathway evolved primarily to degrade biphenyl? The diphenylmethane case. J Bacteriol 195:3563-74.

52. Furukawa K, Suenaga H, Goto M. 2004. Biphenyl dioxygenases: functional versatilities and directed evolution. J Bacteriol 186:5189-96.

53. Suenaga H, Mitsuoka M, Ura Y, Watanabe T, Furukawa K. 2001. Directed evolution of biphenyl dioxygenase: emergence of enhanced degradation capacity for benzene, toluene, and alkylbenzenes. J Bacteriol 183:5441-4.

54. Yu CL, Liu W, Ferraro DJ, Brown EN, Parales JV, Ramaswamy S, Zylstra GJ, Gibson DT, Parales RE. 2007. Purification, characterization, and crystallization of the components of a biphenyl dioxygenase system from *Sphingobium yanoikuyae* B1. J Ind Microbiol Biotechnol 34:311-24.

55. Eaton SL, Resnick SM, Gibson DT. 1996. Initial reactions in the oxidation of 1,2-dihydronaphthalene by *Sphingomonas yanoikuyae* strains. Appl Environ Microbiol 62:4388-94.

56. Klecka GM, Gibson DT. 1980. Metabolism of dibenzo-*p*-dioxin and chlorinated dibenzo-*p*-dioxins by a *Beijerinckia* species. Appl Environ Microbiol 39:288-96.

57. Gibson DT, Cruden DL, Haddock JD, Zylstra GJ, Brand JM. 1993. Oxidation of polychlorinated biphenyls by *Pseudomonas* sp. strain LB400 and *Pseudomonas pseudoalcaligenes* KF707. J Bacteriol 175:4561-4.

58. Khan AA, Wang RF, Nawaz MS, Cerniglia CE. 1997. Nucleotide sequence of the gene encoding *cis*-biphenyl dihydrodiol dehydrogenase (*bphB*) and the expression of an active recombinant His-tagged *bphB* gene product from a PCB degrading bacterium, *Pseudomonas putida* OU83. FEMS Microbiol Lett 154:317-24.

59. Vaillancourt FH, Haro MA, Drouin NM, Karim Z, Maaroufi H, Eltis LD. 2003. Characterization of extradiol dioxygenases from a polychlorinated biphenyl-degrading strain that possess higher specificities for chlorinated metabolites. J Bacteriol 185:1253-60.

60. Yamada A, Kishi H, Sugiyama K, Hatta T, Nakamura K, Masai E, Fukuda M. 1998. Two nearly identical aromatic compound hydrolase genes in a strong polychlorinated biphenyl degrader, *Rhodococcus* sp. strain RHA1. Appl Environ Microbiol 64:2006-12.

61. Seeger M, Timmis KN, Hofer B. 1995. Conversion of chlorobiphenyls into phenylhexadienoates and benzoates by the enzymes of the upper pathway for polychlorobiphenyl degradation encoded by the *bph* locus of *Pseudomonas* sp. strain LB400. Appl Environ Microbiol 61:2654-8.

62. Bhowmik S, Horsman GP, Bolin JT, Eltis LD. 2007. The molecular basis for inhibition of BphD, a C-C bond hydrolase involved in polychlorinated biphenyls degradation: large 3-substituents prevent tautomerization. J Biol Chem 282:36377-85.

63. Zylstra GJ, Kim E, Goyal AK. 1997. Comparative molecular analysis of genes for polycyclic aromatic hydrocarbon degradation. Genet Eng (N Y) 19:257-69.

64. Kim E, Zylstra GJ. 1999. Functional analysis of genes involved in biphenyl, naphthalene, phenanthrene, and *m*-xylene degradation by *Sphingomonas yanoikuyae* B1. J Ind Microbiol Biotechnol 23:294-302.

65. Resnick SM, Gibson DT. 1996. Regio- and stereospecific oxidation of fluorene, dibenzofuran, and dibenzothiophene by naphthalene dioxygenase from *Pseudomonas* sp. strain NCIB 9816-4. Appl Environ Microbiol 62:4073-80.

66. Nojiri H, Nam JW, Kosaka M, Morii KI, Takemura T, Furihata K, Yamane H, Omori T. 1999. Diverse oxygenations catalyzed by carbazole 1,9a-dioxygenase from *Pseudomonas* sp. strain CA10. J Bacteriol 181:3105-13.

67. Schuler L, Ni Chadhain SM, Jouanneau Y, Meyer C, Zylstra GJ, Hols P, Agathos SN. 2008. Characterization of a novel angular dioxygenase from fluorene-degrading *Sphingomonas* sp. strain LB126. Appl Environ Microbiol 74:1050-7.

68. Sambrook J, Fritsch EF, Maniatis T. 1987. Molecular cloning, a laboratory manual 2ed. Cold Spring Harbor Laboratory Press, Cold Spring Harbor, NY.

69. Moody JD, Freeman JP, Doerge DR, Cerniglia CE. 2001. Degradation of phenanthrene and anthracene by cell suspensions of *Mycobacterium* sp. strain PYR-1. Appl Environ Microbiol 67:1476-83.

70. Tomasek PH, Crawford RL. 1986. Initial reactions of xanthone biodegradation by an *Arthrobacter* sp. J Bacteriol 167:818-27.

71. Sutherland JB, Freeman JP, Selby AL, Fu PP, Miller DW, Cerniglia CE. 1990. Stereoselective formation of a K-region dihydrodiol from phenanthrene by *Streptomyces flavovirens*. Arch Microbiol 154:260-6.

72. Zeinali M, Vossoughi M, Ardestani SK. 2008. Degradation of phenanthrene and anthracene by *Nocardia otitidiscaviarum* strain TSH1, a moderately thermophilic bacterium. J Appl Microbiol 105:398-406.

73. Quijano L, Marin S, Millan E, Yusa V, Font G, Pardo O. 2018. Dietary exposure and risk assessment of polychlorinated dibenzo-*p*-dioxins, polychlorinated dibenzofurans and dioxin-like polychlorinated biphenyls of the population in the Region of Valencia (Spain). Food Addit Contam Part A Chem Anal Control Expo Risk Assess 35:740-749.

74. Sakari M. 2012. Depositional history of polycyclic aromatic hydrocarbons: reconstruction of petroleum pollution record in peninsular Malaysia. *In* Puzyn T, Mostrag-Szlichtyng A (ed), Organic Pollutants Ten Years After the Stockholm Convention - Environmental and Analytical Update. IntechOpen, doi:10.5772/31624.

75. Kappell AD, Wei Y, Newton RJ, Van Nostrand JD, Zhou J, McLellan SL, Hristova KR. 2014. The polycyclic aromatic hydrocarbon degradation potential of Gulf of Mexico native coastal microbial communities after the Deepwater Horizon oil spill. Front Microbiol 5:205.

76. Pieper DH, Reineke W. 2000. Engineering bacteria for bioremediation. Curr Opin Biotechnol 11:262-70.

77. Singh S, Kang SH, Mulchandani A, Chen W. 2008. Bioremediation: environmental clean-up through pathway engineering. Curr Opin Biotechnol 19:437-44.

78. Dvorak P, Nikel PI, Damborsky J, de Lorenzo V. 2017. Bioremediation 3.0: Engineering pollutant-removing bacteria in the times of systemic biology. Biotechnol Adv 35:845-866.

79. Aso Y, Miyamoto Y, Harada KM, Momma K, Kawai S, Hashimoto W, Mikami B, Murata K. 2006. Engineered membrane superchannel improves bioremediation potential of dioxin-degrading bacteria. Nat Biotechnol 24:188-9.

80. Nam IH, Kim YM, Schmidt S, Chang YS. 2006. Biotransformation of 1,2,3-tri- and 1,2,3,4,7,8-hexachlorodibenzo-*p*-dioxin by *Sphingomonas wittichii* strain RW1. Appl Environ Microbiol 72:112-6.

81. Gibson DT. 1999. *Beijerinckia* sp strain B1: a strain by any other name. J Ind Microbiol Biotechnol 23:284-293.

82. Mutter T. 2019. Molecular genetic and physiological studies to unravel the mystery of *Sphingomonas wittichii* RW1 dibenzo-*p*-dioxin degradation. Ph.D. Rutgers University, New Brunswick, NJ.

83. Keen NT, Tamaki S, Kobayashi D, Trollinger D. 1988. Improved broad-host-range plasmids for DNA cloning in gram-negative bacteria. Gene 70:191-7.

84. Kim E, Zylstra GJ. 1995. Molecular and biochemical characterization of two meta-cleavage dioxygenases involved in biphenyl and *m*-xylene degradation by *Beijerinckia* sp. strain B1. J Bacteriol 177:3095-103.

85. Figurski DH, Helinski DR. 1979. Replication of an origin-containing derivative of plasmid RK2 dependent on a plasmid function provided in trans. Proc Natl Acad Sci U S A 76:1648-52.

86. Stanier RY, Palleroni NJ, Doudoroff M. 1966. The aerobic pseudomonads: a taxonomic study. J Gen Microbiol 43:159-271.

87. Ruzzini AC, Bhowmik S, Yam KC, Ghosh S, Bolin JT, Eltis LD. 2013. The lid domain of the MCP hydrolase DxnB2 contributes to the reactivity toward recalcitrant PCB metabolites. Biochemistry 52:5685-95.

88. Ruzzini AC, Bhowmik S, Ghosh S, Yam KC, Bolin JT, Eltis LD. 2013. A substrate-assisted mechanism of nucleophile activation in a Ser-His-Asp containing C-C bond hydrolase. Biochemistry 52:7428-38.

89. Tandlich R, Vrana B, Payne S, Dercova K, Balaz S. 2011. Biodegradation mechanism of biphenyl by a strain of *Pseudomonas stutzeri*. J Environ Sci Health A Tox Hazard Subst Environ Eng 46:337-44.

90. Parnell JJ, Park J, Denef V, Tsoi T, Hashsham S, Quensen J, 3rd, Tiedje JM. 2006. Coping with polychlorinated biphenyl (PCB) toxicity: Physiological and genome-wide responses of *Burkholderia xenovorans* LB400 to PCB-mediated stress. Appl Environ Microbiol 72:6607-14.

91. Hu J, Qian M, Zhang Q, Cui J, Yu C, Su X, Shen C, Hashmi MZ, Shi J. 2015. *Sphingobium fuliginis* HC3: a novel and robust isolated biphenyl- and polychlorinated biphenyls-degrading bacterium without dead-end intermediates accumulation. PLoS One 10:e0122740.

92. Hong HB, Chang YS, Nam IH, Fortnagel P, Schmidt S. 2002. Biotransformation of 2,7-dichloro- and 1,2,3,4-tetrachlorodibenzo-*p*-dioxin by S*phingomonas wittichii* RW1. Appl Environ Microbiol 68:2584-8.

93. Nam IH, Kim YM, Schmidt S, Chang YS. 2006. Biotransformation of 1,2,3-tri- and 1,2,3,4,7,8-hexachlorodibenzo-*p*-dioxin by *Sphingomonas wittichii* strain RW1. Appl Environ Micorbiol 72:112-6.

94. Zhao Q, Hu H, Wang W, Peng H, Zhang X. 2015. Genome sequence of *Sphingobium yanoikuyae* B1, a polycyclic aromatic hydrocarbon-degrading strain. Genome Announc 3.

95. Kim E, Aversano PJ, Romine MF, Schneider RP, Zylstra GJ. 1996. Homology between genes for aromatic hydrocarbon degradation in surface and deep-subsurface *Sphingomonas* strains. Appl Environ Microbiol 62:1467-70.

96. Ni Chadhain SM, Moritz EM, Kim E, Zylstra GJ. 2007. Identification, cloning, and characterization of a multicomponent biphenyl dioxygenase from *Sphingobium yanoikuyae* B1. J Ind Microbiol Biotechnol 34:605-13.

97. Zhao Q, Bilal M, Yue S, Hu H, Wang W, Zhang X. 2017. Identification of biphenyl 2, 3-dioxygenase and its catabolic role for phenazine degradation in *Sphingobium yanoikuyae* B1. J Environ Manage 204:494-501.

98. Cerniglia CE, Morgan JC, Gibson DT. 1979. Bacterial and fungal oxidation of dibenzofuran. Biochem J 180:175-85.

99. Dennis JJ, Zylstra GJ. 1998. Improved antibiotic-resistance cassettes through restriction site elimination using Pfu DNA polymerase PCR. Biotechniques 25:772-4, 776.

100. Ho SN, Hunt HD, Horton RM, Pullen JK, Pease LR. 1989. Site-directed mutagenesis by overlap extension using the polymerase chain reaction. Gene 77:51-9.

101. Kumamaru T, Suenaga H, Mitsuoka M, Watanabe T, Furukawa K. 1998. Enhanced degradation of polychlorinated biphenyls by directed evolution of biphenyl dioxygenase. Nat Biotechnol 16:663-6.

102. Suenaga H, Watanabe T, Sato M, Ngadiman, Furukawa K. 2002. Alteration of regiospecificity in biphenyl dioxygenase by active-site engineering. J Bacteriol 184:3682-8.

103. Ohtsubo Y, Shimura M, Delawary M, Kimbara K, Takagi M, Kudo T, Ohta A, Nagata Y. 2003. Novel approach to the improvement of biphenyl and polychlorinated biphenyl degradation activity: promoter implantation by homologous recombination. Appl Environ Microbiol 69:146-53.

104. Gibson DT, Roberts RL, Wells MC, Kobal VM. 1973. Oxidation of biphenyl by a *Beijerinckia* species. Biochem Biophys Res Commun 50:211-9.

105. Eltis LD, Bolin JT. 1996. Evolutionary relationships among extradiol dioxygenases. J Bacteriol 178:5930-7.